Biochemical and Functional Characterization of Induced Terpene Formation in Arabidopsis Roots

Reza Sohrabi

Dissertation submitted to the faculty of the Virginia Polytechnic Institute and State University
in partial fulfillment of the requirements for the degree of

Doctor of Philosophy
In
Biological Sciences

Dorothea Tholl, Committee Chair

Glenda Gillaspy
Khidir Hilu
John Jelesko

July 23rd 2013
Blacksburg Virginia

Keywords: Cytochrome P450, plant volatiles, specialized metabolism, root chemical defense, *Arabidopsis*

Biochemical and Functional Characterization of Induced Terpene Formation in Arabidopsis Roots

Reza Sohrabi

ABSTRACT

Plants have evolved a variety of constitutive and induced chemical defense mechanisms against biotic stress. Emission of volatile compounds from plants facilitates interactions with both beneficial and pathogenic organisms. However, knowledge of the chemical defense in roots is still limited. In this study, we have examined the root-specific biosynthesis and function of volatile terpenes in the model plant *Arabidopsis*. When infected with the root rot pathogen *Pythium irregulare*, *Arabidopsis* roots release the acyclic C_{11}-homoterpene (*E*)-4,8-dimethylnona-1,3,7-triene (DMNT), which is a common constituent of volatile blends emitted from insect-damaged foliage. We have identified a single cytochrome P450 monooxygenase of the CYP705 family that catalyzes a root-specific oxidative degradation of the C_{30}-triterpene precursor arabidiol thereby causing the release of DMNT and a C_{19}-degradation product named arabidonol. We found that DMNT shows inhibitory effects on *P. irregulare* mycelium growth and oospore germination *in vitro*, and that DMNT biosynthetic mutant plants were more susceptible to *P. irregulare* infection. We provide evidence based on genome synteny and phylogenetic analysis that the arabidiol biosynthetic gene cluster containing the arabidiol synthase (*ABDS*) and *CYP705A1* genes possibly emerged via local gene duplication followed by

de novo neofunctionalization. Together, our studies demonstrate differences and plasticity in the metabolic organization and function of terpenes in roots in comparison to aboveground plant tissues.

Additionally, we demonstrated that the arabidiol cleavage product, arabidonol, is further modified by yet unknown enzymatic reactions into three products, which are found in root exudates. We suggested a pathway for their biosynthesis based on precursor feeding experiments and NMR analysis. Although DMNT biosynthetic genes are clustered on chromosome 4 along with several potential modification genes, we did not find a possible role of these genes in the derivatization of arabidonol. Preliminary experimental results using genetic and biochemical approaches for identifying genes involved in the modification steps are also presented.

In summary, this study demonstrates an alternative route for volatile terpene formation belowground different from aboveground plant tissues via triterpene degradation and provides evidence for an unexplored triterpene catabolism pathway in *Arabidopsis*.

ACKNOWLEDGEMENTS

I owe my gratitude to all those people who have made this dissertation possible and because of whom my experience as graduate student has been one that I will treasure forever. First I would like to gratefully and sincerely thank Dr. Dorothea Tholl for her guidance, understanding, patience, and great opportunities she has provided during my graduate studies. She encouraged me to think independently and taught me how to question thoughts and ideas critically.

I am grateful to my committee members Drs. Khidir Hilu, Glenda Gillaspy and John Jelesko for their academic support, valuable comments and discussion, and guidance during all these years. I would like to thanks Dr. Brenda Winkel for all her support and also for accepting to serve as proxy on the defense date. It has been an honor for me to have you all.

I would like to appreciate Dr. Liva Harinantenina for NMR analysis, Dr. Dan Kliebenstein for help in QTL analysis, Dr. Somayesadat Badieyan for protein modeling experiments and Dr. Jim Tokuhisa for his advice and discussions. My special thanks go to all former and current members of the Tholl lab: Jason Lancaster, Jingyu Zhang, Dr. Jung-Hyun Huh, Dr. Sungbeom Lee, Dr. Martha Vaughan, and Dr. Qiang Wang.

Lastly, I would like to express my special thanks to my friends and family members, who have been cheering and supportive of my endeavors during my entire education. I owe great gratitude and appreciation to my mother, father, brothers and sisters for their assurance and encouragement, which were appreciated. Specially, I would like to thank my wife Somayesadat Badieyan for her sincere support and sacrifice throughout my journey and my wonderful daughter Sarah Sohrabi. Both of you are the best things that has ever happened to me and you inspires me with great confidence.

TABLE OF CONTENTS

CHAPTER **PAGE**

ABSTRACT ..... **IV**

ACKNOWLEDGEMENTS ..... **IV**

TABLE OF CONTENTS ..... **V**

LIST OF FIGURES AND TABLES ..... **VII**

1. GENERAL INTRODUCTION AND OVERVIEW OF RESEARCH **1**

CHEMICAL COMMUNICATION IN PLANT–ORGANISM INTERACTIONS 2
THE IMPORTANCE OF VOLATILE TERPENES IN PLANT-ENVIRONMENT INTERACTION 4
DISTRIBUTION AND FUNCTIONS OF C_{11}- AND C_{16}-HOMOTERPENES IN LAND PLANTS 6
BIOSYNTHESIS OF REGULAR TERPENES AND IRREGULAR HOMOTERPENES 12
ARABIDOPSIS AS A MODEL FOR THE FORMATION OF BELOWGROUND VOLATILE TERPENES 16
OVERVIEW OF RESEARCH 17
LITERATURE CITED 20

2. AN ALTERNATIVE BIOSYNTHETIC ROUTE TO THE PATHOGEN-INDUCED VOLATILE HOMOTERPENE DMNT VIA TRITERPENE DEGRADATION IN *ARABIDOPSIS* ROOTS **26**

ABSTRACT 27
INTRODUCTION 28
RESULTS 30
Pythium-Induced Production of DMNT in Arabidopsis Roots *30*
Identification of CYP705A1 as a Root-Specific Gene Involved in DMNT Biosynthesis *32*
Arabidiol is the Precursor in DMNT Biosynthesis in Arabidopsis Roots *35*
Arabidiol is Cleaved into DMNT and the Non-Volatile C_{19} Tricyclic Ketone Arabidonol *38*
Transcript Analysis of ABDS and CYP705A1 in Pythium-Infected and JA-Treated Arabidopsis Roots *40*
Spatial Pattern of DMNT Biosynthetic Gene Expression *42*
DMNT Negatively Effects Pythium Oospore Germination and Growth *44*
DISCUSSION 47
Arabidopsis Roots Produce DMNT via the Breakdown of a Triterpene Precursor *47*
DMNT Biosynthetic Genes are Expressed in Specific Cell Types of the Arabidopsis Root and Respond to Jasmonate and Pathogen Treatment *51*
Arabidiol Breakdown Products are Involved in the Defense Against P. irregulare *53*
Evolution of DMNT Biosynthesis in Arabidopsis via Triterpene Gene Cluster Assembly *54*
METHODS 58
Plant Materials and Growth Conditions *58*
Volatile Collection and Analysis *59*
Genotyping of Plant Materia *60*
Construction and Analysis of Transgenic Plants *60*
Yeast Expression, Arabidonol Purification and Enzyme Assays *61*
Transcript Analysis by RT–PCR and Quantitative Real-Time PCR *63*
Growth and Bioassay Conditions of P. irregulare *64*

Oospore Isolation and Germination of P. irregulare 110305 ..... *65*
SUPPLEMENTAL MATERIALS 66
SUPPLEMENTAL METHODS 90
Growth Inhibition Assay in Vitro *90*
NMR Analysis of Arabidonol Structure *90*
Computational Methods: *91*
LITERATURE CITED: 94

3. IDENTIFICATION OF DOWNSTREAM MODIFICATION PRODUCTS IN THE ARABIDIOL CATABOLIC PATHWAY IN *ARABIDOPSIS* ROOTS 99

ABSTRACT 100
INTRODUCTION 101
RESULTS 103
Arabidiol-Derived Compounds are Detected in Arabidopsis Root Tissue and Exudates *103*
Arabidonol is Converted into Deg-M, Deg-R, and a Third Compound, Deg-I, in Planta *106*
Purification and Structure Elucidation of Arabidonol Modification Products *108*
Application of Individual Derivatives to Confirm the Sequence of Arabidonol Modification Steps *110*
Functional Expression of the Putative Acyltransferase At4g15390 in Yeast *111*
Genetic and Evolutionary Approaches for the Identification of Genes Involved in the Arabidiol Catabolic Pathway *112*
DISCUSSION 115
The Arabidiol Catabolic Pathway Contains Several Modification Steps *115*
Identification of Arabidonol Modifying Enzymes *118*
METHODS 120
Plant Materials and Growth Conditions *120*
Production and Purification of Arabidonol from Yeast Expression Lines *121*
Analysis of Arabidonol Derivatives in Plants *122*
Purification of Modification Products *123*
NMR Analysis of Modification Products *124*
SUPPLEMENTAL MATERIALS 125
LITERATURE CITED 128

4. FINAL DISCUSSION AND FUTURE PERSPECTIVES 131

REGULATION AND FUNCTIONS OF PHYTOCHEMICALS IN THE RHIZOSPHERE 132
CELL-TYPE OR TISSUE SPECIFICITY OF CHEMICAL DEFENSE IN ROOTS 134
EVOLUTION OF DMNT FORMATION IN *ARABIDOPSIS* 137
LITERATURE CITED 140

LIST OF FIGURES AND TABLES

FIGURE/TABLE **PAGE**

Chapter 1

Figure 1.1 Ecological roles of VOCs in plant-environment interactions..... 3
Figure 1.2 Plant families with reported emission of DMNT and TMTT..... 9
Figure 1.3 Biosynthetic pathways of terpenes in plants. 14

Chapter 2

Figure 2.1 DMNT emission in *Arabidopsis* roots is induced by infection with *P. irregulare* or treatment with jasmonic acid. 31
Figure 2.2 Identification of CYP705A1 as a DMNT synthase. 34
Figure 2.3 Arabidiol is the substrate for DMNT biosynthesis. 36
Figure 2.4 Detection of arabidonol in the yeast co-expression system..... 39
Figure 2.5 qRT-PCR Analysis of *CYP705A1* and *ABDS* Transcript Levels. 41
Figure 2.6 Spatial expression pattern of *CYP705A1*. 43
Figure 2.7 DMNT negatively effects *P. irregulare* oospore germination and formation..... 46
Figure 2.8 Docked conformation of arabidiol in the active site of modeled CYP705A1..... 49
Figure 2.9 The proposed mechanism for oxidative degradation of arabidiol by CYP705A1 50
Figure 2.10 Comparative Genome Analysis Maps of ABDS Gene Cluster. 55

Supplemental Figure 2.1 Infection of *Arabidopsis* roots with *P. irregulare*. 66
Supplemental Figure 2.2 DMNT emission from hydroponically grown Arabidopsis roots..... 67
Supplemental Figure 2.3 The *cyp82g1-1* T-DNA insertion mutant is not impaired in JA induced production of DMNT from roots. 68
Supplemental Figure 2.4 Pharmacological study of DMNT formation in *Arabidopsis* hairy root culture. 69
Supplemental Figure 2.5 QTL analysis of natural variation in DMNT biosynthesis among Arabidopsis accessions. 70
Supplemental Figure 2.6 Selection of Candidate P450 Genes for DMNT Biosynthesis..... 72
Supplemental Figure 2.7 RT-PCR Analysis of *CYP705A1*. 73
Supplemental Figure 2.8 DMNT formation in *Arabidopsis* roots is dependent on the mevalonate pathway of terpene precursor biosynthesis. 74
Supplemental Figure 2.9 RT-PCR analysis of *ABDS* and *CYP705A1* genes. 76
Supplemental Figure 2.10 HRESIMS analysis and ^{1}H-NMR spectrum of arabidonol. 77
Supplemental Figure 2.11 Full HMBC NMR spectrum of arabidonol. 78
Supplemental Figure 2.12 HMQC NMR spectrum of arabidonol. 79
Supplemental Figure 2.13 NOESY NMR spectrum of arabidonol..... 80
Supplemental Figure 2.14 COSY NMR spectrum of arabidonol. 81
Supplemental Figure 2.15 Structure of arabidonol. 82
Supplemental Figure 2.16 Induced promoter-GUS activity of *CYP705A1* and *ABDS*..... 85

Supplemental Figure 2.17 Confocal microscopy analysis in response to JA treatment in *ProCYP705A1:CYP705A1-eYFP* lines. 86
Supplemental Figure 2.18 Effect of arabidiol, arabidonol and DMNT on the growth of *P. irregulare* 110305. 87
Supplemental Figure 2.19 Molecular Phylogenetic Analysis of *A. thaliana* and *A. lyrata* CYP705 members on the *ABDS* and *THAS* gene clusters 88
Supplemental Figure 2.20 Sequence alignment of active site residues of CYP705A1 to CYP705A5. 89

Supplemental Table 2.1 DMNT Biosynthesis Gene Candidates. 71
Supplemental Table 2.2 Candidate genes co-expressed with *CYP705A1* evaluated based on the ATTED-II database. 75
Supplemental Table 2.3 Proton and carbon chemical shifts for arabidiol and key correlations from NMR spectra. 83
Supplemental Table 2.4 Sequence of primers used in different experiments. 84

Chapter 3

Figure 3.1 The arabidiol degradation pathway. 103
Figure 3.2 Detection of arabidiol-derived compounds in *Arabidopsis* root tissue. 104
Figure 3.3 Detection of arabidiol-derived compounds in Arabidopsis root exudates. 105
Figure 3.4 Arabidonol is converted into several modification products *in planta.* 107
Figure 3.5 Putative pathway for the formation of arabidonol derivatives. 109
Figure 3.6 Arabidonol is converted to acetyl-arabidonol via two intermediates. 111
Figure 3.7 Natural Variation in the Modification of Arabidiol-Derived Compounds Between Different Accessions of *Arabidopsis*. 113
Figure 3.8 Arabidonol is modified differently in *A. thaliana* and *A. lyrata*. 114

Supplemental Figure 3.1 Genes on the *ABDS*/*BARS* cluster are not highly co-regulated under normal developmental condition. 125
Supplemental Figure 3.2 Genes of the *ABDS*/*BARS* cluster are not co-regulated under stress conditions. 126
Supplemental Figure 3.3 Genome evolution analysis of the ABDS/BARS region. 127

1. General Introduction and Overview of Research

Chemical Communication in Plant–Organism Interactions

Plants, as sedentary organisms, have to adjust to the surrounding environment throughout their life cycle. To compensate for their immobility, plants have evolved several mechanisms for interacting with beneficial and pathogenic organisms including the accumulation of diverse arrays of small molecules with specialized functions. Although many of these phytochemicals were not considered essential for plant survival and were referred to as secondary metabolites (Verpoorte and Alfermann, 2000), they contribute to adaptation under strong selective pressure in specific ecological situations, such as the attraction of pollinators or defense against specific herbivores (Pichersky et al., 2006). The ability to synthesize such "specialized metabolites" has evolved in various plant lineages and these compounds are composed of several classes of metabolites including terpenoids, alkaloids, glucosinolates, and phenolics with estimated numbers exceeding 200,000 compounds (Yonekura-Sakakibara and Saito, 2009).

Among specialized metabolites are volatile organic compounds (VOCs) with more than 1700 VOCs identified from 90 different plant families in both angio- and gymnosperms (Knudsen et al., 2006). VOCs are typically lipophilic liquids with high vapor pressures and can easily cross membranes and be diffused into the surrounding environment in the absence of a barrier (Pichersky et al., 2006). They are primarily derived from four major classes of specialized metabolic pathways including phenylpropanoids/benzenoids, fatty acid derivatives, amino acid derivatives and terpenoids (Dudareva et al., 2006). Plants emit VOCs from their leaves, flowers, and fruits into the atmosphere and from their roots into the soil (Figure 1.1). One of the main functions of volatile compounds is to defend plants against pathogens and herbivores through antimicrobial and direct repellent activities (De Moraes et al., 2001; Kessler and Baldwin, 2001; Vancanneyt et al., 2001). Volatiles also function as indirect defense compounds by attracting

natural enemies of attacking herbivores in tritrophic interactions (Drukker et al., 2000; van Loon et al., 2000). By emitting volatiles in response to insect feeding or pathogen infection, plants can also prime neighboring plants to respond faster to future herbivore or pathogen attack (Shulaev et al., 1997; Kessler et al., 2006). Furthermore, volatile compounds emitted from flowers provide a reproductive advantage by attracting pollinators and seed dispersers (Dudareva et al., 2006). Additionally, VOCs such as isoprene have been implicated in the protection of plants against oxidative stress or sunlight-induced rapid heating (Loreto and Velikova, 2001; Sharkey et al., 2008).

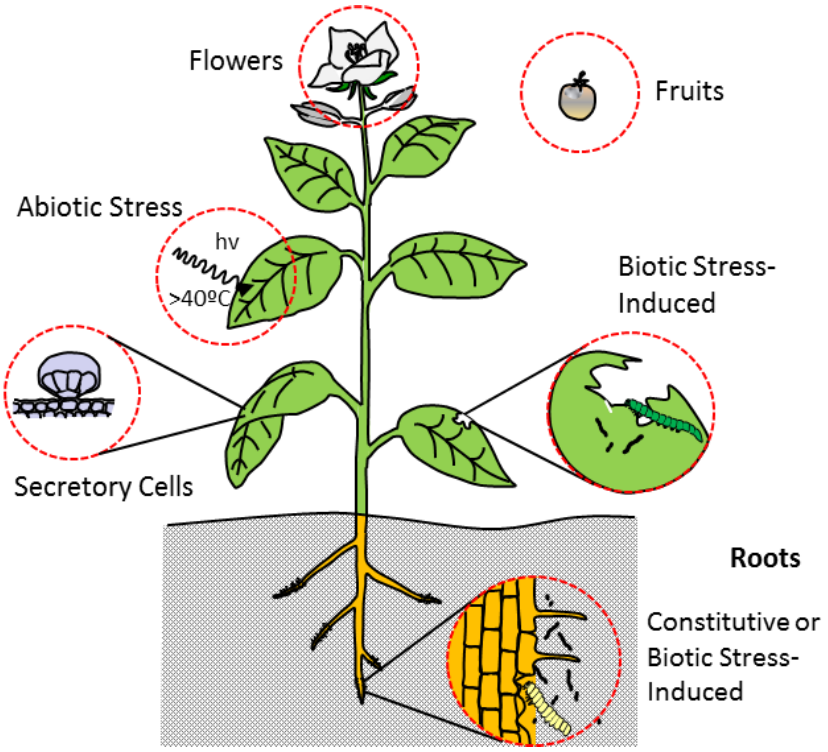

Figure 1.1 Ecological roles of VOCs in plant-environment interactions

Emission of VOCs occurs from aboveground and belowground tissues. VOCs play various roles in plant interaction with different beneficial and pathogenic organisms including pollinators and seed dispersers, and act as antimicrobial or anti-feeding agents. They also play a role in tritrophic interactions. See text for details. Modified from (Tholl, 2006).

The Importance of Volatile Terpenes in Plant-Environment Interaction

Terpenes or terpenoids compose the largest class of plant secondary metabolites with many volatile representatives. Hemiterpenes (C_5), many monoterpenes (C_{10}), sesquiterpenes (C_{15}), homoterpenes (C_{11} and C_{16}), and some diterpenes (C_{20}) have a high vapor pressure allowing their release into the atmosphere. Terpenoids are defined by their carbon backbone consisting of isoprene (2-methylbuta-1-3-diene) units. The generic name "terpene" was originally applied to hydrocarbons found in turpentine, the suffix "ene" indicating the presence of olefinic bonds. Additionally, degradation products of terpenoids in which carbon atoms have been lost through chemical or biochemical processes may contain different numbers of carbon atoms (e.g. C_{11} and C_{16}), but their overall structure indicates their terpenoid origin (Sell, 2003).

Volatile terpenes are often synthesized as constituents of essential oils and stored as liquid in specialized secretory cells and structures (e.g. glandular trichomes and resin ducts), which are frequently found in plant species from the *Coniferae* or *Lamiaceae* family. These structures establish a constitutive chemical defense barrier against herbivores or pathogens. Herbivore contact with plant tissue ruptures the trichomes and results in the release of stored chemicals, leading to plant protection from the attacking herbivore due to toxicity effects of the volatile compounds (Pichersky and Gershenzon, 2002). Additionally, antimicrobial activities of essential oils against animal and plants bacterial pathogens (Dorman and Deans, 2000) are presumably associated with the ability of terpenes to diffuse freely in biological membranes and disrupt the integrity and functionality of membranes (Trombetta et al., 2005).

Although storage of terpene metabolites in specialized structures as essential oils has been implicated in constitutive plant defense, plants have evolved alternative strategies to defend against attacking herbivores or pathogen via localized or systemic *de novo* induction of terpene

metabolites. For example, maize plants release a mixture of volatiles from their leaves including (*E*)-nerolidol, (*E*)-α-bergamotene and (*E*)-β-farnesene upon feeding damage by lepidopteran larvae (van Loon et al., 2000). The majority of these volatiles are emitted only by insect-damaged plants and not by unattacked or artificially damaged plants. The mixture of volatiles released is largely synthesized *de novo* following initial damage by herbivore attack (Pare and Tumlinson, 1997) and can be released from non-damaged plant parts in a systemic response as well (Rose et al., 1996).

In many cases *de novo* plant responses to herbivore attack by emitting volatile terpenes are associated with the attraction of natural enemies of herbivores via tritrophic interactions. For example, lima bean (*Phaseolous lunatus*) plants damaged by the spider mite *Tetranychus urticae*, emit a mixture of monoterpenes, C_{11}- and C_{16}-homoterpenes, and methyl salicylate, which attracts a carnivorous mite, *Phytoseiulus persimilis*, that preys on spider mites (Dicke, 1994). When maize or cotton are attacked by *lepidopteran* larvae, a blend of monoterpenes, sesquiterpenes, homoterpenes and other volatile compounds is released, which attracts parasitic wasps that oviposit on the larvae (Turlings et al., 1995). Additionally *de novo* herbivore-induced volatiles can function as stress signals between neighboring plants. For example, lima bean plants exposed to the terpene volatiles emitted from spider mite (*Tetranychus urticae*) infested neighboring plants show induced defensive gene expression and emission of volatiles and, therefore are primed against the spider mites and are less susceptible (Arimura et al., 2000; Choh et al., 2004).

The induced emission of volatiles is not limited only to aerial parts of plants. Plants also release volatiles from their roots with a chemical and structural diversity comparable to that found in emitted volatiles from aerial plant organs. Similar to aboveground volatile compounds,

root volatiles may contribute to a belowground defense system by acting as antimicrobial or antiherbivore substances, or by attracting enemies of root-feeding herbivores. Infection of *Arabidopsis* roots with either bacterial (*Pseudomonas syringae* strain DC3000) or fungal (*Alternaria brassicola*) pathogens or root-feeding insects (*Diuraphis noxia*) triggers the rapid emission of 1,8-cineole (Steeghs et al., 2004). Previously, the sesquiterpene (*E*)-β-caryophyllene was identified as a first root insect-induced belowground plant signal that strongly attracts the entomopathogenic nematode *Heterorhabditis megidis* under *in situ* laboratory and field conditions (Rasmann et al., 2005). Maize roots released this sesquiterpene in response to feeding by western corn rootworm larvae (*Diabrotica virgifera virgifera*). A five-fold higher nematode infection rate of the larvae was found on a maize variety that produced the signal than on a variety that did not. This finding indicated a communication between plant roots and insect-parasitizing nematodes as the third trophic level in the rhizosphere tritrophic interactions and emphasizes the importance of root emitted volatiles in plant defense belowground.

Distribution and Functions of C_{11}- and C_{16}-Homoterpenes in Land Plants

Homoterpenes are acyclic terpenoid volatiles, found in floral bouquets of night-scented plant species and are also emitted from plants in response to herbivore damage (Bartlet et al., 2004; Bichao et al., 2005). The common C_{11} homo/norterpene 4,8-dimethylnona-1,3,7-triene (DMNT) and the C_{16} homoterpene 4,8,12-trimethyltrideca-1,3,7,11-tetraene (TMTT) are irregular terpenes that are suggested as degradation products of C_{15} and C_{20} terpene precursors, respectively (Boland et al., 1998). To better understand the function and taxonomic distribution of homoterpenes in land plants, we have done a comprehensive survey of the literature on

constitutive and induced emissions of DMNT and TMTT (Tholl et al., 2011) which is summarized in Figure 1.2 and Table 1.1.

Although several terpenes have been found in non-vascular lower plants (such as mosses, liverworts and hornworts) as well as vascular lower plants (pteridophytes) no homoterpene volatile has been reported from these plants. Also, homoterpenes have been rarely reported in gymnosperms. For example, DMNT was found in volatile blends emitted from needles of masson pine (*Pinus massoniana*) upon mechanical damage or insect feeding by larvae of the masson pine moth (*Dendrolimus punctatus*) (Su et al., 2009). Detection of homoterpenes from gymnosperms suggests that their biosynthesis has emerged most likely during the evolution of gymnosperms.

Angiosperms show widespread emission of DMNT and TMTT homoterpenes from numerous plant species. In primitive angiosperms such as species in the *Magnoliaceae* family both homoterpenes are emitted as floral volatiles (Arimura et al., 2008). In many families of monocots and dicots, DMNT and TMTT homoterpenes have been reported as floral volatiles. Indeed, homoterpenes are part the of floral odors contributing to the so-called "white floral image" of night-scented flowers (Kaiser, 1991) in species of *Orchidaceae*, *Magnoliaceae*, and *Liliaceae* and presumably play a role in attracting pollinators.

Interestingly, in several studies homoterpenes have been reported to play a role as insect attractants (kairomones) (Supplemental Table 1.1). DMNT emitted from flowers of the crucifer *Iberis amara* (candytuft) as part of the floral volatile blend has been shown to attract the pollen beetle *Meligethes aeneus* (van Schie et al., 2007). Other examples of homoterpene effects as kairomones include the attraction of strawberry blossom weevil, *Anthonomus rubi* (Aharoni et

al., 2004), the apple maggot fly, *Rhagoletis pomonella* (Nagegowda et al., 2008), and the grapevine moth *Lobesia botrana* (Aharoni et al., 2003).

Plant species, which emit homoterpenes constitutively from their flowers, can also release these compounds in response to herbivore attack from their leaves (Arimura et al., 2008). Interestingly, DMNT and TMTT are emitted from herbivore-damaged foliage of a wide variety of plant species including important crops such as maize, lima bean, tomato, rice, and cucumber (Supplemental Table 1.1). There is growing evidence showing that the increased emission of TMTT and DMNT is likely to play a role in attracting natural enemies of arthropod herbivores (Kant et al., 2004; Kappers et al., 2005). This function is not only limited to herbivore feeding damage but is also implicated in the attraction of egg parasitoids. As an interesting example, egg deposition by the elm leaf beetle *Xanthogaleruca luteola* on leaves of the European elm *Ulmus minor* leads to an induced production of a volatile mixture including DMNT, and subsequent attraction of the egg parasitoid *Oomyzus gallerucae* (Aharoni et al., 2003).

Volatiles released upon herbivore attack can induce or prime defense responses in neighboring plants or different parts within the same plant (Kappers et al., 2005). Interestingly, homoterpene emission upon spider mite attack in lima bean leaves resulted in the induced expression of defense genes such as lipoxygenase (*LOX*) and pathogen-related (PR) protein *PR-2* (β-1,3-glucanase) in the undamaged control plants (Schnee et al., 2002). In addition to this air-borne effect, homoterpenes could possibly function as a stress-induced short range signal which diffuses into adjacent cell layers upon herbivore attack.

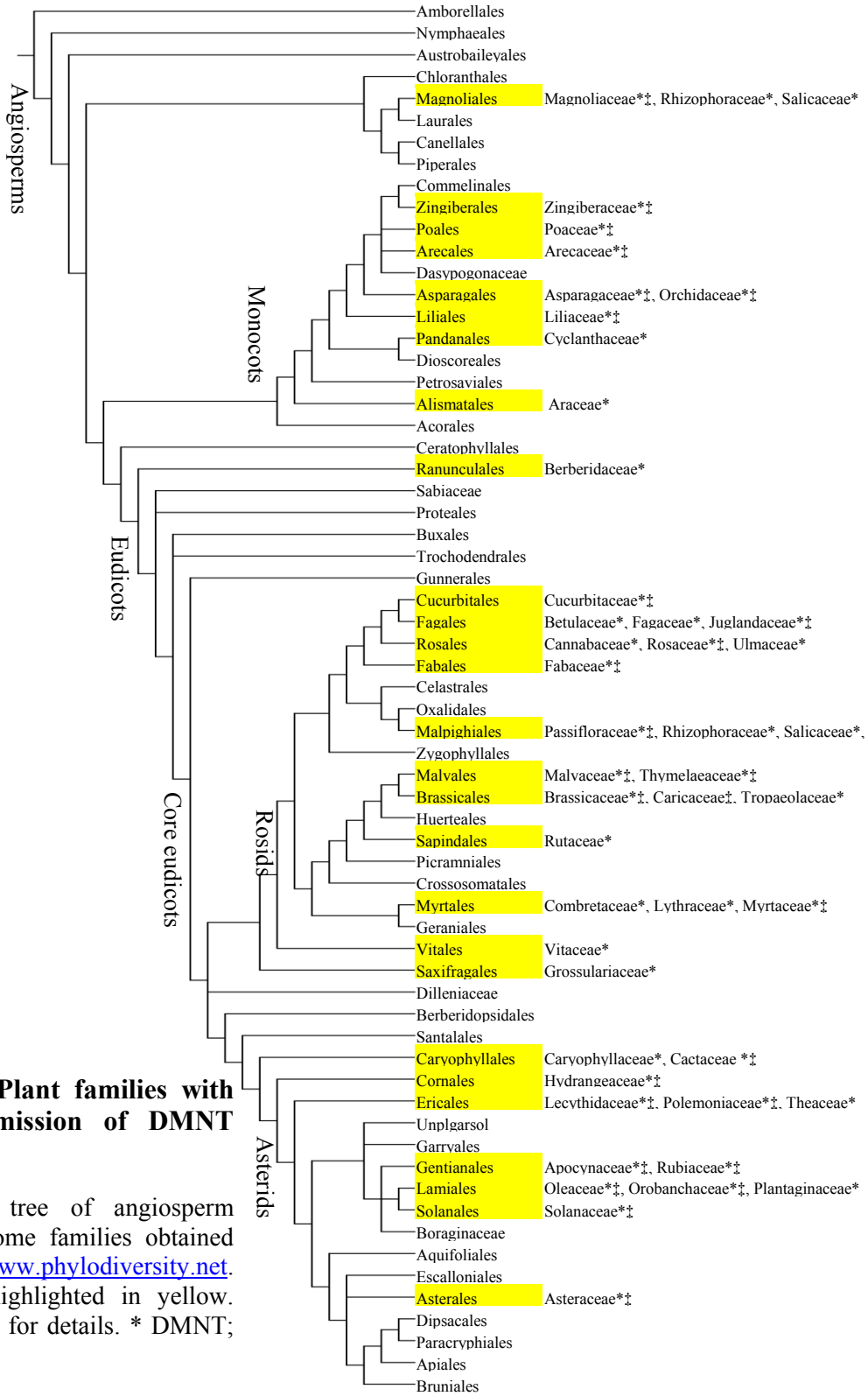

Figure 1.2 Plant families with reported emission of DMNT and TMTT.

Phylogenetic tree of angiosperm orders and some families obtained from http://www.phylodiversity.net. Orders are highlighted in yellow. See Table 1.1 for details. * DMNT; ‡ TMTT.

Table 1.1 Detailed list of DMNT- and TMTT-emitting gymnosperm and angiosperm families

Herbivores and other conditions causing induced homoterpene emissions are listed. No entries were made for constitutive emissions. * DMNT, ‡ TMTT. References are given below if not listed in the text.

Order	Family	Species	Homo-terpene	Tissue	Condition	Ref
Coniferales	*Pinaceae*	*Pinus massoniana*	*	Needle	Mechanical damage and *Dendrolimus punctatus*	(Su et al., 2009)
Magnoliales	*Magnoliaceae*	*Magnolia grandiflora*	*	Leaf and flower	Mechanical damage	(Azuma et al., 1997)
	Magnoliaceae	*Magnolia liliiflora*	* ‡	Flower		(Kaiser, 1991)
	Magnoliaceae	*Liriodendron tulipifera*	* ‡	Flower		(Azuma et al., 1997)
Zingiberales	*Zingiberaceae*	*Elettaria cardamomum*	* ‡	Seed		(Maurer et al., 1986)
	Zingiberaceae	*Hedychium coronarium*	* ‡	Flower		(Knudsen et al., 2006)
Poales	*Poaceae*	*Zea mays*	* ‡	Seedling	*Spodoptera exigua* and *Spodoptera littoralis*	(Turlings et al., 1991)
	Poaceae	*Oryza sativa*	* ‡	Leaf	Jasmonic acid	(Lou et al., 2006)
	Poaceae	*Triticum aestivum*	* ‡	Leaf	*Heliothis virescens* and *Mayetiola destructor*	(Tooker and De Moraes, 2007)
Arecales	*Arecaceae*	*Phytelephas seemannii*	* ‡	Flower		(Knudsen et al., 2006)
Asparagales	*Asparagaceae*	*Yucca filamentosa*	*	Flower		(Svensson et al., 2005)
	Asparagaceae	*Dracaena fragrans*	* ‡	Flower		(Kaiser, 1991)
	Orchidaceae	*Aerangis friesiorum*	* ‡	Flower		(Kaiser, 1991)
Liliales	*Liliaceae*	*Lilium longiflorum*	* ‡	Flower		(Kaiser, 1991)
Pandanales	*Cyclanthaceae*	*Cyclanthus bipartitus*	*	Flower		(Schultz et al., 1999)
Alismatales	*Araceae*	*Spathiphyllum wallisii*	*	Leaf		(Donath and Boland, 1995)
Ranunculales	*Berberidaceae*	*Berberis vulgaris*	*	Flower		(Knudsen et al., 2006)
Cucurbitales	*Cucurbitaceae*	*Cucumis sativus*	* ‡	Leaf	*Tetranychus urticae*	(Takabayashi et al., 1994b)
Fagales	*Betulaceae*	*Betula pubescens*	*	Leaf	*Epirrita autumnata*	(Mantyla et al., 2008)
	Fagaceae	*Fagus sylvatica*	*	Leaf	*Phyllaphis fagi*	(Joo et al., 2010)
	Fagaceae	*Quercus ilex*	*	Leaf	*Lymantria dispar*	(Staudt and Lhoutellier, 2007)
	Juglandaceae	*Juglans regia*	* ‡	Green walnut husk	*Cydia pomonella*	(Buttery et al., 2000)
Rosales	*Cannabaceae*	*Humulus lupulus*	*	Leaf		(Donath and Boland, 1995)
	Rosaceae	*Malus domestica*	* ‡	Leaf	*Tetranychus urticae*	(Takabayashi et al., 1994a) , (Bengtsson et al., 2001)
	Rosaceae	*Crataegus monogyna*	*	Fruit		(Nojima et al., 2003)
	Rosaceae	*Fragaria x ananassa*	*	Flower (blossom)	*Anthonomus rubi*	(Bichao et al., 2005)

	Ulmaceae	*Ulmus minor*	*		Leaf	*Xanthogaleruca luteola*, egg deposition and herbivory	(Wegener et al., 2001)
Fabales	*Fabaceae*	*Medicago truncatula*	*	‡	Leaf	*Spodoptera exigua*	(Arimura et al., 2008)
	Fabaceae	*Phaseolus lunatus*	*	‡	Leaf	*Tetranychus urticae*	(Takabayashi et al., 1991) (Dicke et al., 1990)
	Fabaceae	*Phaseolus lunatus*	*	‡	Leaf	O3	(Vuorinen et al., 2004)
	Fabaceae	*Trifolium pratense*	*		Leaf	*Spodoptera littoralis*	(Kigathi et al., 2009)
	Fabaceae	*Lotus japonicus*	*		Leaf	*Tetranychus urticae*	(Ozawa et al., 2000)
	Fabaceae	*Phaseolus vulgaris*	*	‡	Leaf	*Tetranychus urticae*	(Maeda et al., 1998)
	Fabaceae	*Medicago sativa*	*	‡	Foliage	*Lygus hesperus*	(Blackmer et al., 2004)
	Fabaceae	*Vigna unguiculata*	*	‡	Leaf	*Spodoptera frugiperda*	(Schmelz et al., 2006)
	Fabaceae	*Robinia pseudoacacia*	*	‡	Flower		(Kaiser, 1991)
	Fabaceae	*Vicia faba*		‡	Leaf	Feeding and egg deposition by *Nezara viridula*	(Colazza et al., 2004)
Malpighiales	*Passifloraceae*	*Passiflora adenopoda*	*	‡	Flower		(Knudsen et al., 2006)
	Rhizophoraceae	*Bruguiera gymnorrhiza*	*		Flower		(Knudsen et al., 2006)
	Salicaceae	*Populus trichocarpa*	*		Leaf	*Malacosoma disstria*	(Arimura et al., 2004)
Malvales	*Malvaceae*	*Gossypium hirsutum*	*		Seedling	*Helicoverpa zea*	(Mccall et al., 1994)
	Malvaceae	*Gossypium hirsutum*	*	‡	Leaves	*Spodoptera exigua*	(Rose et al., 1996)
	Malvaceae	*Gossypium hirsutum*	*	‡	Flower buds (squares)	*Helicoverpa zea*	(Rose et al., 1996)
	Malvaceae	*Gossypium herbaceum*	*		Blossom, Leaf	Unknown	(Donath and Boland, 1995)
	Thymelaeaceae	*Daphne cneorum*	*	‡	Flower		(Kaiser, 1991)
Brassicales	*Brassicaceae*	*Arabidopsis thaliana*	*	‡	Root	*Pythium irregulare*	(Unpublished data)
	Brassicaceae	*Arabidopsis thaliana*	*	‡	Leaf	*Several herbivores*	(Herde et al., 2008)
	Brassicaceae	*Brassica oleracea*	*	‡	Leaf	*Pieris rapae* and *Pieris brassicae*	(Geervliet et al., 1997)
	Brassicaceae	*Brassica rapa*	*		Leaf	Methyl jasmonate	(Loivamaki et al., 2004)
	Brassicaceae	*Iberis amara*	*		Flower		(Bartlet et al., 2004)
	Caricaceae	*Carica papaya*		‡	Flower		(Knudsen et al., 2006)
	Tropaeolaceae	*Tropaeolum majus*	*		Leaf	*Pieris rapae*	(Geervliet et al., 1997)
Sapindales	*Rutaceae*	*Citrus madurensis*	*		Flower		(Knudsen et al., 2006)
Myrtales	*Combretaceae*	*Lumnitzera racemosa*	*		Flower		(Knudsen et al., 2006)
	Lythraceae	*Pemphis acidula*	*		buds and pedicels		(Knudsen et al., 2006)
	Myrtaceae	*Eucalyptus dunnii*	*	‡	Leaf	Mechanical damage	(Zini et al., 2003)
Vitales	*Vitaceae*	*Vitis riparia*	*		Leaf and fruit		(Tasin et al., 2005) (Tasin et al., 2006)
Saxifragales	*Grossulariaceae*	*Ribes nigrum*	*		leaves	Unknown	(Griffiths et al., 1999)
Caryophyllales	*Caryophyllaceae*	*Agrostemma githago*	*		Flower		(Knudsen et al., 2006)
	Portulacacineae	*Selenicereus hamatus*	*	‡	Flower		(Kaiser, 1991)
Cornales	*Hydrangeaceae*	*Philadelphus coronarius*	*	‡	Flower		(Kaiser, 1991)

Ericales	*Lecythidaceae*	*Couroupita guianensis*	*	‡	Flower		(Knudsen et al., 2006)
	Polemoniaceae	*Phlox drummondii*	*	‡	Flower		(Knudsen et al., 2006)
	Theaceae	*Camellia sinensis*	*		Leaf	*Tetranychus kanzawai*	(Ishiwari et al., 2007)
Gentianales	*Apocynaceae*	*Trachelospermum jasminoides*	*	‡	Flower		(Kaiser, 1991)
	Apocynaceae	*Plumeria alba*	*	‡	Flower		(Kaiser, 1991)
	Apocynaceae	*Hoya carnosa*	*	‡	Flower		(Kaiser, 1991)
	Rubiaceae	*Warszewiczia coccinea*	*	‡	Flower		(Knudsen et al., 2006)
Lamiales	*Oleaceae*	*Osmanthus fragrans*	*	‡	Flower		(Kaiser, 1991)
	Orobanchaceae	*Escobedia grandiflora*	*	‡	Flower		(Knudsen et al., 2006)
	Plantaginaceae	*Plantago lanceolata*	*		Leaf	*Spodoptera littoralis*	(Fontana et al., 2009)
	Scrophulariaceae	*Buddleja davidii*	*		Flower		(Knudsen et al., 2006)
	Verbenaceae	*Lantana camara*	*	‡	Flower		(Knudsen et al., 2006)
Solanales	*Solanaceae*	*Lycopersicon esculentum*	*	‡	Leaf	*Tetranychus urticae*	(Kant et al., 2004)
	Solanaceae	*Solanum tuberosum*	*	‡	Leaf	*Leptinotarsa decemlineata*	(Bolter et al., 1997)
Asterales	*Asteraceae*	*Gerbera jamesonii*	*		Leaf	*Tetranychus urticae*	(Gols et al., 1999)
	Asteraceae	*Gerbera jamesonii*	*		Leaf		(Donath and Boland, 1995)
	Asteraceae	*Solidago altissima*	*	‡	Leaf	*Heliothis virescens*	(Tooker et al., 2008)

In summary, homoterpenes can serve various functions in plants. These functions are primarily associated with enhancing plant defense response directly or indirectly as part of a volatile blend emitted upon herbivore attack. In addition homoterpenes have been exploited by herbivores to localize a suitable host as well. However, no specific insect anti-feeding or antimicrobial activities have been reported for homoterpenes.

Biosynthesis of Regular Terpenes and Irregular Homoterpenes

Although terpenes are extraordinarily diverse, they all originate from the condensation of the universal five-carbon precursors, isopentenyl diphosphate (IPP) and dimethylallyl diphosphate (DMAPP). In higher plants, two independent pathways that are located in separate intracellular compartments are involved in the biosynthesis of IPP and DMAPP (Figure1.3). In

the cytosol, IPP is derived from the classic mevalonic acid (MVA) pathway that starts from the condensation of three acetyl Coenzyme A (acetyl-CoA) molecules to form the C_6 compound 3-hydroxy-3-methylglutaryl CoA (HMG-CoA), which in turn is reduced to mevalonic acid, phosphorylated twice and subsequently decarboxylated to yield C_5-IPP. IPP is then converted to DMAPP via an IPP isomerase enzymatic activity. In plastids, IPP is formed from pyruvate and glyceraldehyde 3-phosphate via the methylerythritol phosphate (MEP or non-mevalonate) pathway. A C_2-unit derived from pyruvate is combined with glyceraldehyde-3-phosphate to form 1-deoxy-D-xylulose-5-phosphate which successively is transformed into IPP and DMAPP by seven enzymatic steps (Gershenzon and Kreis, 1999; Hunter, 2007).

Initial research indicated that cytosolic IPP serves as a precursor of farnesyl diphosphate (FPP, C_{15}) which is the primary substrate for sesquiterpene and triterpene formation, whereas plastidial IPP and DMAPP are converted into geranyl diphosphate (GPP, C_{10}) and geranylgeranyl diphosphate (GGPP, C_{20}), the substrates in monoterpene and diterpene biosynthesis. Although the subcellular compartmentation of MVA and MEP pathways allows them to operate independently, metabolic "crosstalk" between these two pathways mediated by specific metabolite transporters was discovered (Bick and Lange, 2003), with a preferential transport of IPP from plastids to the cytosol (Laule et al., 2003; Dudareva et al., 2005). Although cross talk between two different IPP biosynthetic pathways has been documented, the relative contribution of each pathway to the biosynthesis of various classes of terpenes remains uncertain.

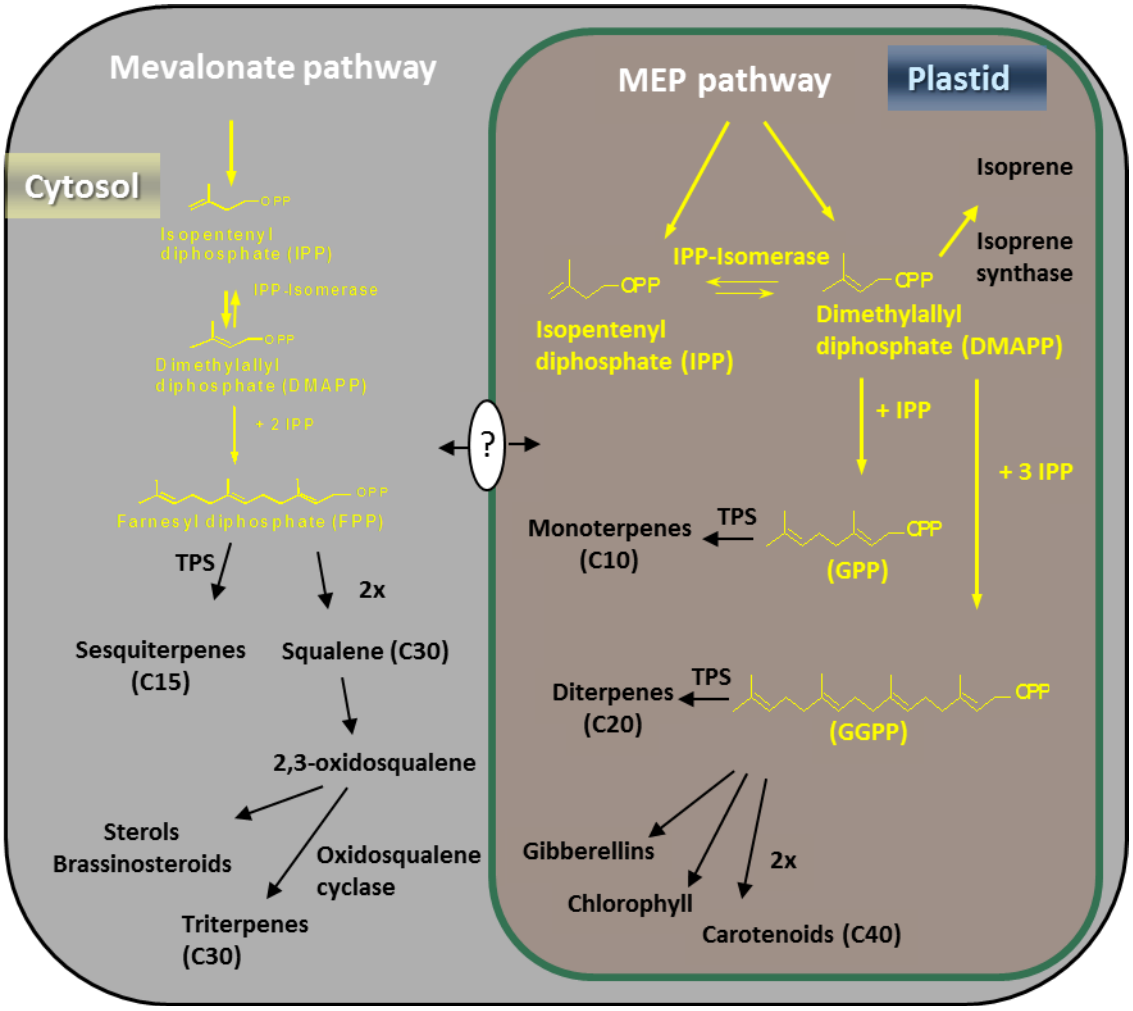

Figure 1.3 Biosynthetic pathways of terpenes in plants.

IPP, isopentenyl diphosphate; DMAPP, dimethylallyl diphosphate; GPP, geranyldiphosphate; FPP, farnesyl diphosphate and GGPP, geranylgeranyl diphosphate. TPS, terpene synthase,

The next step in the biosynthesis of terpenes is catalyzed by terpene synthases or terpene cyclases which convert the prenyl diphosphate substrates (FPP, GPP, and GGPP) into different classes of terpene compounds with higher molecular weight terpenes including triterpenes (C30), Carotenoids (C40), chlorophyll, sterols and brassinosteroids. Terpene synthases are dependent on a divalent metal ion cofactor such as Mg^{2+} for catalysis. The reaction of most terpene synthases starts with the cleavage of the diphosphate moiety leading to the formation of a

carbocation intermediate which undergoes a series of structural rearrangements that may include hydride shifts, alkyl shifts, deprotonation, reprotonation, and additional cyclizations prior to a deprotonation reaction or capture of a water molecule as a final step. Alternatively, ionization of prenyl diphosphates can also occur by the protonation of the double bond at the opposite end of the molecule from the diphosphate moiety. This mechanism is characteristic for several diterpene synthases, including the enzymes synthesizing *ent*-copalyl diphosphate (CPP) a precursor in gibberellin formation (Gershenzon and Kreis, 1999; Tholl, 2006).

Several studies using stable-isotope precursors have been performed to elucidate the biosynthesis of the volatile homo-/norterpenes DMNT and TMTT. Early experiments in cotton showed that DMNT is synthesized *de novo* in response to herbivore attack, since labeled DMNT was detected after [^{13}C]CO_2 pulse-labeling experiments (Pare and Tumlinson, 1997a). Using deuterium labeled precursors, it was demonstrated that DMNT is derived from the sesquiterpene (*E*)-nerolidol (Donath and Boland, 1994). Later on, nerolidol synthase enzyme activities and corresponding genes were identified in different species such as cucumber, maize and lima bean (Bouwmeester et al., 1999, Degenhardt and Gershenzon, 2000). Boland and coworkers reported that (*E*)-nerolidol undergoes a C–C oxidative bond cleavage reaction, which proceeds by *syn*-elimination of the polar head together with the allylic hydrogen atom at the β-carbon atom (β-cleavage) (Boland et al., 1998). More recently, is has been shown that the structural analog of (*E*)-nerolidol, (*E*,*E*)-geranyllinalool, undergoes oxidative degradation to produce TMTT, the structural analog of DMNT in *Arabidopsis* (Lee et al., 2010). However, because of the absence of endogenous (*E*)-nerolidol synthase activity in *Arabidopsis* leaf and root tissue (Vaughan et al., 2013), we concluded that DMNT in *Arabidopsis* roots is not made from the C_{15} precursor (*E*)-

nerolidol. Elucidation of the DMNT biosynthetic pathway will be important for a complete understanding of the ecological role of DMNT in plants.

Arabidopsis as a Model for the Formation of Belowground Volatile Terpenes

Arabidopsis thaliana has been shown to be a promising model plant for studying biosynthesis, regulation and function of terpene secondary metabolites in plant-environment interaction (Aharoni et al., 2003; Chen et al., 2003). The *Arabidopsis* genome contains 32 genes that are annotated as terpene synthase genes. Recent investigations by the Tholl laboratory on the biosynthesis of volatile terpenes in *Arabidopsis* flowers led to the identification of two monoterpene synthases and two sesquiterpene synthases, which are responsible for the formation of the *Arabidopsis* floral volatile blend (Tholl et al., 2005). In *Arabidopsis* leaves, the emission of volatile terpenes such as myrcene, β-ocimene, (*E,E*)-α-farnesene and the C_{16}-homoterpene TMTT is induced in response to herbivore feeding (Tholl and Lee, 2011). The induced volatile blend has been shown to attract the parasitic wasp *Cotesia rubecula* leading to increased plant fitness (Van Poecke et al., 2001). Similar to aboveground volatile compounds, root volatiles may contribute to a belowground defense system by acting as antimicrobial or anti-herbivore substances, or by attracting natural enemies of root-feeding herbivores. But to date only few studies have focused on the biochemical and molecular analysis of root volatile terpenes. Infection of *Arabidopsis* roots with either bacterial or fungal pathogens or root-feeding insects triggers the rapid emission of 1,8-cineole (Steeghs et al., 2004). It has been shown that a root-specific monoterpene synthase gene is responsible for the formation of 1,8-cineole in *Arabidopsis* roots (Chen et al., 2004). Additionally a recently characterized diterpene volatile

from Arabidopsis roots has been suggested as a defense metabolite against root herbivory by the larvae of fungus gnats (*Bradysia spp*) (Vaughan et al., 2013). *Arabidopsis* has been selected as a model for studying the formation and function of root volatile terpenes, since 14 terpene synthase genes are expressed in the *Arabidopsis* root.

We have discovered for the first time that sterile and non-sterile cultures of *Arabidopsis* roots emit the C_{11}-homoterpene DMNT in response to infection with root-rot pathogen (*Pythium irregulare*) suggesting a possible new role for this homoterpene volatile as an antimicrobial factor. Although DMNT is known as floral and insect-induced volatile terpene with suggested functions in mediating interactions with arthropod insects, its presence has not been reported in plant roots before. DMNT emission is also induced upon treatment with the defense hormone jasmonic acid as the main volatile induced in *Arabidopsis* roots. The emission of DMNT from Arabidopsis roots in not only induced by JA treatment but also to some extent by root-feeding larvae of the flea beetle *Phyllotreta spp*. (Dr. Stefan Schütz, Georg-August University, Göttingen, Germany Lab), suggesting that insect-feeding can induce JA-mediated production of volatile terpene from *Arabidopsis* roots. A detailed study of the role of DMNT in plant organism interactions requires elucidation of the biosynthetic pathway and functional characterization of genes involved in its biosynthesis.

Overview of Research

The induced formation of volatile terpenes has been investigated as a defense mechanism in plant-insect and plant-pathogen interactions. Research on volatile terpenes has focused primarily on aerial parts of plants, and there are limited numbers of studies concerning the role of volatile emissions from roots. Recent studies in the Tholl lab have suggested that volatile

terpenes can function as anti-feedants against herbivores of *Arabidopsis* roots (Vaughan et al., 2013). Also here we show that volatile DMNT could be induced in response to pathogens. Therefore, we hypothesized similar defensive functions for pathogen-induced volatiles in the rhizosphere. Here we present our study on the identification of DMNT biosynthetic genes in *Arabidopsis* roots and evaluate the defensive activities of DMNT by using bioassays with the root pathogen *Pythium irregulare*. Our experimental work revealed a DMNT biosynthetic pathway via the degradation of a triterpene precursor resulting in the production of DMNT and a non-volatile breakdown compound, which is further modified *in planta*. We performed structural studies of triterpene degradation products in roots and did preliminary studies on the identification of enzymatic activities associated with their biosynthesis.

The specific objectives of this study were to:

I. Identify DMNT biosynthetic genes in *Arabidopsis* roots and understand the role of DMNT in the interaction of *Arabidopsis* with the root pathogen *Pythium irregulare*

II. Identify downstream derivatives and putative enzymatic steps in the DMNT producing, triterpene-specific catabolic pathway

Chapter II presents the biochemical and functional characterization of the DMNT biosynthetic pathway in *Arabidopsis*. Experimental evidence based on genetic analysis and gene expression experiments is provided showing that DMNT is biosynthesized by a so far unknown pathway via the oxidative degradation of the triterpene alcohol, arabidiol, into DMNT and a C_{19} ketone product. We show that the reaction is catalyzed by the crucifer-specific cytochrome P450 monooxygenase CYP705A1, which clusters and is co-regulated with the gene encoding an

arabidiol synthase. Additionally, we evaluate the biological activity of DMNT against root pathogen *Pythium* using oospore germination and root infection assays. In summary, our results suggest that DMNT contributes to defense in *Arabidopsis* roots.

Chapter III presents a study on the "non-volatile" branch of the arabidiol catabolic pathway by identifying derivatives of the C_{19} ketone breakdown product of arabidiol. We provide evidence for the detection of these metabolites from root tissue and from root exudates and suggest a pathway for their formation based on NMR analysis and precursor feeding experiments. Preliminary experimental results using genetic and biochemical approaches for identifying genes involved in the modification steps are also presented.

Chapter IV presents the final discussion and future perspectives of the described research.

Literature Cited

Aharoni, A., Verstappen, F.W., Schwab, W., Giri, A.P., and Bouwmeester, H.J. (2004). Gain and loss of fruit flavor compounds produced by wild and cultivated strawberry species. Abstracts of Papers of the American Chemical Society **228,** U51-U51.

Aharoni, A., Giri, A.P., Deuerlein, S., Griepink, F., de Kogel, W.J., Verstappen, F.W.A., Verhoeven, H.A., Jongsma, M.A., Schwab, W., and Bouwmeester, H.J. (2003). Terpenoid metabolism in wild-type and transgenic Arabidopsis plants. Plant Cell **15,** 2866-2884.

Arimura, G., Huber, D.P.W., and Bohlmann, J. (2004). Forest tent caterpillars (Malacosoma disstria) induce local and systemic diurnal emissions of terpenoid volatiles in hybrid poplar (Populus trichocarpa x deltoides): cDNA cloning, functional characterization, and patterns of gene expression of (-)-germacrene D synthase, PtdTPS1. Plant J **37,** 603-616.

Arimura, G., Ozawa, R., Shimoda, T., Nishioka, T., Boland, W., and Takabayashi, J. (2000). Herbivory-induced volatiles elicit defence genes in lima bean leaves. Nature **406,** 512-515.

Arimura, G.I., Garms, S., Maffei, M., Bossi, S., Schulze, B., Leitner, M., Mithoefer, A., and Boland, W. (2008). Herbivore-induced terpenoid emission in Medicago truncatula: concerted action of jasmonate, ethylene and calcium signaling. Planta **227,** 453-464.

Azuma, H., Thien, L.B., Toyota, M., Asakawa, Y., and Kawano, S. (1997). Distribution and differential expression of (E)-4,8-dimethyl-1,3,7-nonatriene in leaf and floral volatiles of Magnolia and Liriodendron taxa. J Chem Ecol **23,** 2467-2478.

Bartlet, E., Blight, M.M., Pickett, J.A., Smart, L.E., Turner, G., and Woodcock, C.M. (2004). Orientation and feeding responses of the pollen beetle, Meligethes aeneus, to candytuft, Iberis amara. J Chem Ecol **30,** 913-925.

Bengtsson, M., Backman, A.C., Liblikas, I., Ramirez, M.I., Borg-Karlson, A.K., Ansebo, L., Anderson, P., Lofqvist, J., and Witzgall, P. (2001). Plant odor analysis of apple: antennal response of codling moth females to apple volatiles during phenological development. J Agr Food Chem **49,** 3736-3741.

Bichao, H., Borg-Karlson, A.K., Araujo, J., and Mustaparta, H. (2005). Five types of olfactory receptor neurons in the strawberry blossom weevil Anthonomus rubi: Selective responses to inducible host-plant volatiles. Chemical Senses **30,** 153-170.

Bick, J.A., and Lange, B.M. (2003). Metabolic cross talk between cytosolic and plastidial pathways of isoprenoid biosynthesis: unidirectional transport of intermediates across the chloroplast envelope membrane. Archives of Biochemistry and Biophysics **415,** 146-154.

Blackmer, J.L., Rodriguez-Saona, C., Byers, J.A., Shope, K.L., and Smith, J.P. (2004). Behavioral response of Lygus hesperus to conspecifics and headspace volatiles of alfalfa in a Y-tube olfactometer. J Chem Ecol **30,** 1547-1564.

Boland, W., Gabler, A., Gilbert, M., and Feng, Z.F. (1998). Biosynthesis of C-11 and C-16 homoterpenes in higher plants; Stereochemistry of the C-C-bond cleavage reaction. Tetrahedron **54,** 14725-14736.

Bolter, C.J., Dicke, M., vanLoon, J.J.A., Visser, J.H., and Posthumus, M.A. (1997). Attraction of Colorado potato beetle to herbivore-damaged plants during herbivory and after its termination. J Chem Ecol **23,** 1003-1023.

Buttery, R.G., Light, D.M., Nam, Y., Merrill, G.B., and Roitman, J.N. (2000). Volatile components of green walnut husks. J Agr Food Chem **48,** 2858-2861.

Chen, F., Tholl, D., D'Auria, J.C., Farooq, A., Pichersky, E., and Gershenzon, J. (2003). Biosynthesis and emission of terpenoid volatiles from Arabidopsis flowers. Plant Cell **15,** 481-494.

Chen, F., Ro, D.K., Petri, J., Gershenzon, J., Bohlmann, J., Pichersky, E., and Tholl, D. (2004). Characterization of a root-specific Arabidopsis terpene synthase responsible for the formation of the volatile monoterpene 1,8-cineole. Plant Physiology **135,** 1956-1966.

Choh, Y., Shimoda, T., Ozawa, R., Dicke, M., and Takabayashi, J. (2004). Exposure of lima bean leaves to volatiles from herbivore-induced conspecific plants results in emission of carnivore attractants: Active or passive process? Journal of Chemical Ecology **30,** 1305-1317.

Colazza, S., McElfresh, J.S., and Millar, J.G. (2004). Identification of volatile synomones, induced by Nezara viridula feeding and oviposition on bean spp., that attract the egg parasitoid Trissolcus basalis. J Chem Ecol **30,** 945-964.

De Moraes, C.M., Mescher, M.C., and Tumlinson, J.H. (2001). Caterpillar-induced nocturnal plant volatiles repel conspecific females. Nature **410,** 577-580.

Dicke, M. (1994). Local and Systemic Production of Volatile Herbivore-Induced Terpenoids - Their Role in Plant-Carnivore Mutualism. Journal of Plant Physiology **143,** 465-472.

Dicke, M., Sabelis, M.W., Takabayashi, J., Bruin, J., and Posthumus, M.A. (1990). Plant strategies of manipulating predator-prey interactions through allelochemicals - prospects for application in pest-control. J Chem Ecol **16,** 3091-3118.

Donath, J., and Boland, W. (1995). Biosynthesis of acyclic homoterpenes - enzyme selectivity and absolute-configuration of the nerolidol precursor. Phytochemistry **39,** 785-790.

Dorman, H.J., and Deans, S.G. (2000). Antimicrobial agents from plants: antibacterial activity of plant volatile oils. Journal of applied microbiology **88,** 308-316.

Drukker, B., Bruin, J., Jacobs, G., Kroon, A., and Sabelis, M.W. (2000). How predatory mites learn to cope with variability in volatile plant signals in the environment of their herbivorous prey. Experimental and Applied Acarology **24,** 881-895.

Dudareva, N., Negre, F., Nagegowda, D.A., and Orlova, I. (2006). Plant volatiles: Recent advances and future perspectives. Critical Reviews in Plant Sciences **25,** 417-440.

Dudareva, N., Andersson, S., Orlova, I., Gatto, N., Reichelt, M., Rhodes, D., Boland, W., and Gershenzon, J. (2005). The nonmevalonate pathway supports both monoterpene and sesquiterpene formation in snapdragon flowers. Proceedings of the National Academy of Sciences of the United States of America **102,** 933-938.

Fontana, A., Reichelt, M., Hempel, S., Gershenzon, J., and Unsicker, S.B. (2009). The effects of arbuscular mycorrhizal fungi on direct and indirect defense metabolites of Plantago lanceolata L. J Chem Ecol **35,** 833-843.

Geervliet, J.B.F., Posthumus, M.A., Vet, L.E.M., and Dicke, M. (1997). Comparative analysis of headspace volatiles from different caterpillar-infested or uninfested food plants of Pieris species. J Chem Ecol **23,** 2935-2954.

Gershenzon, J., and Kreis, W. (1999). Biochemistry of terpenoids: monoterpenes, sesquiterpens, diterpenes, sterols, cardiac glycosides and steroid saponins. In M. Wink, ed, Biochemistry of Plant Secondary Metabolism. Annual Plant Reviews **2,** 222-249.

Gols, R., Posthumus, M.A., and Dicke, M. (1999). Jasmonic acid induces the production of gerbera volatiles that attract the biological control agent Phytoseiulus persimilis. Entomol Exp Appl **93,** 77-86.

Griffiths, D.W., Robertson, G.W., Birch, A.N.E., and Brennan, R.M. (1999). Evaluation of thermal desorption and solvent elution combined with polymer entrainment for the analysis of volatiles released by leaves from midge (Dasineura tetensi) resistant and susceptible blackcurrant (Ribes nigrum L.) cultivars. Phytochem Analysis **10,** 328-334.

Herde, M., Gartner, K., Kollner, T.G., Fode, B., Boland, W., Gershenzon, J., Gatz, C., and Tholl, D. (2008). Identification and regulation of TPS04/GES, an Arabidopsis geranyllinalool synthase catalyzing the first step in the formation of the insect-induced volatile C16-homoterpene TMTT. Plant Cell **20,** 1152-1168.

Hunter, W.N. (2007). The Non-mevalonate Pathway of Isoprenoid Precursor Biosynthesis. J. Biol. Chem. **282,** 21573-21577.

Ishiwari, H., Suzuki, T., and Maeda, T. (2007). Essential compounds in herbivore-induced plant volatiles that attract the predatory mite Neoseiulus womersleyi. J Chem Ecol **33,** 1670-1681.

Joo, E., Van Langenhove, H., Simpraga, M., Steppe, K., Amelynck, C., Schoon, N., Muller, J.F., and Dewulf, J. (2010). Variation in biogenic volatile organic compound emission pattern of Fagus sylvatica L. due to aphid infection. Atmos Environ **44,** 227-234.

Kaiser, R. (1991). Trapping, investigation and reconstitution of flower scents. (Essex, UK: Elsevier Science Publishers).

Kant, M.R., Ament, K., Sabelis, M.W., Haring, M.A., and Schuurink, R.C. (2004). Differential timing of spider mite-induced direct and indirect defenses in tomato plants. Plant Physiology **135,** 483-495.

Kappers, I.F., Aharoni, A., van Herpen, T.W.J.M., Luckerhoff, L.L.P., Dicke, M., and Bouwmeester, H.J. (2005). Genetic engineering of terpenoid metabolism attracts, bodyguards to Arabidopsis. Science **309,** 2070-2072.

Kessler, A., and Baldwin, I.T. (2001). Defensive function of herbivore-induced plant volatile emissions in nature. Science **291,** 2141-2144.

Kessler, A., Halitschke, R., Diezel, C., and Baldwin, I.T. (2006). Priming of plant defense responses in nature by airborne signaling between Artemisia tridentata and Nicotiana attenuata. Oecologia **148,** 280-292.

Kigathi, R.N., Unsicker, S.B., Reichelt, M., Kesselmeier, J., Gershenzon, J., and Weisser, W.W. (2009). Emission of volatile organic compounds after herbivory from Trifolium pratense (L.) under laboratory and field conditions. J Chem Ecol **35,** 1335-1348.

Knudsen, J.T., Eriksson, R., Gershenzon, J., and Stahl, B. (2006). Diversity and distribution of floral scent. Bot Rev **72,** 1-120.

Laule, O., Furholz, A., Chang, H.-S., Zhu, T., Wang, X., Heifetz, P.B., Gruissem, W., and Lange, M. (2003). Crosstalk between cytosolic and plastidial pathways of isoprenoid biosynthesis in Arabidopsis thaliana. Proceedings of the National Academy of Sciences **100,** 6866-6871.

Loivamaki, M., Holopainen, J.K., and Nerg, A.M. (2004). Chemical changes induced by methyl jasmonate in oilseed rape grown in the laboratory and in the field. J Agr Food Chem **52,** 7607-7613.

Loreto, F., and Velikova, V. (2001). Isoprene produced by leaves protects the photosynthetic apparatus against ozone damage, quenches ozone products, and reduces lipid peroxidation of cellular membranes. Plant Physiology **127,** 1781-1787.

Lou, Y.G., Hua, X.Y., Turlings, T.C.J., Cheng, J.A., Chen, X.X., and Ye, G.Y. (2006). Differences in induced volatile emissions among rice varieties result in differential

attraction and parasitism of Nilaparvata lugens eggs by the parasitoid Anagrus nilaparvatae in the field. J Chem Ecol **32,** 2375-2387.

Maeda, T., Takabayashi, J., Yano, S., and Takafuji, A. (1998). Factors affecting the resident time of the predatory mite Phytoseiulus persimilis (Acari : Phytoseiidae) in a prey patch. Appl Entomol Zool **33,** 573-576.

Mantyla, E., Alessio, G.A., Blande, J.D., Heijari, J., Holopainen, J.K., Laaksonen, T., Piirtola, P., and Klemola, T. (2008). From plants to birds: higher avian predation rates in trees responding to insect herbivory. PLoS One **3,** -.

Maurer, B., Hauser, A., and Froidevaux, J.C. (1986). (E)-4,8-Dimethyl-1,3,7-nonatriene and (E,E)-4,8,12-Trimethyl-1,3,7,11-tridecatetraene, 2 unusual hydrocarbons from Cardamom oil. Tetrahedron Lett **27,** 2111-2112.

Mccall, P.J., Turlings, T.C.J., Loughrin, J., Proveaux, A.T., and Tumlinson, J.H. (1994). Herbivore-induced volatile emissions from Cotton (Gossypium-hirsutum L) seedlings. J Chem Ecol **20,** 3039-3050.

Nagegowda, D.A., Gutensohn, M., Wilkerson, C.G., and Dudareva, N. (2008). Two nearly identical terpene synthases catalyze the formation of nerolidol and linalool in snapdragon flowers. Plant Journal **55,** 224-239.

Nojima, S., Linn, C., Morris, B., Zhang, A.J., and Roelofs, W. (2003). Identification of host fruit volatiles from hawthorn (Crataegus spp.) attractive to hawthorn-origin Rhagoletis pomonella flies. J Chem Ecol **29,** 321-336.

Ozawa, R., Shimoda, T., Kawaguchi, M., Arimura, G., Horiuchi, J., Nishioka, T., and Takabayashi, J. (2000). Lotus japonicus infested with herbivorous mites emits volatile compounds that attract predatory mites. J Plant Res **113,** 427-433.

Pare, P.W., and Tumlinson, J.H. (1997). Induced synthesis of plant volatiles. Nature **385,** 30-31.

Pichersky, E., and Gershenzon, J. (2002). The formation and function of plant volatiles: perfumes for pollinator attraction and defense. Current Opinion in Plant Biology **5,** 237-243.

Pichersky, E., Noel, J.P., and Dudareva, N. (2006). Biosynthesis of plant volatiles: nature's diversity and ingenuity. Science **311,** 808-811.

Rasmann, S., Kollner, T.G., Degenhardt, J., Hiltpold, I., Toepfer, S., Kuhlmann, U., Gershenzon, J., and Turlings, T.C.J. (2005). Recruitment of entomopathogenic nematodes by insect-damaged maize roots. Nature **434,** 732-737.

Rose, U.S.R., Manukian, A., Heath, R.R., and Tumlinson, J.H. (1996). Volatile semiochemicals released from undamaged cotton leaves - A systemic response of living plants to caterpillar damage. Plant Physiol **111,** 487-495.

Schmelz, E.A., Carroll, M.J., LeClere, S., Phipps, S.M., Meredith, J., Chourey, P.S., Alborn, H.T., and Teal, P.E.A. (2006). Fragments of ATP synthase mediate plant perception of insect attack. P Natl Acad Sci USA **103,** 8894-8899.

Schnee, C., Kollner, T.G., Gershenzon, J., and Degenhardt, J. (2002). The maize gene terpene synthase 1 encodes a sesquiterpene synthase catalyzing the formation of (E)-beta-farnesene, (E)-nerolidol, and (E,E)-farnesol after herbivore damage. Plant Physiology **130,** 2049-2060.

Schultz, K., Kaiser, R., and Knudsen, J.T. (1999). Cyclanthone and derivatives, new natural products in the flower scent of Cyclanthus bipartitus Poit. Flavour Frag J **14,** 185-190.

Sell, C.S. (2003). In A fragrant Introduction to Terpenoid Chemistry (The Royal Society of Chemistry), pp. 1-5.

Sharkey, T.D., Wiberley, A.E., and Donohue, A.R. (2008). Isoprene emission from plants: why and how. Ann Bot-London **101,** 5-18.

Shulaev, V., Silverman, P., and Raskin, I. (1997). Airborne signalling by methyl salicylate in plant pathogen resistance. Nature **385,** 718-721.

Staudt, M., and Lhoutellier, L. (2007). Volatile organic compound emission from hohn oak infested by gypsy moth larvae: evidence for distinct responses in damaged and undamaged leaves. Tree Physiol **27,** 1433-1440.

Steeghs, M., Bais, H.P., de Gouw, J., Goldan, P., Kuster, W., Northway, M., Fall, R., and Vivanco, J.M. (2004). Proton-transfer-reaction mass spectrometry as a new tool for real time analysis of root-secreted volatile organic compounds in arabidopsis. Plant Physiology **135,** 47-58.

Su, J.W., Zeng, J.P., Qin, X.W., and Ge, F. (2009). Effect of needle damage on the release rate of Masson pine (Pinus massoniana) volatiles. J Plant Res **122,** 193-200.

Svensson, G.P., Hickman, M.O., Bartram, S., Boland, W., Pellmyr, O., and Raguso, R.A. (2005). Chemistry and geographic variation of floral scent in Yucca filamentosa (Agavaceae). Am J Bot **92,** 1624-1631.

Takabayashi, J., Dicke, M., and Posthumus, M.A. (1991). Induction of indirect defense against spider-mites in uninfested lima bean leaves. Phytochemistry **30,** 1459-1462.

Takabayashi, J., Dicke, M., and Posthumus, M.A. (1994a). Volatile herbivore-induced terpenoids in plant mite interactions - variation caused by biotic and abiotic factors. J Chem Ecol **20,** 1329-1354.

Takabayashi, J., Dicke, M., Takahashi, S., Posthumus, M.A., and Vanbeek, T.A. (1994b). Leaf age affects composition of herbivore-induced synomones and attraction of predatory mites. J Chem Ecol **20,** 373-386.

Tasin, M., Backman, A.C., Bengtsson, M., Ioriatti, C., and Witzgall, P. (2006). Essential host plant cues in the grapevine moth. Naturwissenschaften **93,** 141-144.

Tasin, M., Anfora, G., Ioriatti, C., Carlin, S., De Cristofaro, A., Schmidt, S., Bengtsson, M., Versini, G., and Witzgall, P. (2005). Antennal and behavioral responses of grapevine moth Lobesia botrana females to volatiles from grapevine. J Chem Ecol **31,** 77-87.

Tholl, D. (2006). Terpene synthases and the regulation, diversity and biological roles of terpene metabolism. Curr Opin Plant Biol **9,** 297-304.

Tholl, D., and Lee, S. (2011). Terpene Specialized Metabolism in Arabidopsis thaliana. The Arabidopsis book / American Society of Plant Biologists **9,** e0143.

Tholl, D., Sohrabi, R., Huh, J.H., and Lee, S. (2011). The biochemistry of homoterpenes--common constituents of floral and herbivore-induced plant volatile bouquets. Phytochemistry **72,** 1635-1646.

Tholl, D., Chen, F., Petri, J., Gershenzon, J., and Pichersky, E. (2005). Two sesquiterpene synthases are responsible for the complex mixture of sesquiterpenes emitted from Arabidopsis flowers. Plant Journal **42,** 757-771.

Tooker, J.F., and De Moraes, C.M. (2007). Feeding by Hessian fly [Mayetiola destructor (Say)] larvae does not induce plant indirect defences. Ecol Entomol **32,** 153-161.

Tooker, J.F., Rohr, J.R., Abrahamson, W.G., and De Moraes, C.M. (2008). Gall insects can avoid and alter indirect plant defenses. New Phytol **178,** 657-671.

Trombetta, D., Castelli, F., Sarpietro, M.G., Venuti, V., Cristani, M., Daniele, C., Saija, A., Mazzanti, G., and Bisignano, G. (2005). Mechanisms of antibacterial action of three monoterpenes. Antimicrob Agents Ch **49,** 2474-2478.

Turlings, T.C.J., Tumlinson, J.H., Heath, R.R., Proveaux, A.T., and Doolittle, R.E. (1991). Isolation and identification of allelochemicals that attract the larval parasitoid, Cotesia-marginiventris (Cresson), to the microhabitat of one of Its hosts. J Chem Ecol **17,** 2235-2251.

Turlings, T.C.J., Loughrin, J.H., Mccall, P.J., Rose, U.S.R., Lewis, W.J., and Tumlinson, J.H. (1995). How Caterpillar-Damaged Plants Protect Themselves by Attracting Parasitic Wasps. Proceedings of the National Academy of Sciences of the United States of America **92,** 4169-4174.

van Loon, J.J.A., de Boer, J.G., and Dicke, M. (2000). Parasitoid-plant mutualism: parasitoid attack of herbivore increases plant reproduction. Entomologia Experimentalis Et Applicata **97,** 219-227.

Van Poecke, R.M.P., Posthumus, M.A., and Dicke, M. (2001). Herbivore-induced volatile production by Arabidopsis thaliana leads to attraction of the parasitoid Cotesia rubecula: Chemical, behavioral, and gene-expression analysis. Journal of Chemical Ecology **27,** 1911-1928.

van Schie, C.C.N., Haring, M.A., and Schuurink, R.C. (2007). Tomato linalool synthase is induced in trichomes by jasmonic acid. Plant Molecular Biology **64,** 251-263.

Vancanneyt, G., Sanz, C., Farmaki, T., Paneque, M., Ortego, F., Castañera, P., and Sánchez-Serrano, J.J. (2001). Hydroperoxide lyase depletion in transgenic potato plants leads to an increase in aphid performance. Proceedings of the National Academy of Sciences **98,** 8139-8144.

Vaughan, M.M., Wang, Q., Webster, F.X., Kiemle, D., Hong, Y.J., Tantillo, D.J., Coates, R.M., Wray, A.T., Askew, W., O'Donnell, C., Tokuhisa, J.G., and Tholl, D. (2013). Formation of the unusual semivolatile diterpene rhizathalene by the Arabidopsis class I terpene synthase TPS08 in the root stele is involved in defense against belowground herbivory. Plant Cell **25,** 1108-1125.

Verpoorte, R., and Alfermann, A.W. (2000). Plant secondary metabolism. In Metabolic engineering of plant secondary metabolism, R. Verpoorte and A.W. Alfermann, eds (Dordrecht ; Boston, MA: Kluwer Academic Publishers), pp. 1-29.

Vuorinen, T., Nerg, A.M., and Holopainen, J.K. (2004). Ozone exposure triggers the emission of herbivore-induced plant volatiles, but does not disturb tritrophic signalling. Environ Pollut **131,** 305-311.

Wegener, R., Schulz, S., Meiners, T., Hadwich, K., and Hilker, M. (2001). Analysis of volatiles induced by oviposition of elm leaf beetle Xanthogaleruca luteola on Ulmus minor. J Chem Ecol **27,** 499-515.

Yonekura-Sakakibara, K., and Saito, K. (2009). Functional genomics for plant natural product biosynthesis. Natural Product Reports **26,** 1466-1487.

Zini, C.A., Zanin, K.D., Christensen, E., Caramao, E.B., and Pawliszyn, J. (2003). Solid-phase microextraction of volatile compounds from the chopped leaves of three species of Eucalyptus. J Agr Food Chem **51,** 2679-2686.

2. An alternative Biosynthetic Route to the Pathogen-Induced Volatile Homoterpene DMNT via Triterpene Degradation in *Arabidopsis* Roots

Other Contributors:

Jung-Hyun Huh, former PhD student, did screening of *TPS* mutants, and performed and analyzed results for all *Pythium* experiments in this study.

Somayesadat Badieyan, postdoctoral associate in the Biochemistry Department at Virginia Tech, did the protein modeling and mechanism predictions.

Liva Harinantenaina, postdoctoral associate in the Chemistry Department at Virginia Tech, did the NMR analysis.

Daniel Kliebenstein, professor at the University of California at Davis, performed the analysis of the QTL data.

ABSTRACT

Plant-derived volatile compounds such as terpenes exhibit substantial structural variation and serve multiple ecological functions. Despite their structural diversity, volatile terpenes are generally produced from a small number of core five- to twenty-carbon intermediates. Here we present unexpected plasticity in volatile terpene biosynthesis by showing that irregular homo/norterpenes can arise from different biosynthetic routes in a tissue specific manner. While *Arabidopsis* and other angiosperms are known to produce the homoterpene (*E*)-4,8-dimethyl-1,3,7-nonatriene (DMNT) or its C_{16}-analog (*E*,*E*)-4,8,12-trimethyl-1,3,7,11-tridecatetraene (TMTT) by the breakdown of sesquiterpene and diterpene tertiary alcohols in aboveground tissues, we demonstrate that *Arabidopsis* roots biosynthesize DMNT by the degradation of the C_{30} triterpene diol, arabidiol. The reaction is catalyzed by the *Brassicaceae*-specific cytochrome P450 monooxygenase CYP705A1 and transiently induced in a jasmonate-dependent manner by infection with the root-rot pathogen *Pythium irregulare*. *CYP705A1* clusters with the arabidiol synthase gene *ABDS* and both genes are co-expressed constitutively in the root endodermis and pericycle. We further provide *in vitro* and *in vivo* evidence for the role of arabidiol and DMNT in resistance against *P. irregulare*. Our results suggest convergent evolution in DMNT biosynthesis in land plants via the assembly of triterpene gene clusters and presents biochemical and genetic evidence for volatile compound formation via triterpene degradation in plants.

INTRODUCTION

Plants employ volatile compounds of diverse structure to interact with their environment. Volatile terpenes have been implicated with multiple functions in the attraction of insects, defense against herbivores or pathogens, and plant-plant interactions (McGarvey and Croteau, 1995; Dudareva et al., 2006; Pichersky et al., 2006), and these activities often correlate with the tissue and cell type specific biosynthesis of terpenes. Independent of their tissue specific origin, the specific classes of terpene compounds are supposed to be derived from the same central intermediates. For example, regular terpenes such as C_{10} monoterpenes, C_{15} sesquiterpenes, and C_{20} diterpenes are assembled from the 5-carbon units isopentenyl diphosphate (IPP) and dimethylallyl diphosphate (DMAPP), which are condensed to the core C_{10}, C_{15}, and C_{20} trans- or cis-prenyl diphosphate substrates of terpene synthases (Bohlmann et al., 1998; Fridman and Pichersky, 2005; Chen et al., 2011).

The C_{15} and C_{20} tertiary alcohols, (*E*)-nerolidol and (*E*,*E*)-geranyl linalool, have been shown to function as precursors of the irregular C_{11}-homo/norterpene volatile (*E*)-4,8-dimethyl-1,3,7-nonatriene (DMNT) and its C_{16}-analog (*E*,*E*)-4,8,12-trimethyl-1,3,7,11-tridecatetraene (TMTT), respectively. DMNT and TMTT are common constituents of floral and herbivore- or pathogen-induced volatile blends of angiosperms and they contribute to the deterrence or attraction of insect pests and their parasites or predators (Mumm and Dicke, 2010; Tholl et al., 2011). For example, both homoterpenes occur as floral volatiles of night-scented, moth-pollinated orchids (Kaiser, 1991; Donath and Boland, 1995). Several studies have supported the role of DMNT and TMTT in indirect defense against spider mite attack by promoting the attraction of predatory mites (Dicke et al., 1990; De Boer et al., 2004; Kappers et al., 2005). Moreover, homoterpenes have been shown to induce defense gene expression in plant-plant

interactions (Arimura et al., 2000). The formation of DMNT and TMTT in leaf or flower tissues usually occurs by the oxidative breakdown of (*E*)-nerolidol or (*E*,*E*)-geranyl linalool (Boland et al., 1998). The C-C cleavage reaction is catalyzed by cytochrome P450 monooxygenases, of which only a single enzyme, CYP82G1, has so far been identified in *Arabidopsis* (Lee et al., 2010). CYP82G1, which is induced in *Arabidopsis* leaves upon insect feeding damage, produces DMNT and TMTT *in vitro* but functions as a TMTT synthase *in planta* because of the presence of (*E*,*E*)-geranyllinalool (Herde et al., 2008) but not (*E*)-nerolidol in *Arabidopsis* leaves.

Here we show that *Arabidopsis* can produce DMNT via an unexpected novel alternative pathway in a tissue specific manner by the oxidative degradation of arabidiol a tricyclic triterpene diol in *Arabidopsis* roots. We demonstrate that CYP705A1, a member of *Brassicaceae*-specific CYP705 family, cleaves the prenyl side chain of arabidiol to produce DMNT and the non-volatile C_{19}-ketone derivative arabidonol. The reaction is induced by the root rot oomycete pathogen *Pythium irregulare* and treatment with the plant defense hormone jasmonic acid (JA) and contributes to *Arabidopsis* root defense. The *CYP705A1* gene clusters with the arabidiol synthase (*ABDS*) (Xiang et al., 2006) as part of a larger triterpene biosynthetic gene cluster on chromosome 4. Our results provide evidence for convergent evolution and biosynthetic plasticity in the formation of functionally active volatiles. We discuss how alternative pathways in the production of the same homoterpene compound may evolve depending on the tissue-specific expression of biosynthetic terpene synthase/P450 gene modules. Our findings also support the notion that triterpenes, similar to C_{40} carotenoids, can undergo enzyme-mediated degradation to serve as precursors of plant volatiles.

RESULTS

Pythium-Induced Production of DMNT in Arabidopsis Roots

We investigated whether *Arabidopsis* roots release volatile compounds in response to infection by the soilborne pathogen *Pythium irregulare*. *Pythium* is an oomycete pathogen causing seedling damping off, root rot and vascular wilt disease in various plant species including *Arabidopsis* (Armstrong and Armstrong, 1981; Agrios, 1997). *Arabidopsis* plants were grown in liquid axenic and hydroponic culture, and inoculated with a uniform suspension of mycelium and oospores of the oosporic *P. irregulare* isolate 110305. Root tissue was detached at different time points after inoculation and root volatiles were analyzed by solid phase microextraction gas chromatography-mass spectrometry (SPME-GC/MS). We found that DMNT was transiently released in response to *P. irregulare* treatment (Figure 2.1 B). Emission of DMNT was highest 3 h after inoculation with a 7-fold increase over constitutive background levels and then decreased over the following 10 to 20 h (Figure 2.1 B). DMNT was detected at approximately 10 ng/g root fresh weight at the peak of emission. Light microscopy analysis of *Pythium*-inoculated roots showed that the release of DMNT coincided with the attachment of hyphae and oospores to the root surface and the germination of oospores to produce infection hyphae (Supplemental Figure 2.1). A transient emission of DMNT was also observed in roots grown under non-sterile, hydroponic conditions (Supplemental Figure 2.1 A).

Since *Pythium* produces elicitors such as lytic enzymes and phytotoxins (Brandenburg, 1950; Deacon, 1979) we tested the effect of a soluble *Pythium* filtrate on DMNT emission. Furthermore, we examined whether treatment with *Escherichia coli*, a non-plant pathogen, could cause induction of DMNT emission. Transient DMNT emission was observed only following

inoculation with a suspension of *P. irregulare* containing mycelium and oospores and neither inoculation with the soluble filtrate nor treatment with an *E. coli* suspension could mimic this response (Figure 2.1 B).

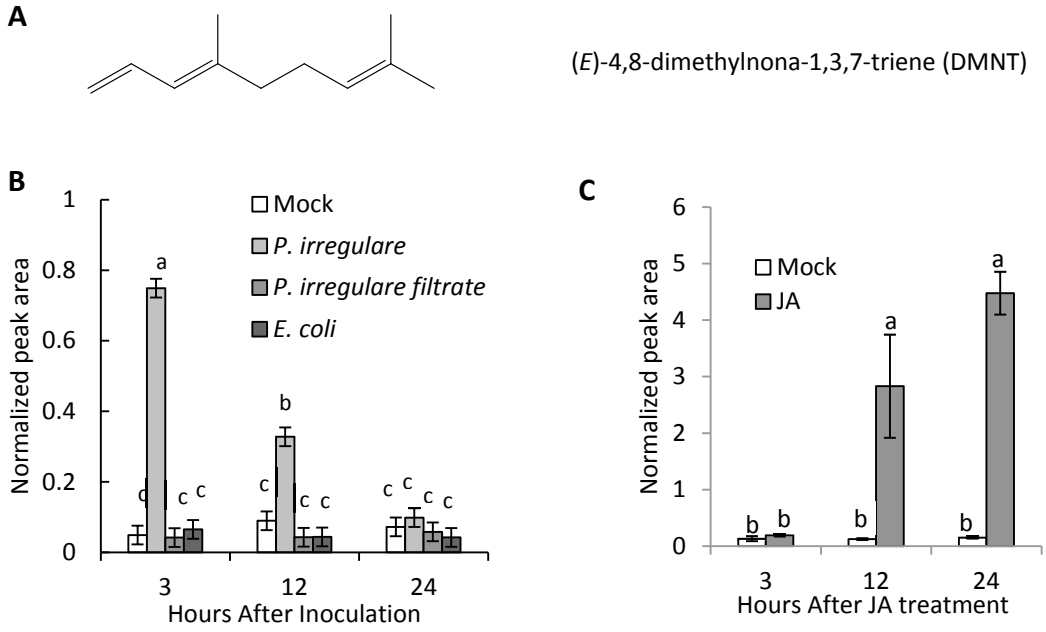

Figure 2.1 DMNT emission in *Arabidopsis* roots is induced by infection with *P. irregulare* or treatment with jasmonic acid.

(A) Structure of the acyclic-irregulare terpene DMNT. (B) Axenically grown *Arabidopsis* roots were infected with a suspension of *P. irregulare* mycelium and oospores, a *P. irregulare* filtrate, or with a suspension of *E. coli*. (C) Treatment of axenically grown roots with 100 µM JA. Root volatiles were analyzed from detached roots at different time points by SPME-GC/MS. Normalized peak areas are shown. Values represent the mean ± SE of three biological replicates. Results were analyzed by two-way ANOVA, and Tukey-Kramer HSD test; $P < 0.001$. The experiment was repeated at least two times with similar results.

The importance of the defense hormone jasmonic acid (JA) in plant defense against *Pythium* has been reported previously (Vijayan et al., 1998). To further understand the role of JA in DMNT formation in *Arabidopsis* roots, axenically grown *Arabidopsis* plants were treated with 100 µM JA. Roots were excised and headspace volatiles were measured by SPME-GC/MS. DMNT

emission was induced at 12 h after the beginning of treatment and peaked at 24 h with approximately 70 ng/g fresh weight (Figure 2.1C). JA-inducible DMNT production was also observed in hydroponically grown roots (Supplemental Figure 2.2 B).

Identification of CYP705A1 as a Root-Specific Gene Involved in DMNT Biosynthesis

Previous studies on the formation of TMTT in *Arabidopsis* leaves elucidated a two-step biosynthetic pathway consisting of the formation of the tertiary alcohol (*E*,*E*)-geranyllinalool (GL) catalyzed by the GL synthase TPS04 (Herde et al., 2008) and the subsequent breakdown of GL to (*E*)-TMTT catalyzed by CYP82G1(Lee et al., 2010). Even though the CYP82G1 enzyme can convert (*E*)-nerolidol into DMNT *in vitro* (Lee et al., 2010) and possibly *in planta* (Kappers et al., 2005), *CYP82G1* is not expressed in roots (Lee et al., 2010) and the null mutant *cyp82g1-1* is not impaired in root-specific DMNT biosynthesis (Supplemental Figure 2.3) indicating that this P450 is not involved in the formation of DMNT in *Arabidopsis* roots. Since treatments of *Arabidopsis* hairy roots with the cytochrome P450-specific azole inhibitors miconazole and clotrimazole severely reduced JA-induced emission of DMNT (Supplemental Figure 2.4), we hypothesized that DMNT is most likely produced by a different root-specific P450 enzyme.

To identify P450 gene(s) involved in DMNT formation, we performed quantitative trait locus (QTL) analysis of DMNT emission using recombinant inbred lines of the accession Cave Verdi Island (CVI), a non-DMNT emitter, and the DMNT-emitting accession Landsberg erecta (L*er*) (Alonso-Blanco et al., 1998) (Supplemental Figure 2.5 A). This analysis suggested that only a single region on chromosome 4 contributes to the natural variation in DMNT biosynthesis (Supplemental Figure 2.5B). To further refine this analysis, we searched for the expression of all *Arabidopsis* P450 genes in publically available microarray data sets using GENEVESTIGATOR,

(Zimmermann et al., 2004) under the treatment with methyl jasmonate (MeJA) or wounding assuming that the expression of the target P450 gene would be induced in roots under these conditions. This approach again excluded *CYP82G1* and resulted in a final list of 9 candidate genes (Supplemental Table 2.1). We then conducted a comparative RT-PCR analysis of transcripts of the selected candidate genes with and without JA-treatment in hydroponically grown roots of wild type plants and the JA-insensitive mutant *coi1-1* (Xie et al., 1998). As a result, two P450 genes, *CYP705A1* and *CYP81D1*, were found, whose transcripts accumulated upon JA-treatment in wild type but not *coi1-1* roots (Supplemental Figure 2.6). Of these two genes only *CYP705A1* resides in the identified QTL region on chromosome 4. SPME-GC-MS analysis of volatiles emitted from roots of the gene knockout line *cyp705a1-1* (SALK_043195) with a T-DNA insertion in the second exon (Figure 2.2 A) lacked emission of DMNT upon JA-treatment while a second line carrying a T-DNA insertion in the *CYP705A1* promoter region *cyp705a1-2* (SALK_090621) produced wild type levels of DMNT (Figure 2.2 B) and the *CYP705A1* transcript (Supplemental Figure 2.7 A). This finding suggested that *CYP705A1* is involved in DMNT biosynthesis in *Arabidopsis* roots.

To further study the role of the *CYP705A1* gene in DMNT production, the *cyp705a1-1* mutant was complemented with a full length *CYP705A1* cDNA in C-terminal fusion to enhanced yellow fluorescent protein (eYFP) under the control of a 1.5 kb fragment of the native *CYP705A1* promoter. Additionally, the full length *CYP705A1* transcript was fused to the *CaMV 35S* promoter for ectopic expression in the *cyp705a1-1* mutant background. In *ProCYP705A1:CYP705A1-eYFP* lines accumulation of the full length *CYP705A1* transcript was detected upon JA treatment, while only basal transcript levels of the gene were observed in *CaMV35S-CYP705A1* lines with no JA-dependent increase of transcript abundance

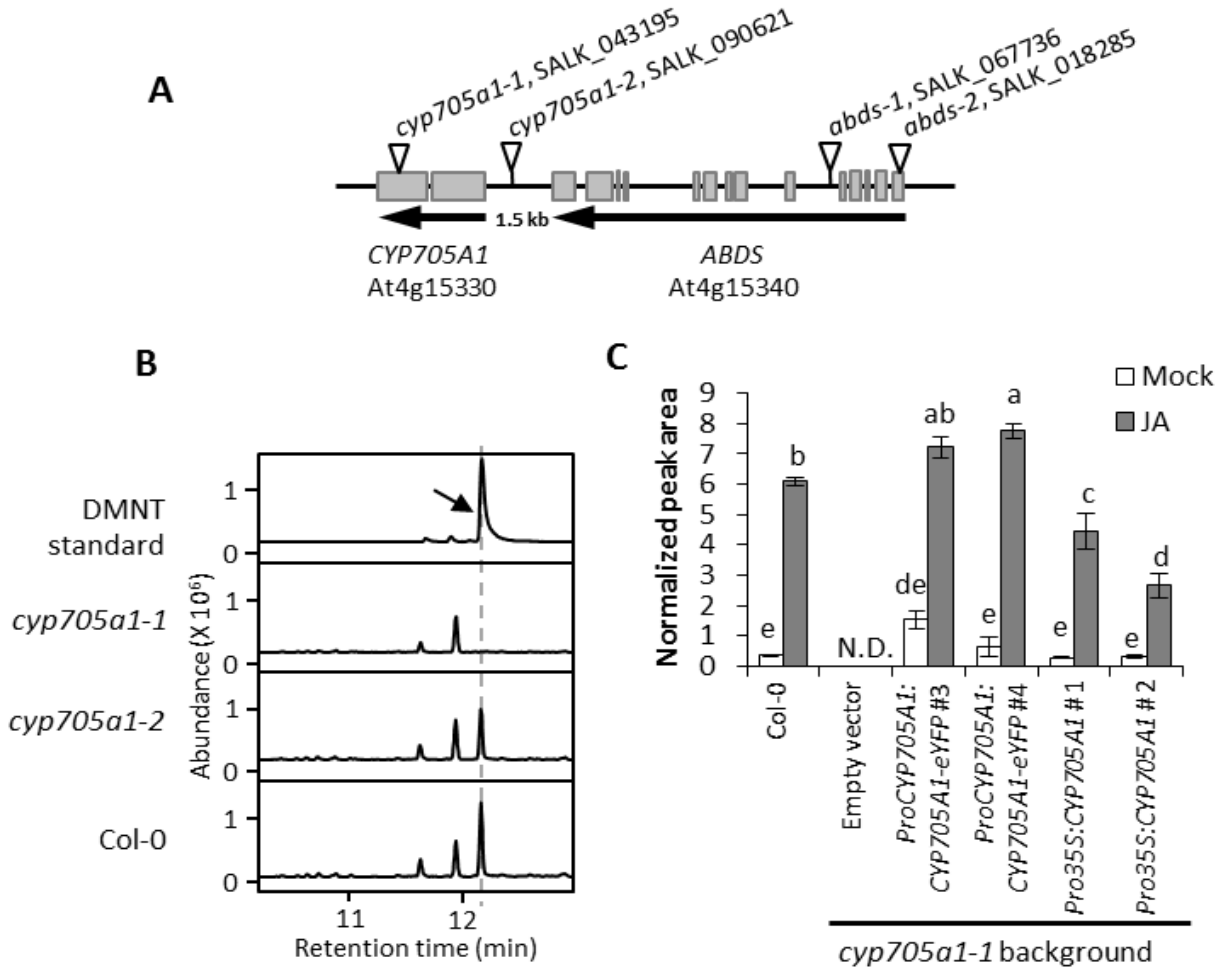

Figure 2.2 Identification of CYP705A1 as a DMNT synthase.

(A) Schematic showing the genomic locus of *Arabidopsis CYP705A1* (At4g15330) in tandem with the arabidiol synthase (*ABDS*) gene. Exons are represented by grey boxes. Introns and intergenic regions are represented by the black line. Insertion sites of the T-DNA mutants used in this study are marked with inverted triangles. **(B)** DMNT emission in roots of wild-type, and *cyp705a1* mutants after 24 h of JA treatment. The retention time for DMNT authentic standard is marked with a dotted line. **(C)** DMNT emission in mock- and JA-treated plants in wild-type background compared to representative transgenic lines. Volatiles were collected from roots after 24 h of JA treatment and analyzed by SPME-GC/MS. Mock controls were treated with ethanol (EtOH). Normalized peak areas are shown and the values represent the mean ± SE of three biological replicates. Letters show significant differences based on two-way ANOVA and Tukey-Kramer HSD test, $P < 0.001$. N.D. indicates that no volatile was detected.

(Supplemental Figure 2.7 B). Consistent with the transcript accumulation, DMNT volatile formation was restored in both transgenic lines (Figure 2.2C) further supporting the role of CYP705A1 in the DMNT biosynthetic pathway.

Arabidiol is the Precursor in DMNT Biosynthesis in Arabidopsis Roots

Despite our prediction that DMNT would be produced from (*E*)-nerolidol, we were unable to detect this precursor in the headspace or in organic extracts of JA-treated roots. In addition, an analysis of T-DNA insertion lines of several root-expressed *TPS* genes (Vaughan et al., 2013) did not lead to the identification of a gene involved in DMNT formation. However, treatment of *Arabidopsis* hairy roots with lovastatin, an inhibitor of the IPP producing mevalonate (MVA) pathway in the cytosol, severely reduced jasmonate-induced emission of DMNT, while this was not the case when fosmidomycin, an inhibitor of the plastidial methylerythritol phosphate (MEP) pathway, was applied (Supplemental Figure 2.8). This result suggested a major contribution of the MVA pathway and a possibly FPP-derived precursor in the DMNT biosynthetic pathway.

Since P450s are often co-expressed with genes of the same biosynthetic pathway (Ehlting et al., 2008; Field and Osbourn, 2008; Lee et al., 2010), we applied an in silico gene co-expression approach using the ATTED II database (http://atted.jp/) to identify genes that may be responsible for the formation of the DMNT precursor. According to this analysis, a gene encoding a triterpene synthase called arabidiol synthase (*ABDS*) (Xiang et al., 2006) was highly co-expressed with *CYP705A1* (Supplemental Table 2.2). Moreover, both genes clustered in tandem on chromosome 4, which strongly suggested a contribution to the same biosynthetic pathway (Figure 2.2 A). Arabidiol has a 6,6,5-tricyclic ring system with two hydroxyl groups,

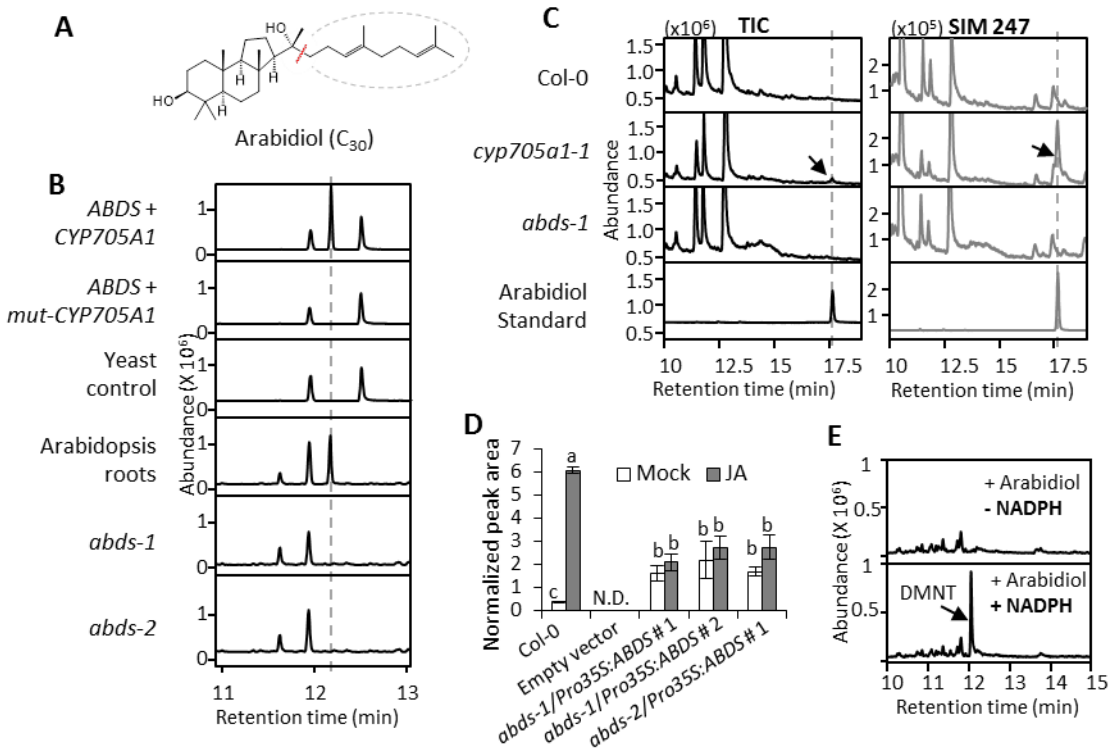

Figure 2.3 Arabidiol is the substrate for DMNT biosynthesis.

(A) Structure of arabidiol. We predicted that DMNT could be produced from the arabidiol hydrophobic tail via C-C bond cleavage catalyzed by CYP705A1. (B) DMNT emission in yeast and *Arabidopsis* plants. DMNT was detected from WAT11 yeast cells co-expressing *ABDS* with a wild type *CYP705A1* cDNA but not a mutated version of *CYP705A1* (*mut-CYP705A1*). The yeast control line expressed *ABDS* and the empty vector used for expression of *CYP705A1*. Volatile analysis of Col-0 roots and *abds* mutants after 24 h of 100 µM JA treatment is shown. No DMNT was detected from *abds* mutants. Volatile products were analyzed in the yeast culture or plant tissue headspace by SPME-GC/MS. (C) Arabidiol detection from *Arabidopsis* roots. GC chromatograms of liquid extracts from 1 g JA-treated roots of wild type Col-0, *atpen1-1* and *cyp705a1-1* are depicted. Arabidiol was only detected in the *cyp705a1-1* mutant after JA treatmentas shown in TIC (total ion chromatogram) and in single ion monitoring (SIM) mode for *m/z* 247. (D) DMNT emission from roots in wild type Col-0 and three *ABDS* 35S overexpression line in two different mutant backgrounds treated with JA for 24 h. Normalized peak areas are shown. Normalized peak areas are shown. Values represent the mean ± SE of three biological replicates. Results were analyzed by two-way ANOVA, and Tukey-Kramer HSD test; $P < 0.001$. (E) Microsomal preparations expressing *CYP705A1* converted arabidiol to DMNT in the presence of 2.4 mM of the P450 cofactor NADPH.

whose tricyclic backbone is covalently linked to a C_{13}-prenylalcohol side chain (Figure 2.3 A). We predicted that the tertiary hydroxyl group of this side chain made arabidiol a suitable substrate for oxidative degradation by a P450 enzyme to produce a compound resembling DMNT and a second non-volatile degradation product (Figure 2.3 A).

To test this hypothesis, we co-expressed the *CYP705A1* and *ABDS* genes in *Saccharomyces cerevisiae* WAT11 cells. In addition, co-expression of *ABDS* with a truncated *CYP705A1* gene lacking the heme binding domain was performed to control for any possible non-specific or yeast-mediated conversion of arabidiol to DMNT. Volatile headspace analysis of the respective yeast cultures demonstrated that DMNT was detected only after induction with galactose and when a functional copy of both biosynthetic genes was expressed (Figure 2.3B). Involvement of arabidiol in DMNT biosynthesis was further confirmed by the absence of JA-induced DMNT emission in two independent T-DNA insertion mutants of the *ABDS* gene, SALK_018285 (*abds-1*) and SALK_067736 (*abds-2*), (Figure 2.3 B) both of which lack a full length *ABDS* transcript (Supplemental Figure 2.9A). To detect arabidiol from *Arabidopsis* plants we performed organic solvent extraction from JA-treated roots of wild type and DMNT biosynthetic mutants (Figure 2.3 C). Arabidiol was neither detected in the *abds-1* mutant nor in wild type plants presumably due to an immediate conversion into DMNT. However, an accumulation of arabidiol was observed in *cyp705a1-1* missing a functional arabidiol degradation enzyme. Additionally, complementation of the two *abds* mutants with the full length *ABDS* cDNA driven by the *CaMV 35S* promoter led to a restoration of DMNT emission in both mutants (Figure 2.3 D). Treatment with JA did not further enhance volatile emission from these lines because of the absence of the JA-responsive *ABDS* promoter (Supplemental Figure 2.9B). Finally, purified microsomal fractions from yeast expressing only *CYP705A1* converted arabidiol

into DMNT in the presence of the cofactor NADPH (Figure 2.3 D). In conclusion, these findings suggest that both CYP705A1 and ABDS are necessary and sufficient for the biosynthesis of DMNT.

Arabidiol is Cleaved into DMNT and the Non-Volatile C_{19} Tricyclic Ketone Arabidonol

In analogy to examples of P450-mediated C-C cleavage reactions such as the dealkylation of steroids (Akhtar and Wright, 1991) and the oxidative degradation of (+)-marmesin to the furanocoumarin psoralen and acetone (Larbat et al., 2007), we expected CYP705A1 to catalyze an oxidative C-C cleavage of arabidiol at its C_{14}-C_{15} bond. We proposed that a double bond is introduced in the isoprenyl side chain to produce DMNT and the tertiary hydroxyl group at C_{14} is converted into a ketone group resulting in a C_{19} tricyclic ketone cleavage product (Figure 2.4C). We then searched for the presence of a non-volatile C_{19} compound with a ketone functional group and a predicted molecular weight of 292 in yeast lines expressing *ABDS* with either *CYP705A1* or *mut-CYP705A1*. A *m/z* 292 molecular ion was detected in ethyl acetate extracts of yeast expressing *ABDS* and *CYP705A1* but not in lines expressing the non-functional *CYP705A1* gene (Figure 2.4A). This result suggested the formation of the predicted C_{19} degradation product which we named arabidonol.

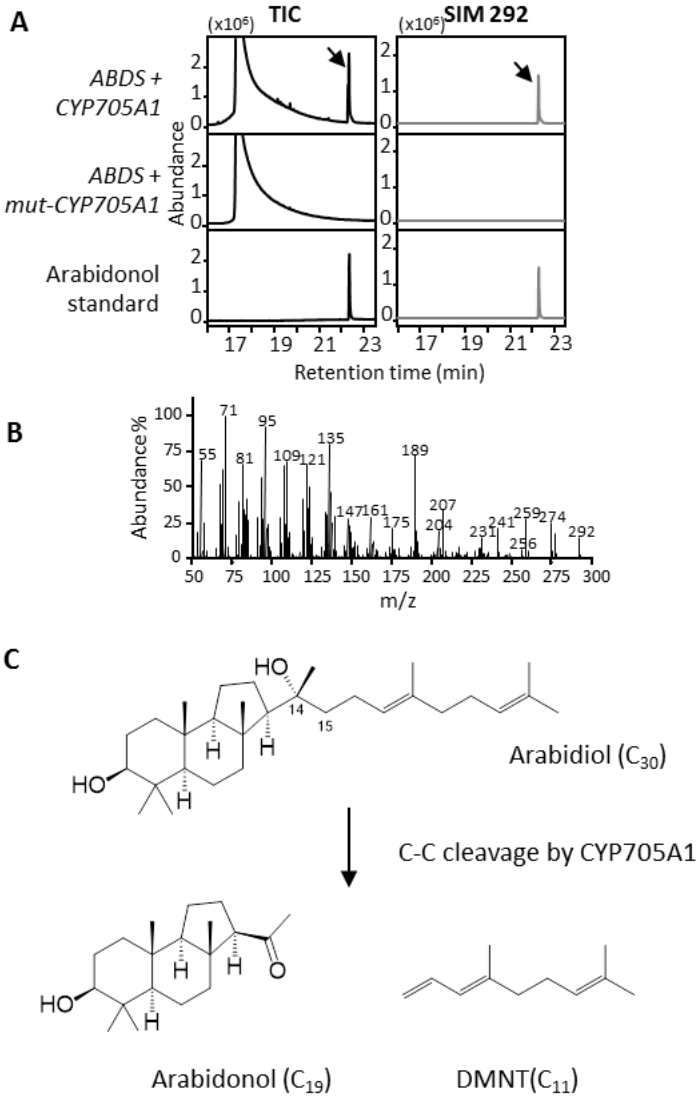

Figure 2.4 Detection of arabidonol in the yeast co-expression system.

(A) The C_{19} degradation product arabidonol was detected in WAT11 yeast cells expressing *ABDS* and *CYP705A1* but not the *mut-CYP705A1*. The GC chromatogram of the purified degradation product is depicted. TIC: total ion chromatogram; SIM; single ion monitoring (B) MS spectrum of arabidonol with a *m/z* 292 molecular ion. (C) The pathway for arabidiol degradation to DMNT and arabidonol. The molecular structure of arabidonol was determined by NMR analysis.

For a rigorous structural analysis, arabidonol was purified from *ABDS* and *CYP705A1* expressing yeast cells using ethyl acetate extraction followed by flash chromatography

separation and thin layer chromatography. GC-MS analysis of purified arabidonol showed a single peak at t_R= 22.65 min with the expected molecular ion of *m/z* 292 (Figure 2.4 B). The molecular formula of $C_{19}H_{32}O_2$ was then tentatively assigned to arabidonol. The pseudomolecular ion peak at *m/z* 275.2362, $[M\text{-}OH]^+$ (calculated for $C_{19}H_{31}O$: 275.2369) observed in high resolution electrospray ionization mass spectrometry (HRESIMS) analysis confirmed the proposed molecular formula with four degrees of unsaturation (Supplemental Figure 10 A). The arabidonol structure was then further determined using proton ^{1}H-NMR (Supplemental Figure 10B), HMBC, HMQC, NOESY and COSY (Supplemental Figure 2.11 to 2.14). Proton and carbon chemical shifts are listed in Supplemental Table 2.3 and key correlations are shown in Supplemental Figure 2.15. This analysis confirmed formation of a ketone group at the cleavage site of arabidiol (Figure 2.4 C).

Transcript Analysis of ABDS and CYP705A1 in Pythium-Infected and JA-Treated Arabidopsis Roots

To understand whether the biosynthesis of DMNT is regulated by the transcription of *ABDS* and *CYP705A1*, transcript levels of both genes were monitored by quantitative real-time PCR (qRT-PCR) in axenically grown roots upon *Pythium* infection and treatment with JA. Both genes showed some constitutive expression at time point 0 of treatment. During the early stage of *Pythium* infection (1, 3, 12 h post-inoculation), when DMNT emission is observed, (Figure 2.5A-B) no significant changes in transcript levels of *ABDS* were found in comparison to those at the start of inoculation By contrast, expression of *CYP705A1* was induced 2 fold one hour after inoculation prior to a decline to transcript levels similar to those prior to inoculation. Since this transient increase of *CYP705A1* mRNA precedes the emission of DMNT, we conclude that the

Pythium-induced formation of DMNT appears to be, at least in part, regulated by the expression of *CYP705A1* but not *ABDS*.

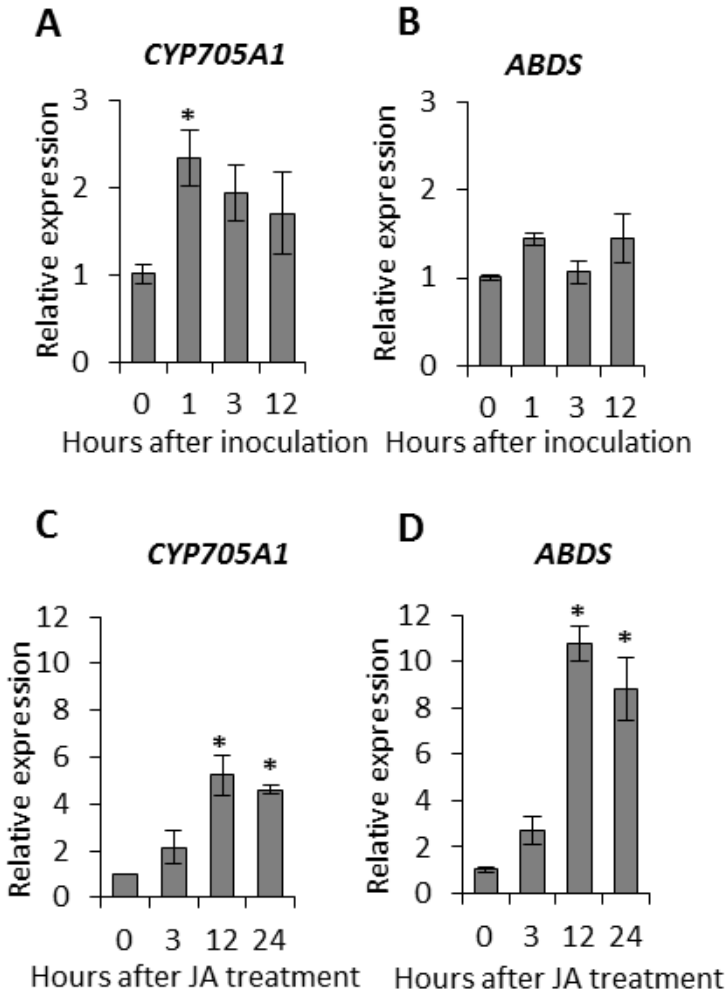

Figure 2.5 qRT-PCR Analysis of *CYP705A1* and *ABDS* Transcript Levels.

Relative transcript levels of *CYP705A1* and *ABDS* were determined in Col-0 plants inoculated with *Pythium* (A and B) or treated with JA (C and D) over a series of several time points. Values were normalized to those of UBC21 and represent means ± SE of three biological replicates. Transcript levels at 0 h time point were arbitrary set to 1. Asterisk indicates statistically significant differences among means compared to transcript levels at 0 h time point calculated by one-way ANOVA and student *t*-test ($P < 0.005$). No significant difference was found in *ABDS* transcript levels upon inoculation with *Pythium*.

Upon JA treatment, transcript accumulation was significantly higher for both genes at 12 h and 24 h after the beginning of JA treatment. Transcripts of *ABDS* and *CYP705A1* were induced 10 fold and 5-fold, respectively, over constitutive levels suggesting a significant contribution of both *ABDS* and *CYP705A1* in JA-induced DMNT formation.

Spatial Pattern of DMNT Biosynthetic Gene Expression

We further examined the tissue specific expression of the DMNT biosynthetic genes by performing promoter activity assays in *Arabidopsis* transgenic lines expressing the β-glucuronidase gene (GUS) under the control of the native *CYP705A1* and *ABDS* promoters In 12-day-old seedlings grown on MS medium, promoter activities of both genes were primarily observed in roots and only weak *ProCYP705A1*-GUS and *ProABDS*-GUS activity was found in the vasculature of cotyledons and in true leaves, respectively (Figure 2.6 .A and B and Supplemental Figure 2.16). In roots of *ProCYP705A1-GUS* lines, GUS staining was mainly detected in the stele in addition to weak activity in the cortex and epidermis at the root differentiation zone. GUS staining expanded to all cell layers proximal to the cell elongation-differentiation zone boundary (Figures 2.6 A-E). No GUS activity was observed in the cell elongation area but, curiously, a cell type specific activity was found in the quiescent center at the root meristematic zone (Figure 6D-E). Similar expression patterns were detected in lateral roots (Figures 2.6).

GUS activity driven by the promoter of the *ABDS* gene largely co-localized to the same areas where *ProCYP705A1*-GUS activity was observed. However, *ProABDS*-GUS activity was confined to the stele in the differentiation and elongation zones and was very strong in all cells of the root meristematic zone (Supplemental Figure 2.16).

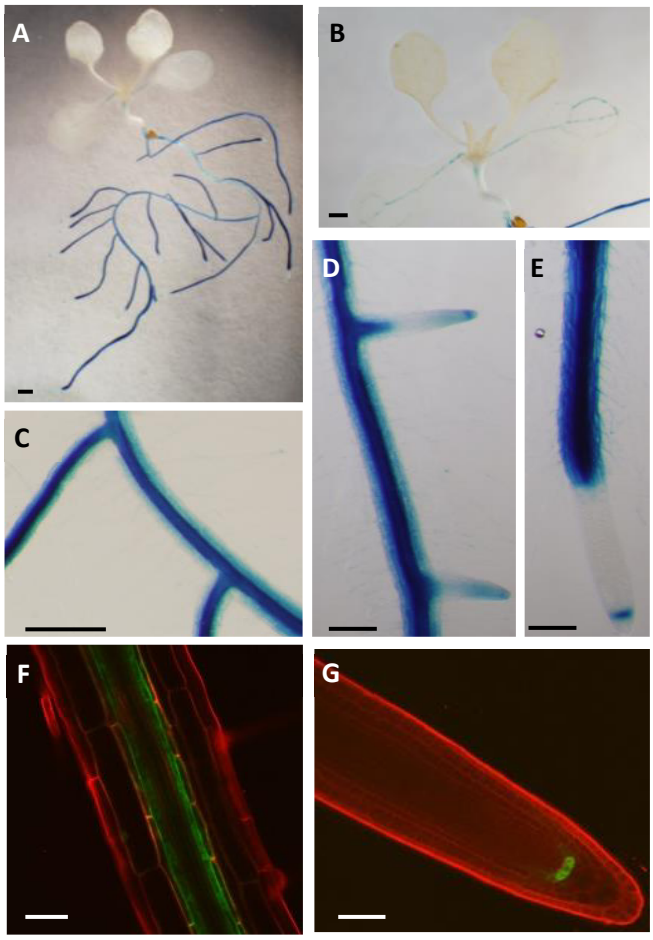

Figure 2.6 Spatial expression pattern of *CYP705A1*.

(A) to (E) GUS activity in twelve-day-old *ProCYP705A1-GUS* transgenic lines. (A) Whole seedling. (B) Main root at the root hair zone. (C) and (D) Lateral roots. (E) Main root. For (A) Bar = 1 mm and for (A) to (E) Bar = 200 µm. (F) and (G) Protein expression pattern in *ProCYP705A1:CYP705A1-eYFP* transgenic plants. (F) Localization of CYP705A1-eYFP protein in the pericycle in the root hair zone and the quiescent center in the root meristematic zone (G). Bar = 50 µm.

To further evaluate the tissue specificity of constitutive DMNT production at the protein level, we examined the cell type specific localization of the CYP705A1 protein in *ProCYP705A1:CYP705A1-eYFP* lines. Confocal microscopy analysis of three independent transgenic lines suggested that the CYP705A1 protein is expressed primarily in the pericycle and very weakly in the endodermis, cortex, and stele at the root differentiation zone (Figure 2.6F).

Observation of a YFP signal in the quiescent center confirmed CYP705A1 expression in the root meristem (Figure 2.6G) under normal developmental conditions.

Since we observed DMNT at high levels upon JA treatment, we also analyzed spatial patterns of GUS activity and YFP-fusion protein expression in 12-days old transgenic seedlings treated with 100 μM JA for 12 h. in three independent transgenic lines. Jasmonate treatment induced strong *CYP705A1* promoter activity in the root meristem and cell elongation zone in main and lateral roots but at the differentiation zone much stronger activity was detected in lateral roots compared to the main roots (Supplemental Figure 2.16). Enhanced *ProCYP705A1*-GUS activity was also observed in the vasculature of cotyledons but not in true leaves suggesting that the induced breakdown of arabidiol and emission of DMNT is largely confined to roots (Supplemental Figure 2.16). Patterns of JA-induced *ABDS* promoter-GUS activity were similar to those found for the *CYP705A1* promoter except that no changes were detected in leaves in comparison to mock controls (Supplemental Figure 2.16).

At the protein level, JA treatment appeared to enhance CYP705A1-YFP expression largely in the area of the pericycle at the root differentiation zone (Supplemental Figure 2.17) without major systemic effects in this root zone. In the root meristematic zone, expression of the CYP705A1-YFP protein expanded from the quiescent center to the endodermis and cortex but was excluded from the stele and columella lateral root cap, epidermis, and pericycle and.

DMNT Negatively Effects Pythium Oospore Germination and Growth

Since we had observed highest emission levels of DMNT within hours of oospore germination and germ tube penetration, we examined a possible effect of DMNT on *Pythium* oospore germination. Since an accurate quantitative assessment of these effects under in vivo

conditions proved too difficult, we observed oospore germination rates in vitro on corn meal agar plates supplemented with DMNT at different concentrations. Oospore germination was inhibited by about 50% at concentrations as low as 50 ρM DMNT (Figure 2.7A). Higher DMNT concentrations caused only minor additional inhibitory effects, which may suggest a dose-specific response. We also tested whether DMNT had any effect on the mycelium growth rate of the oomycete by comparing the growth area of the mycelium on potato dextrose agar (PDA) at different DMNT concentrations. Incubation with 10 nM DMNT resulted in approximately 30% reduction of *Pythium* growth (Supplemental Figure 2.18), but again no strong dose-specific responses were observed at higher concentrations. In summary, these results indicate that DMNT can inhibit oospore germination and to some extend retard *Pythium* growth specifically at low concentrations under *in vitro* conditions similar to the inhibitory effects of DMNT on *Pythium* mycelium growth although at about 200-fold lower concentrations. Measurement of DMNT effects on mycelium growth rate was done by Incubation with DMNT resulted in approximately 30% reduction *Pythium* growth at 10nM concentration (Supplemental Figure 2.18) with no strong dose-specific effect. These results indicate that DMNT can primarily inhibit oospore germination and to some extend retard *Pythium* growth *in vitro*. Incubation with DMNT resulted in approximately 60% reduction in *Pythium* growth at 13 nM concentration (Supplemental Figure 2.18) with a small further decrease at 133 nM wich may suggest a dose-specific effect. These results indicate that DMNT can retard *Pythium* growth and inhibit oospore germination *in vitro*.

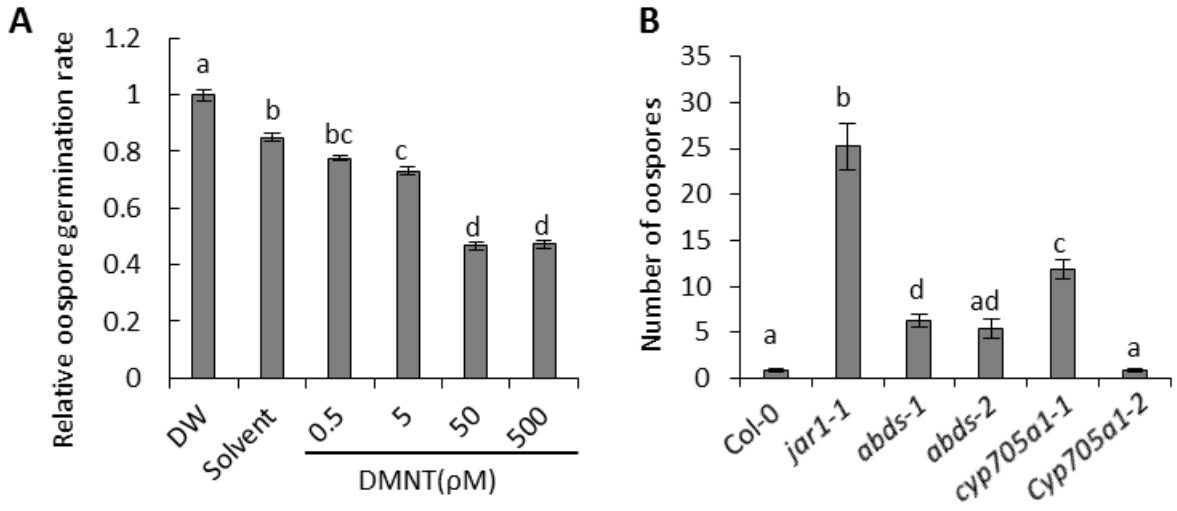

Figure 2.7 DMNT negatively effects *P. irregulare* oospore germination and formation.

(A) Effect of DMNT on oospore germination of *P. irregulare*. DMNT was applied at different concentrations in 10 ml of corn meal agar containing streptomycin. Oospore suspensions were added into each plate and incubated at 27 °C in the dark. Germination rates were determined 24 h after inoculation. Thirty percent of the oospores germinated in the control treatment. The results were plotted relative to distilled water (DW) and oospore germination rate for DW was arbitrary set to 1. (B) Root infection assay of *P. irregulare* in wild-type, DMNT biosynthetic mutants (*abds-1, abds-2, cyp705a1-1*) and the control line *cyp705a1-2*. Representative root segments were taken three weeks after infection of soil grown plants with the pathogen to measure oospore formation. Oospores were counted approximately 10 mm behind the root tips. Statistical analysis was done using one-way ANOVA and Tukey-Kramer HSD test. The values represent the mean ± SE of 5 replicates ($P < 0.01$) for (A) and at least six root segments from 3 different plants ($P < 0.05$) for (B).

We further investigated whether the formation of arabidiol or its volatile and non-volatile break-down products had any long term effects on the root infection level of wild type and *abds* and *cyp705a1* mutant plants grown in potting substrate. To this end, roots of six-week-old plants were harvested three weeks post inoculation and stained with acid-fuchsin lactophenol to observe and count oospores inside root tissues in a 10-mm zone behind the root tip (Figure 2.7B). Whereas few oospores were found in roots of wild-type plants and the *cyp705a1-2* line (DMNT

wild type phenotype), both *abds-1* mutants and the *cyp705a1-1* exhibited higher levels of oospores inside infected root tissues (significant for *abds-1* and *cyp705a1*). However, the abundance of oospores in these mutants was significantly lower than that of the highly susceptible *jar1-1*, which is deficient in the formation of the JA-Ile conjugate (Staswick et al., 1998). Together, these results indicate that arabidiol biosynthesis and breakdown contribute to the plant defense response to the selected *P. irregulare* isolate.

DISCUSSION

Arabidopsis Roots Produce DMNT via the Breakdown of a Triterpene Precursor

Our results provide genetic and biochemical evidence for a novel pathway for DMNT formation via oxidative degradation of the triterpene alcohol, arabidiol, in *Arabidopsis* roots. This finding was rather unexpected since previous biochemical studies administrating stable isotope precursors had demonstrated that DMNT in aerial parts of plants is derived from the sesquiterpene alcohol (*E*)-nerolidol (Donath and Boland, 1995; Boland et al., 1998). Additionally, transgenic *Arabidopsis* plants carrying a nerolidol synthase from cultivated strawberry (FaNES1) were shown to emit DMNT from leaves (Kappers et al., 2005). These studies were further supported by the characterization of the leaf-specific and insect-induced *Arabidopsis* P450 enzyme CYP82G1, which catalyzes the *in vitro* conversion of both (*E*)-nerolidol and (*E*,*E*)-geranyllinalool into DMNT and TMTT, respectively. Although, only TMTT is produced in wild type *Arabidopsis* leaves by CYP82G1 activity (Lee et al., 2010), the root specific emission of DMNT is not impaired in *cyp82g1-1* plants confirming no contribution of CYP82G1 in the formation of DMNT in *Arabidopsis* roots. However, because of the absence of

endogenous (*E*)-nerolidol synthase activity in *Arabidopsis* leaf (Lee et al., 2010) as well as root tissue (Vaughan et al., 2013), we concluded that DMNT biosynthesis in *Arabidopsis* roots is not via C_{15} precursor (*E*)-nerolidol. Our findings rather suggested a novel pathway for volatile DMNT biosynthesis via degradation of a C_{30} triterpene arabidiol in *Arabidopsis*.

To explore the mechanism of tricyclic triterpene arabidiol cleavage, docking of arabidiol to the active site of a homology based protein model of CYP705A1 was performed. The most energetically favorable orientation of arabidiol in the CYP705A1 active site is illustrated in Figure 2.8. The C_3-OH atom makes a hydrogen bond to both the main and side chain of Thr213; however, the hydroxyl group on C_{14} is not involved in any hydrogen binding. The H-bond made by the C_3-OH group and the orientation of the tricyclic moiety in the active site are comparable to the positioning of abiraterone (an sterol based inhibitor) in the active site of CYP17A1, the template used for homology modeling (PDB:3RUK) (DeVore and Scott, 2012). Two Phe residues (F223 and F224) mainly shape the active site and along with A371, T372, and V376 are in hydrophobic interaction to the alkyl chain of arabidiol (Figure 2.8).

The predicted coordination of arabidiol in the active site may properly be allied with the C-C bond cleavage through the radical attack by [Fe(III)-O-O]$^{\bullet}$ and hydrogen abstraction from C_{16} of the arabidiol molecule followed by an internal atomic rearrangement that leads to the C-C bond breakage (Figure 2.9). In addition, the relative position of C_{16} indicates the hydrogen abstraction is probably a *syn* elimination reaction since the hydrogen atom on the same side of the hydroxyl group is closer to the Fe atom (Figure 2.9). This is in agreement with previous studies on homology modeling of CYP82G1 and substrate docking experiments, which suggested that the oxidative degradation of the alcohol substrates (*E*)-nerolidol and (*E*,*E*)-geranyllinalool proceeds via syn-elimination of the polar head, together with an allylic C-5

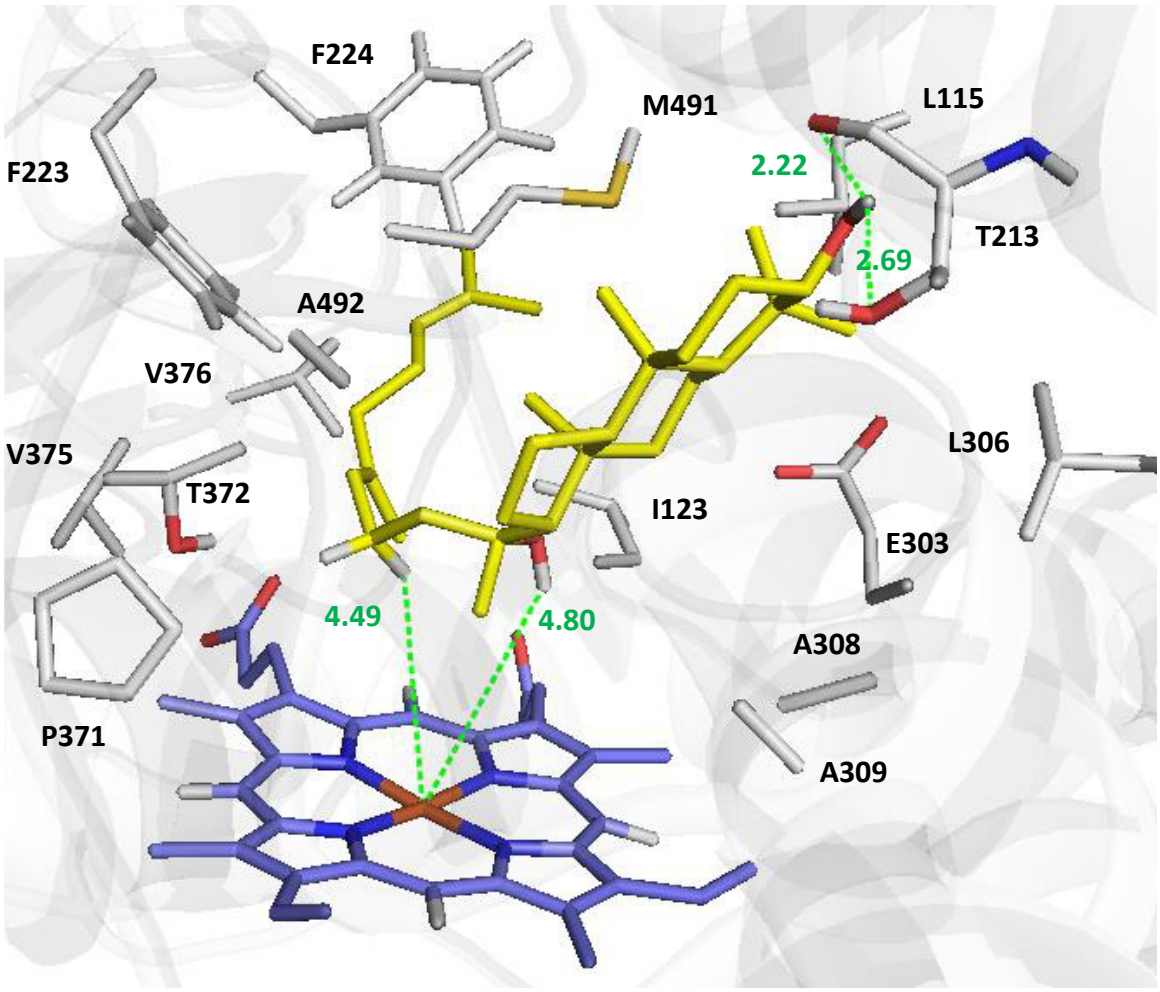

Figure 2.8 Docked conformation of arabidiol in the active site of modeled CYP705A1.

Docking was performed using AutoDock-Vina. The structure of the arabidiol molecule to be docked into the active site of modeled CYP705A1 was taken form ZINC database (ZINC 59211647). The most energetically favorable orientation of arabidiol with -8.9 Kcal/mol binding affinity is shown. The side chains of residues in 5 Å of substrate are illustrated. The main chain of Thr213 forms a H-bond to C_3-OH of arabidiol. The figure is prepared by PyMol.

hydrogen atom (Lee et al., 2010). Similar cleavage reactions of a tertiary alcohol catalyzed by P450s have been described for the dealkylation of 22-hydroxycholesterol into androstenolone (Akhtar and Wright, 1991) and the formation of the furanocoumarin psoralen from its precursor (+)-marmesin (Larbat et al., 2007). CYP705A1, a P450 enzyme of the Brassicaceae-specific

CYP705 family, shares only about 31% amino acid sequence identity with CYP82G1 however, the configuration of the arabidiol substrate with a tertiary hydroxyl group at its prenyl side chain makes a C-C cleavage mechanism equivalent to that catalyzed by CYP82G1 and marmesin synthase very likely. While it is not yet well understood whether CYP82G1 produces DMNT or TMTT in a single cleavage step or in two sequential steps, our results clearly demonstrate that CYP705A1 synthesizes DMNT by a one-step cleavage reaction with arabidonol as the second product (Figure 2.4C). Our analysis of JA-treated roots of the *cyp705a1* mutant showed an accumulation of small amounts of arabidiol, but the compound was not detected in JA-treated wild type roots, suggesting a rapid breakdown of the triterpene precursor. Since we were not able to detect arabidonol in roots of JA-treated wild type plants using GC-MS analysis, it is possible that this compound is further modified by additional downstream reaction steps.

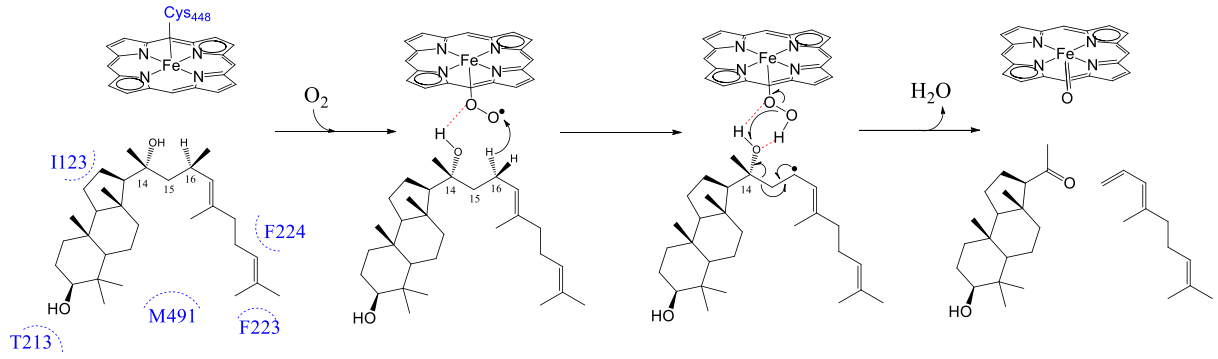

Figure 2.9 The proposed mechanism for oxidative degradation of arabidiol by CYP705A1

The coordination of arabidiol in the active site based on docking experiments is shown. Radical attack by [Fe(III)-O-O]$^{\bullet}$, hydrogen abstraction and subsequent internal atomic rearrangement are proposed for the C-C bond breakage of arabidiol to form arabidonol and DMNT. The figure is prepared by Ultra ChemDraw.

DMNT Biosynthetic Genes are Expressed in Specific Cell Types of the Arabidopsis Root and Respond to Jasmonate and Pathogen Treatment

According to their promoter GUS activities, both DMNT biosynthetic genes, *ABDS* and *CYP705A1*, are co-expressed primarily in the root vasculature under constitutive conditions. These expression patterns are consistent with those found in high resolution root gene expression maps (Birnbaum et al., 2003; Brady et al., 2007). Specifically, fine scale transcript profiles indicated an expression of *CYP705A1* in the pericycle at the root differentiation zone, which was confirmed in our study by the tissue-specific localization of the CYP705A1-eYFP fusion protein (Figure 2.6). Interestingly, we also found a highly cell type specific expression of the P450 protein in the quiescent center of the meristematic zone (Figure 2.6). In contrast to the *CYP705A1* gene, *ABDS* appears to be expressed in the entire meristematic zone. It is possible, that the specific activity of CYP705A1 in the root stem cells is required to remove the arabidiol precursor from this cell area because of putative inhibiting effects. A recent study supports this idea by showing stunted growth and root hair deficiency in oat triterpene biosynthetic mutants that accumulate triterpene intermediates in the epidermis (Mylona et al., 2008).Additionally a pericycle-specific expression at the root differentiation zone could be important both under constitutive and induced conditions as a barrier to avoid vasculature invasion by root pathogens such as nematodes. A similar pericycle specific expression profile was found for rhizathalene synthase in response to herbivore attack in *Arabidopsis* roots (Vaughan et al., 2013). The expanded expression in the elongation zone an area that is preferred by microbial pathogen infection positively correlates with potential defensive functions of arabidiol derived compounds. However it was difficult to observe induced gene expression with promoter-GUS assays *in vivo* upon Pythium infection primarily due to the transient nature of infection and the overall weaker

response compared to JA treatment.

While treatment with JA resulted in 10- and 5-fold transcript induction for *ABDS* and *CYP705A1*, respectively, inoculation with *P. irregulare* caused only a two-fold transient increase in expression of *CYP705A1* but had no effect on *ABDS* expression. Although both genes are required for the production of DMNT (Figure 4C), the induced formation of DMNT may not be regulated at gene transcript levels alone. Besides post-translational modifications, an increase in metabolite flux toward squalene and 2,3-oxidosqualene (Fulton et al., 1994), the common precursor in triterpene biosynthesis, might contribute to the enhanced formation of arabidiol and its breakdown products.

We observed only a transient breakdown of arabidiol and formation of DMNT at the time when oospores make initial contact with the root tissue and germ tubes start to penetrate the epidermis. Accordingly, expression of *CYP705A1* was transiently induced prior to highest emission levels of DMNT 3 h post-inoculation. A similar transient accumulation of transcripts was found for marker genes of JA- and SA-dependent pathways (e.g. *PR1*, *PDF1.2*) within the first 5 h of inoculation of *Arabidopsis* roots with the oomycete, *Phytophthora parasitica* (Attard et al., 2010). In accordance with these observations, the transient nature of DMNT production might be resulted from activity of pathogen effectors that suppress host-specific defense responses within several hours after penetration of the pathogen. Previous studies on the infection of *Arabidopsis* seedlings with *P. irregulare* suggested an infection process similar to that of a hemibiotrophic pathogen with the formation of biotrophic appressoria and haustoria at the beginning of the infection followed by a nectrotrophic movement of hyphae through the vasculature and invasion of all tissues. The suppression of host responses benefits a hemibiotrophic lifestyle, as described for *Phytophthora*-plant root pathosystems with biotrophic

growth of the pathogen in the root at an early stage of infection and a later switch to necrotrophic growth causing root loss (Schlink, 2010).

Arabidiol Breakdown Products are Involved in the Defense Against P. irregulare

Our results support a role of DMNT in chemical defense against *Pythium* showing that DMNT reduces *Pythium* mycelium growth and oospore germination *in vitro*. Although it is somewhat difficult to compare the actual concentration of DMNT released at the root surface with those in the *in vitro* assays, the concentrations of DMNT with inhibitory effects were in the range of the amounts emitted per g fresh weight of hydroponically grown roots. Due to the highly lipophilic nature of terpenes, it is assumed that terpenes exhibit antimicrobial activity by interfering with the integrity of the cellular membrane (disruption/alteration), which leads to ion leakage, membrane potential reduction, proton pump dysfunction and ATP pool depletion (Mann et al., 2000; Kalemba et al., 2002; Bakkali et al., 2008; Field and Osbourn, 2008b).

Despite the fact that the breakdown of arabidiol seems to occur only within the first hours of infection, our comparative studies on long term disease assessment using oospore counting assays in wild type and arabidiol and DMNT biosynthesis mutants demonstrate that metabolites of the arabidiol degradation pathway have a partial contribution from the onset of infection to slow down the infection process in roots. The volatile and non-volatile breakdown products might exhibit different activities in this process. While DMNT appears to be primarily effective at the stage of oospore germination and penetration, it may also have signaling or priming effects. It has been shown that volatile blends including homoterpenes that are released from a site of wounding or infection can function as systemic signals by priming non-affected parts of the plant for defense responses (Frost et al., 2007). Since arabidonol did not have inhibitory

activity *in vitro*, we assume that its derivatives that are modified in the root tissue are functionally more important defense compounds. Strong antifungal activities have previously been described for root-produced triterpene saponins such as avenacin that is secreted from oat roots (Mary et al., 1986). Since the concentrations of arabidiol and other triterpenes in *Arabidopsis* are low compared to those in the roots of other plants such as oat, they represent only one component in the chemical defense machinery of *Arabidopsis* roots. Bednarek et al. (2005) reported that the infection of *Arabidopsis* roots with *P. sylvaticum* in axenic culture induced changes in the concentrations of secondary metabolite changes including indole glucosinolates and phenylpropanoids. Together, these specialized metabolites combined with other chemical and physical responses such as the formation of ROS or the reinforcement of cell walls (Adie et al., 2007; Oliver et al., 2009) may contribute to the comparatively mild pathogenicity of the *P. irregulare* strain investigated in this work on mature wild-type *Arabidopsis* plants.

Evolution of DMNT Biosynthesis in Arabidopsis via Triterpene Gene Cluster Assembly

To obtain insights on the evolution of the DMNT biosynthetic pathway in *A. thaliana* roots, we compared the chromosomal region of the *ABDS* and *CYP705A1* gene loci to those in close relatives of *Arabidopsis* including *Capsella rubella* (belonging to a genus close to *Arabidopsis*) and *A. lyrata*. Based on this genome synteny analysis and phylogenetic analysis of several genes on the *ABDS* gene cluster, we propose a genome evolutionary history for arabidiol biosynthesis and cleavage as depicted in Figure 2.10. The *ABDS* region in *A. thaliana* contains two triterpene synthase genes, *ABDS* and a baroul synthase (BARS), which has 84% amino acid sequence identity to the ABDS protein. *ABDS* and *BARS* cluster with 4 members of the

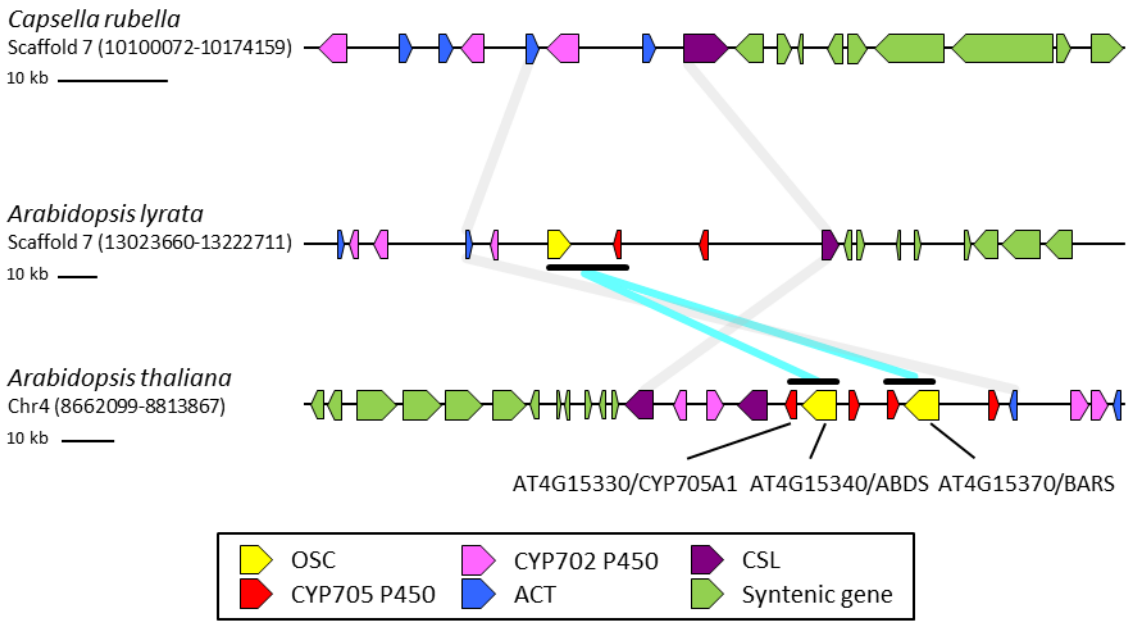

Figure 2.10 Comparative Genome Analysis Maps of ABDS Gene Cluster.

Synteny map for ABDS cluster between *C. rubella*, *A. lyrata*, and *A. thaliana* is shown. No OSC gene ortholog was found on highly syntenic region in *C. rubella*. One OSC and two CYP705 P450 members were present in *A. lyrata*. In *A. thaliana* two OSC and four CYP705 members were found. A duplication of CYP705A3 and BARS gene orthologs in the common ancestor followed by inversion of CYP705 gene in *A. thaliana* could be likely source of DMNT biosynthesis gene evolution. Different gene families are color coded. Syntenic region flanking ABDs gene cluster are connected with grey line. The syntenic regions for DMNT biosynthesis gene are shown with cyan line.

Brassicaceae specific CYP705 family, *CYP705A1*, *A2*, *A3* and *A4*. Interestingly, neither a triterpene synthase nor a CYP705 member was found on the *ABDS* syntenic region in *C. rubella* (Figure 2.10), but in *A. lyrata* a single triterpene synthase gene with 92% amino acid sequence identity to *BARS* and two P450s (*CYP705A2* and *CYP705A3*) are present in this region. According to a phylogenetic analysis of *CYP705A* genes on the syntenic regions (Supplemental Figure 19), *ABDS* and *CYP705A1* presumably have evolved after the divergence of *A. lyrata* and *A. thaliana* from their common ancestor of 5 Mya via a localized segmented duplication of *BARS*

and *CYP705A3* followed by an inversion of *CYP705A1* and neofunctionalizatoin of both genes in *A. thaliana* (Figure 2.10).

A related, highly coordinated triterpene gene cluster has recently been described for the formation and modification of the triterpene thalianol in *Arabidopsis* roots (Field and Osbourn, 2008b). Thalianol is a tricyclic triterpene similar to arabidiol with no hydroxyl group in the prenyl side chain. Because of the lack of the tertiary hydroxyl group, thalianol is not cleaved by CYP705A1. Instead, thalianol undergoes hydroxylation of the tricyclic moiety and desaturation at the prenyl side chain, catalyzed by two P450 enzymes, CYP708A2 and CYP705A5, respectively (Field and Osbourn, 2008b). A second functional triterpene/P450 gene cluster has been described for the biosynthesis and modification of marneral, an unusual monocyclic triterpene aldehyde, in *Arabidopsis* with a high degree of co-regulation for clustered genes (Field et al., 2011).

To study the underlying evolution of arabidiol cleavage activity in CYP705A1, we used a substrate docking and comparative protein homology modeling approach to examine the properties of the CYP705A1 active site and other CYP705 members on the gene cluster. Sequence alignment and homology modeling indicate variation in the active site between CYP705A1 and the other Arabidopsis CYP705A paralogs. Particularly, the active site of CYP705A5 involved in desaturation of the thalianol side chain is not conserved in comparison to that of CYP705A1 (Supplemental Figure 2.20). Only four residues (L115, F223, P371 and M491 based on sequence numbering of CYP705A1) out of 18 active site residue are conserved residues among CYP705A1-A5 suggesting enzyme-substrate specificity has diverged extensively after gene duplication events. Homology modeling of A2-A5 using the structure of CYP705A1 as the template suggests several alterations in the active site may be associated with their lack of

activity toward arabidiol. Residue T213, which form a H-bond to the C3-OH group of arabidiol is replace by V/A in other members. Furthermore, F223 that faces toward the active site and plays a major role in shaping the binding cavity in CYP705A1 is replaced by amino acids with smaller side chain (I, L, H). Two tandem alanine residues (A308 and A309) are replaced in all the other members of family by GT. These replacements reduce the hydrophobicity of the microenvironment and may affect the orientation of C_{14}-OH of arabidiol. Docking of arabidiol into the active site of modeled CYP705A2-A5 proteins did not result in reactive coordination of arabidiol and this molecule was bond in reverse orientation compared to its docked configuration in the active site of A1. In this orientation, C14 and C15 atoms of arabidiol are not accessible by oxygen activated heme. Therefore, the amino acid combinations in the active site of CYP705A2-A5 more likely interfere with the binding of arabidiol than affecting the mechanism. In conclusion, the ability of CYP705A1 to cleave arabidiol has been evolved presumably by substitution of several amino acids in the active site (including T213 and G223) after gene duplication events in the *ABDS* gene cluster region.

It is possible that other genes of the *ABDS* gene cluster are involved in downstream modifications of the arabidonol cleavage product such as hydroxylation and/or glycosylation, although these genes are not as tightly co-expressed with *CYP705A1* and *ABDS,* which is also the case in the thalianol cluster. Gene clusters such as those described for thalianol and marneral have been found in other terpene metabolic pathways such as the one responsible for the biosynthesis of diterpenes in rice (Shimura et al., 2007). The selective forces driving the evolution of gene cluster assembly in terpene metabolism are not well understood and require further attention. In summary, the formation of DMNT in *Arabidopsis* roots evolved as part of a

triterpene biosynthesis gene cluster indicating plasticity in the biosynthesis of homoterpene volatiles and differences of specialized metabolic pathways above- and belowground.

METHODS

Plant Materials and Growth Conditions

Arabidopsis mutants (*abds-1, abds-2, cyp705a1-1,* and *cyp705a1-2)* used in this study were from the wild-type Col-0 genetic background and were acquired from the ABRC stock center (Alonso et al., 2003). The *coi1-1* was kindly provided by John G. Turner (Xie et al., 1998). All plants were grown in short day (10-h light/14-h dark photoperiod) under standard growth conditions ($150\,\mu$mol $m^{-2}\,s^{-1}$ photosynthetically active radiation (PAR), 22°C, 55 % relative humidity (RH).

Axenic plants were maintained as described by Hetu et al. (2005). Two days before treatments and harvesting the root tissue, the MS medium was changed to reduce the sucrose concentration to 1%. JA treatment was done by applying 100 µM JA (Sigma Aldrich, St. Louis, MO) directly to root cultures in the liquid medium. Hydroponic cultures were established by transferring 4-week-old soil grown plants to plastic containers containing Hoagland's medium under constant aeration as previously described (Gibeaut et al., 1997). Plants were grown for three to four weeks in hydroponic culture before volatile analysis. *Arabidopsis* hairy root cultures was kindly provided by Dr. John Jelekso lab and were grown on Gamborg's B5 liquid media with 2% sucrose. Cultures were kept at room temperature under dark conditions and with constant shaking at 75 rpm for two weeks at before treatment and analysis. JA treatment was done as described for axenic culture. P450 inhibitor treatments were done at 5 and 50 µM

concentration along with JA treatment for 24 h.

Volatile Collection and Analysis

Root volatiles from axenically or hydroponically grown plants were collected in the head space and analyzed by SPME-GC/MS. One gram of roots (fresh weight) was detached from plants and placed in screw-capped vials (20 mL) containing 1 mL of distilled water with 10 ng of 1-bromodecane as an internal standard. Root volatiles were adsorbed with a 100 µm polydimethylsiloxane fiber (Supelco) for 30 min at room temperature following incubation at 30ºC for 30 min in the headspace of a screw-capped vial (20-mL GC vial). Volatile compounds were desorbed from the fiber at 240°C (4-min) with a splitless injection and analyzed with a Shimadzu GC/MS-QP2010S. Separation was performed on an Rxi-XLB column (Restek) of 30 m x 0.25 mm i.d. x 0.25 μm film thickness. Helium was the carrier gas (1.4 mL min^{-1} flow rate), and a temperature gradient was applied at 4°C min^{-1} from 40°C (2-min hold) to 220°C followed by a gradient of 5°C min^{-1} from 40°C to 220°C and 20°C min^{-1} from 220°C to 240°C (2-min hold). Identification of all volatile compounds was achieved by comparison of their retention times and mass spectra with those of authentic standards and with mass spectra of the National Institute of Standards and Technology and Wiley libraries (John Wiley & Sons, Inc., New York, NY).

Standardization of the SPME-based volatile analysis for C_{11}-homoterpene 4,8-dimethyl-1,3,7-nonatriene (DMNT) was validated by performing the volatile analysis with and without root materials. Incubation was carried out in the presence of DMNT and 1-bromodecane standard with or without root material, and volatiles were analyzed as described above. Linear calibration was obtained between 5 and 50 ng (for 1-bromodecane, $R^2 = 0.99$; DMNT, $R^2 = 0.99$).

Genotyping of Plant Material

A T-DNA insertion line of the *CYP705A1* gene (*cyp705a1-1*, SALK_043195) with an insertion in the second exon was obtained from ABRC. Also, two independent T-DNA insertion lines, *abds-1* (SALK_018285) and *abds-2* (SALK_067736), with insertions in exon 1 and intron 5, respectively were obtained for the *ABDS* gene. Homozygous mutants were confirmed by PCR and the absence of full-length transcript in these mutant lines was verified by RT-PCR.

Construction and Analysis of Transgenic Plants

The full-length cDNAs of the *CYP705A1* and *ABDS* genes were prepared from 1 µg of total RNA extracted using the Tri reagent (Fisher) (Huang et al., 2010) from axenically grown Col-0 roots treated with JA for 24 h with full length cloning primers listed in Supplemental Table 2.4 using proofreading enzyme P*fx* Turbo Cx hot start (Stratagene). The amplified fragments were cloned into the pENTR/D-TOPO vector (Invitrogen). For construction of *CaMV 35S* over-expression lines, the *ABDS* and *CYP705A1* cDNAs were subcloned into the pB7WG2 vector (Karimi et al., 2002) using LR recombination (Invitrogen). For construction of promoter:GUS fusion vectors, 1.5 kb and 2.6 kb fragments upstream of the start codon for *CYP705A1* and *ABDS*, respectively, were amplified from genomic DNA, cloned into pENTR/D-TOPO and recombined into pKGWFS7 (Karimi et al., 2002). Plant transformation was done with the *Agrobacterium tumefaciens* strain GV3101 using the vacuum infiltration method (Bechtold et al., 1993). Transformants were screened on half strength MS plates with 1% (w/v) sucrose and 75 µg mL^{-1} kanamycin. Histochemical GUS assays were performed as previously described (Vitha et

al., 1993) for least three independent lines in the T_2 generation. GUS staining was observed with an Olympus SZX16 microscope.

To construct the *ProCYP705A1:CYP705A1-eYFP* line, first the 1.5 kb promoter region upstream of start codon was subcloned into the pDONR P4-P1R vector (Invitrogen) via BP reaction using primers P5 and P6 (Invitrogen). Then, the LR reaction was done using pDONR P4-P1R and pENTR/D-TOPO vectors carrying promoter and gene fragments, respectively, with the pB7Y24WG binary destination vector (Tholl Lab) carrying the eYFP coding sequence. The pB7Y24WG was constructed by replacing the attR1 and promoter elements region in pB7YWG2 with attR4 region from pK7m24GW using *Eco*RI and *Sac*I digestion and ligation reactions. Upon introduction of the *ProCYP705A1:CYP705A1-eYFP* construct into *A. tumefaciens* strain GV3101, *cyp705a1-1* plant transformation was done by floral vacuum infiltration. Transgenic plants were identified by spraying soil grown plants with 0.01% BASTA solution. Root samples from three independent T2 transgenic lines were mounted on a microscope slide with distilled water and visualized using a Zeiss Axiovert 200 inverted fluorescence microscope with FITC (*l*ex = 480 nm; *l*em = 535 nm), Texas Red (*l*ex = 570 nm; *l*em = 625 nm) fluorescent filter sets, an attached MRc5 Axiocamcolor digital camera, and an LD Achroplan 40X objective. Propidium iodine (PI) staining was done in liquid growth medium by incubating with 10 µg/mL of PI up to 30 min before confocal microscopy analysis.

Yeast Expression, Arabidonol Purification and Enzyme Assays

For establishing yeast co-expression lines, the full-length cDNA of *CYP705A1* was amplified using primers P7 and P8, and directionally cloned into the multiple cloning site1 region of the pESC-TRP vector (Stratagene) and was expressed under the galactose-inducible

promoter GAL10. The *mut-CYP705A1* cDNA with a truncation in the heme binding domain was amplified using primers P7 and P9 and subcloned into pESC-TRP as described above. The *ABDS* full-length cDNA was recombined into the Gateway yeast expression vector YEp352-GW under control of the constitutive *ADH1* promoter (Takahashi et al., 2007). Both vector constructs were simultaneously transformed into the yeast line WAT11 (Urban et al., 1997) by following the protocol described by the provider of the pESC-TRP vector (Stratagene). Transgenic yeast strains were grown in yeast selective media (SGI) and protein expression was done as described previously (Takahashi et al., 2007). For DMNT production assays in yeast expression lines, 4 ml of yeast culture induced with 2% galactose for 16 h was transferred to a screw cap SPME vial and allowed to grow for another 4 h at 28 ºC at 220 rpm , followed by direct headspace volatile analysis using SPME-GC/MS. Protein expression for microsomal purification was done according to Takahashi et al. (2007) and enzyme assays were performed as described in (Lee et al., 2010) with 55 µM arabidiol substrate purified as described previously (Xiang et al., 2006).

To produce arabidonol in large quantities, we used transgenic yeast lines expressing *ABDS* and *CYP705A1*. A 2 L of yeast culture was prepared in YPI medium and induced with 2% of galactose. DMNT levels were monitored every day to ensure continuous degradation of arabidiol and production of arabidonol. After 3 days of galactose induction, 0.5 L of acetone was added to yeast culture to burst open cells followed by three times extraction with 1 L of ethyl acetate. The ethyl acetate extracts were combined and organic solvent was removed to dryness under low pressure using a rotary evaporator (Cole-Parmer). Then, the extract was subjected to flash chromatography over silica gel (Merck grade 9385, pore size 60 Å, 230-400 mesh, Sigma). For transferring the extract to the column, first, a slurry of extract was prepared by adding 50 mL of ethyl acetate and 3 g of silica gel to the round bottom flask followed by rotary evaporation to

obtain dried silica particles attached to the extracts. Then the silica gel with the extract was loaded onto a silica gel flash chromatography column preconditioned with 5:2 Ethyl acetate:Hexane and several fractions were collected. Upon verification of presence of arabidonol in fractions by GC-MS aliquots of fractions containing arabidonol were individually loaded on preparative thin layer chromatography (TLC) plates (20 x 20 cm silica gel pore size 60 Å (250 µm) with 2.5 x 20 cm concentration zone) and developed with a 5:2 mixture of hexanes:ethyl acetate as described before. Silica gel was scraped from the plates at an R_f value similar to that of arabidonol and the purity of the extracted compound was evaluated by GC-MS analysis.

Transcript Analysis by RT–PCR and Quantitative Real-Time PCR

Total RNA was extracted from 100 mg of root tissue using the TRIzol reagent (Invitrogen) according to (Huang et al., 2010). Two µg of total RNA was converted into cDNA using SuperScript II (Invitrogen) according to the manufacturer's instructions. The expression of P450 candidates in root tissues was monitored by semi-quantitative RT-PCR according to (Huang et al., 2010) using gene specific primers designed by Prime-BLAST (Ye et al., 2012) listed in Supplemental Table 2.4. Homozygous mutants were identified using PCR based genotyping and full length *ABDS* and *CYP705A1* transcript expression was analyzed by RT-PCR using corresponding gene specific full length primer pairs (Supplemental Table 2.4). Quantitative real-time PCR was done according to Lee et al. (2010) using gene specific primers (Supplemental Table 2.4). Threshold cycle (Ct) values for *ABDS* and *CYP705A1* were normalized to the ubiquitin conjugating enzyme (*UBC21*) using primers listed in (Supplemental Table 2.4).

Growth and Bioassay Conditions of P. irregulare

P. irregulare 110305 was grown and maintained as described by (Huffaker et al., 2006) and kindly provided by Dr. Clarence A. Ryan. One-week-old *P. irregulare* cultures were collected from the plates into sterile water and lightly ground with a mortar and pestle to yield a uniform suspension. Aliquots (300 µL) of the suspension (≈ 2.475 X 10^3 propagules) or water (used as a control) were added to the growth medium of axenically grown cultures containing approximately 20 plants per flask. Microscopy analysis of *Arabidopsis* root infection was done using five-day-old *Arabidopsis* seedlings grown on six-well plates containing 3 mL of ½ x MS media with 1% sucrose under short day conditions infected with *P. irregulare* as described previously (Adie et al., 2007). To observe *P. irregulare* on root tissues lactophenol-trypan blue staining (Koch and Slusarenko, 1990) was performed and followed by sample mounting in 50% glycerol and observed under a Olympus SV-16 stereomicroscope.

Disease assessment with *Pythium* on wild-type and DMNT biosynthetic mutants was performed by measuring oospore abundance 18 days after infection of plants in potting substrate. Plants were grown in jiffy pots (Φ 5 cm, height 6 cm) for three weeks under short day conditions (10-h light/14-h dark). *Jar1-1* (jasmonate signaling mutant) was used as a positive control for disease assessment due to its high susceptibility to *Pythium* (Staswick et al., 1998). Randomly selected individual plants were then transplanted along with the jiffy pot into single pots (6x6x8 cm^3) containing *Pythium*-infested potting substrate (Sunshine mix 1). *Pythium*-infested substrate was prepared by slicing Potato Dextrose agar (PDA) containing one week-old *P. irregulare* mycelium, mixing it with the substrate, and incubating the mixture for two days for a uniform infestation. For mock treatments, sliced PDA pieces without *Pythium* were mixed with the substrate. Disease assessment was performed by counting the abundance of oospores inside root

tissues by staining of roots with acid-fuchsin lactophenol (Vijayan et al., 1998).

Oospore Isolation and Germination of P. irregulare 110305

Oospores were prepared following previous studies with minor changes (Yuan and Crawford, 1995; Manici et al., 2000). Briefly, an agar plug from 4-day-old cultures on PDA was inoculated on a V8 juice (Campbell Juice co.) agar plate and incubated at room temperature under dark conditions. After 10 days, V8 agar plugs containing mycelium were transferred into distilled water and further incubated for 10 days under dark conditions. The cultures containing abundantly produced oospores were comminuted with distilled water by a Polytron tissue homogenizer. The homogenized mycelial and oospore mixture was filtered through two layers of cheesecloth, and then the filtrate was subjected to centrifugation (4,500 x *g* for 10 min). The pellet was suspended in distilled water, and the concentration of oospores was determined using a hemacytometer.

To determine the germination rate of oospores according to chemical treatment, oospore germination conditions were applied as described by (Ruben and Stanghellini, 1978). Oospores were induced to germinate directly on corn meal agar (Difco) containing different concentrations of DMNT with 15 μg mL^{-1} streptomycin. One hundred microliters of oospore suspension were applied to the surface of an agar plate (about 200 oospores per plate) and incubated for 24 h in an incubator at 27ºC under dark conditions. The oospore germination rate was measured by counting oospores with emerging germ tubes using light microscopy.

SUPPLEMENTAL MATERIALS

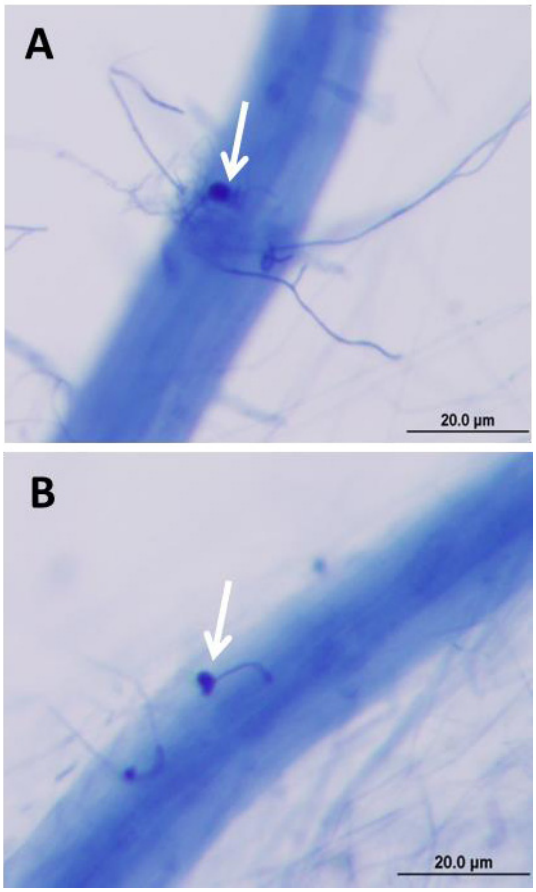

Supplemental Figure 2.1 Infection of *Arabidopsis* roots with *P. irregulare*.

Five-day-old *Arabidopsis* seedlings were used to monitor the infection process. A uniform suspension of mycelium and oospores of a one week-old *P. irregulare* culture grown on potato dextrose agar (PDA) plates was used for infection. According to different time points, approximately ten seedlings were observed after staining with lactophenol-tryphan blue. Arrows show *Pythium* oospores attached to the root surface with germinated infection hyphae three hours post inoculation (A and B).

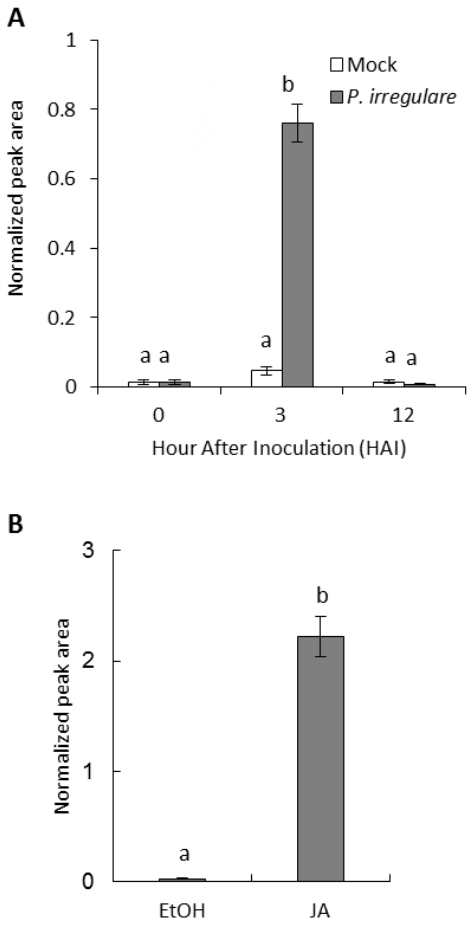

Supplemental Figure 2.2 DMNT emission from hydroponically grown Arabidopsis roots.

Hydroponically grown *Arabidopsis* roots were infected with *P. irregulare* (A) or treated with 100 µM JA (B). Root volatiles were analyzed at different time points (3 h, 12 h and 24 h for *Pythium,* 24 h for JA) by SPME-GC/MS. Normalized peak areas are shown. Values represent the mean ± SE of three biological replicates. $P < 0.05$, One-way ANOVA, Tukey-Kramer HSD test for all comparisons of mock and treatments (A) , $P<0.01$, Student t-test (B).

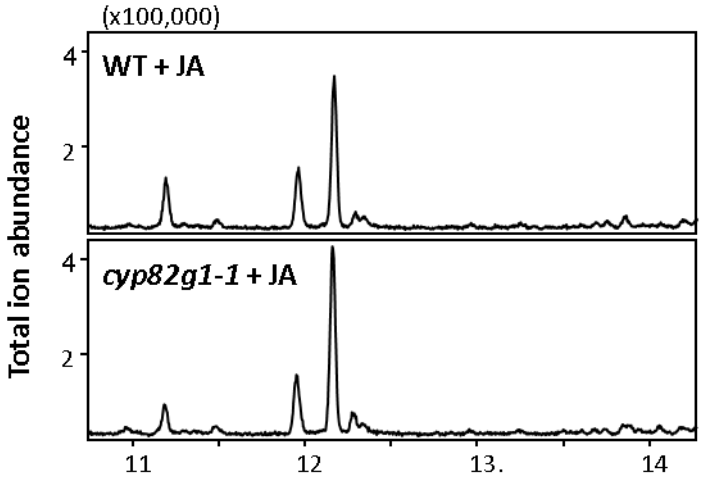

Supplemental Figure 2.3 The *cyp82g1-1* T-DNA insertion mutant is not impaired in JA induced production of DMNT from roots.

GC chromatograms of induced emission of DMNT upon JA-treatment in the *cyp82g1-1* mutant and wild type Col-0 plants are shown. DMNT emission is not impaired in the *cyp82g1-1* mutant suggesting a role for other cytochrome P450 enzymes in root-specific DMNT formation.

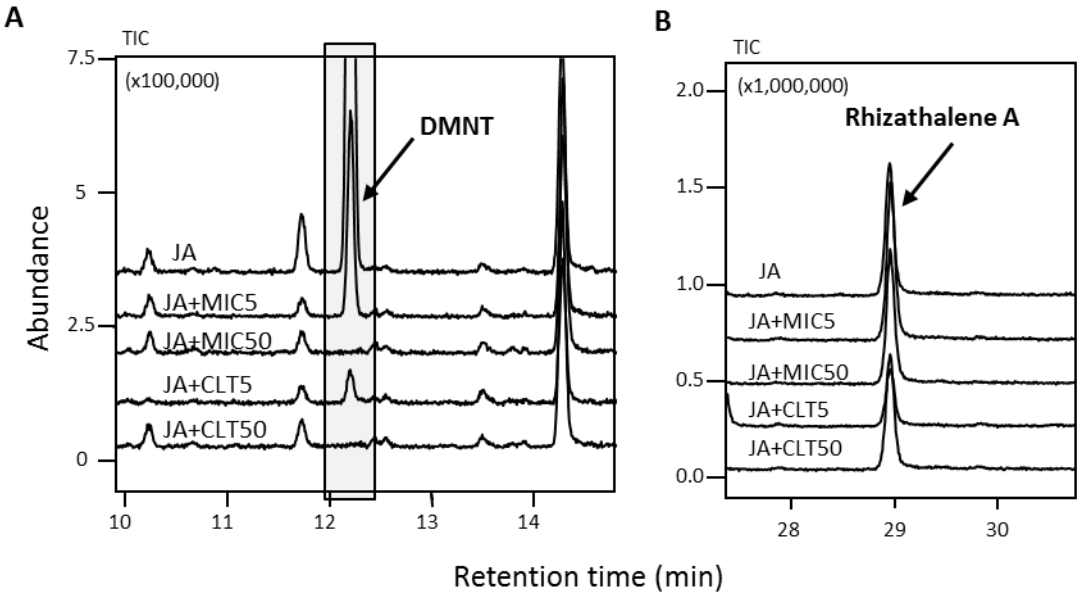

Supplemental Figure 2.4 Pharmacological study of DMNT formation in *Arabidopsis* hairy root culture.

(A) Treatment of hairy roots with the cytochrome P450 monooxygenase-specific azole inhibitors miconazole (MIC) and clotrimazole (CLT) at 50 μM concentration resulted in abolishing the production of DMNT. (C) Production of recently characterized volatile diterpene rhizathalene was not affected by inhibitor treatment.

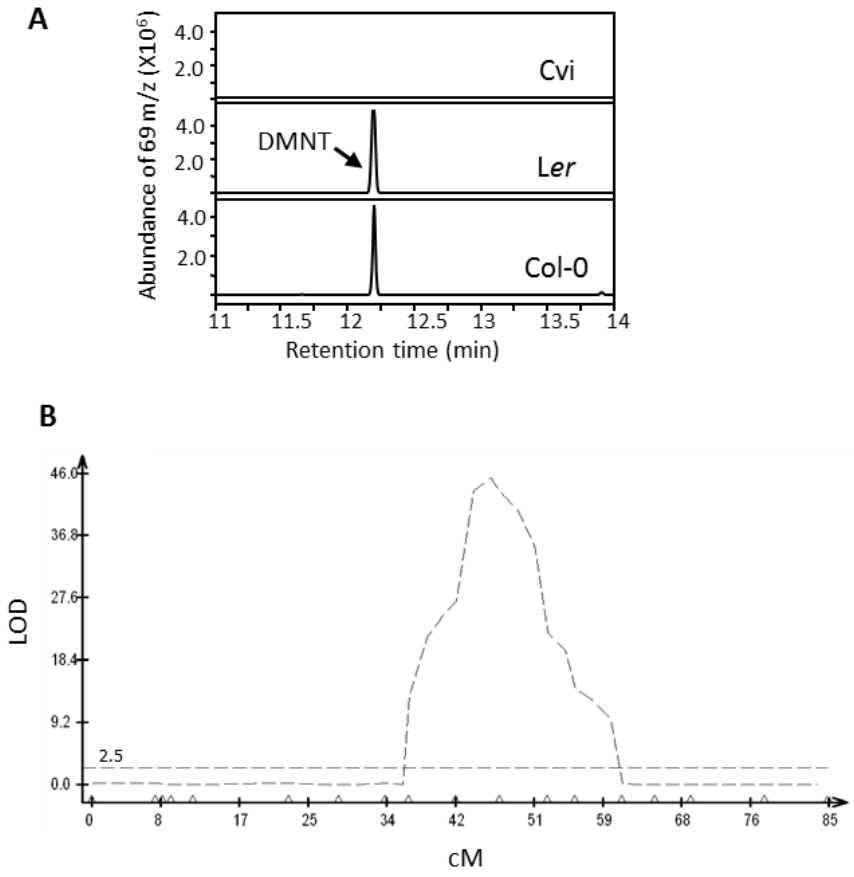

Supplemental Figure 2.5 QTL analysis of natural variation in DMNT biosynthesis among Arabidopsis accessions.

(A) GC chromatograms of induced emissions of DMNT after 24 h of JA treatment in the L*er*, Cvi and Col-0 *Arabidopsis* accessions. No DMNT was detected from the Cvi accession while the volatile was produced from roots of Col-0 and L*er*. (B) Identification of the QTL region for DMNT formation in the L*er* X Cvi RILs. The y axis is in log of the odds units, and the x axis is in centimorgan (cM); the horizontal lines represent the 0.05 significance threshold determined by 1,000 permutations (Hansen et al., 2008).

Selection criteria	Gene name	AGI number
MJ and wounding	CYP71A19	AT4G13290
MJ and wounding	CYP71A20	AT4G13310
MJ and wounding	CYP81D11	At3G28740
MJ and wounding	CYP81D1	AT5G36220
MJ and wounding	CYP705A12	AT5G42580
MJ and wounding	CYP708A3	AT1G78490
MJ and wounding	CYP705A1	AT4G15330
MJ and wounding	CYP71A12	At2G30750
MJ and wounding	CYP81D8	AT4G37370
TPS co-expression	CYP76C4	AT2G45550
TPS co-expression	CYP78A8	AT1G01190
TPS co-expression	CYP705A4	AT4G15380
TPS co-expression	CYP705A18	AT3G20090
TPS co-expression	CYP705A13	AT2G14100

Supplemental Table 2.1 DMNT Biosynthesis Gene Candidates.

List of all initial gene candidates and their corresponding name and Arabidopsis Genome Initiative (AGI) locus number is listed. Genes on the selected QTL region on chromosome 4 are highlighted in grey.

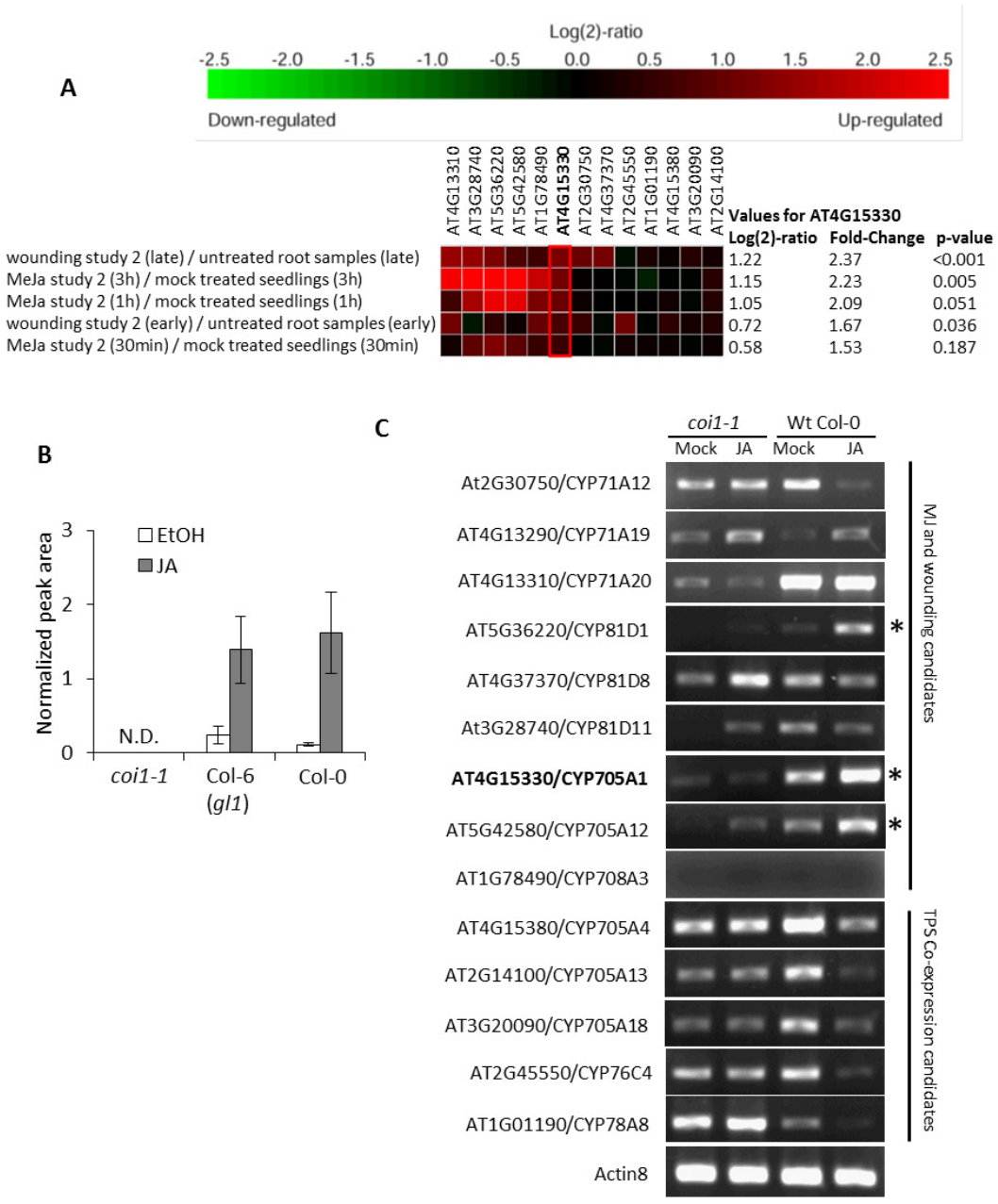

Supplemental Figure 2.6 Selection of Candidate P450 Genes for DMNT Biosynthesis.

(A) Expression of selected P450 candidate genes in wounding and methyl jasmonate (MJ) treatment datasets. (B) Volatile analysis in roots of *coi1-1*, and its corresponding background genotype Col-6 (gl1), and in wild type Col-0. No DMNT was detected in hydroponically grown *coi1-1* plants upon JA treatment. (C) RT-PCR analysis of candidate gene expression in *coi1-1* and WT Col-0 plants in JA and mock (ethanol) treatment. JA inducible and *coi1-1* regulated genes are marked with asterisks. Error bars represent SD ± mean values of three replicates.

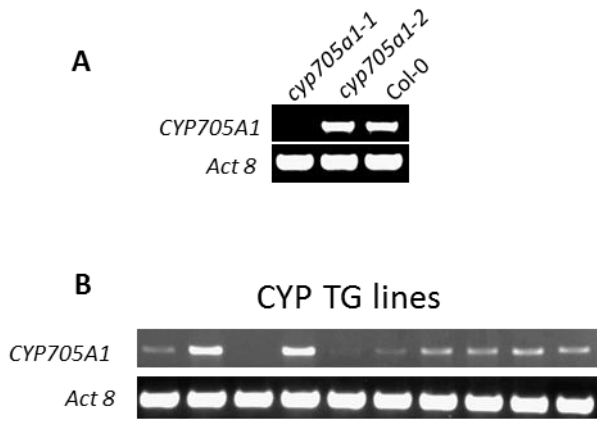

Supplemental Figure 2.7 RT-PCR Analysis of *CYP705A1*.

RT-PCR analysis was performed on mRNA extracted from roots treated with JA for 24 h. The full length *CYP705A1* gene was amplified from cDNA prepared from different lines. Internal transcript of *Actin 8* was used as a control. (A) RT-PCR analysis roots in wild type Col-0 and two *cyp705a1* T-DNA insertion lines. (B) RT-PCR analysis of gene expression in roots of wild type Col-0 plants and two transgenic lines expressing *CYP705A1* under control of the native promoter fused to eYFP and the *CaMV 35S* promoter in the background of the *cyp70aa1-1* mutant

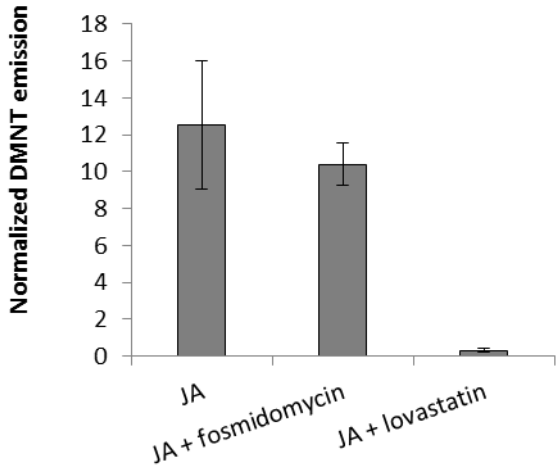

Supplemental Figure 2.8 DMNT formation in *Arabidopsis* roots is dependent on the mevalonate pathway of terpene precursor biosynthesis.

DMNT formation is not effected by fosmidomycin treatment at 400 µM. Volatile DMNT emission was significantly reduced in response to treatment with the mevalonate pathway inhibitor lovastatin at 50 µM suggesting a mevalonate dependent terpene biosynthetic route. LVS, lovastatin; FOS, fosmidomycin. Error bars represent SD ± mean values of three replicates.

COR	AGI No.	Gene annotation
0.781	At4g15340	pentacyclic triterpene synthase 1 (Arabidiol synthase)
0.65	At4g31100	wall-associated kinase, putative
0.62	At4g22610	Bifunctional inhibitor/lipid-transfer protein/seed storage 2S albumin superfamily protein

Supplemental Table 2.2 Candidate genes co-expressed with *CYP705A1* evaluated based on the ATTED-II database.

Annotation and correlation coefficients (COR) were adopted from ATTED-II (http://atted.jp/).

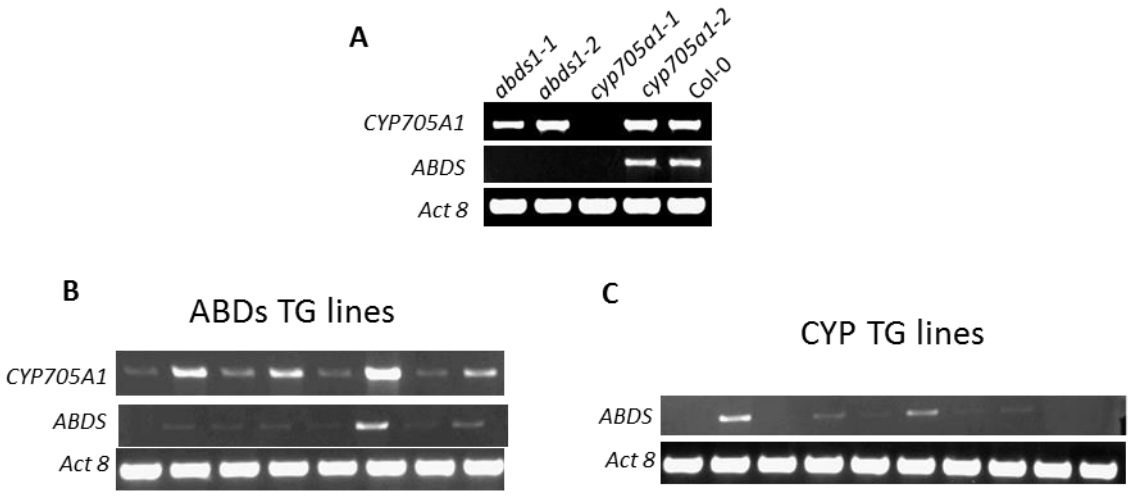

Supplemental Figure 2.9 RT-PCR analysis of *ABDS* and *CYP705A1* genes.

RT-PCR analysis was performed on samples treated with 100 μM JA for 24 h. The full length *ABDS* and *CYP705A1* genes were amplified from cDNA prepared from different lines. Internal transcript of *Actin 8* was used as a control.

(A) Transcript levels in DMNT biosynthetic mutants.

(B) Transcript levels in *ABDS* transgenic lines.

(C) *ABDS* and *Actin 8* transcript levels in *CYP705A1* transgenic lines.

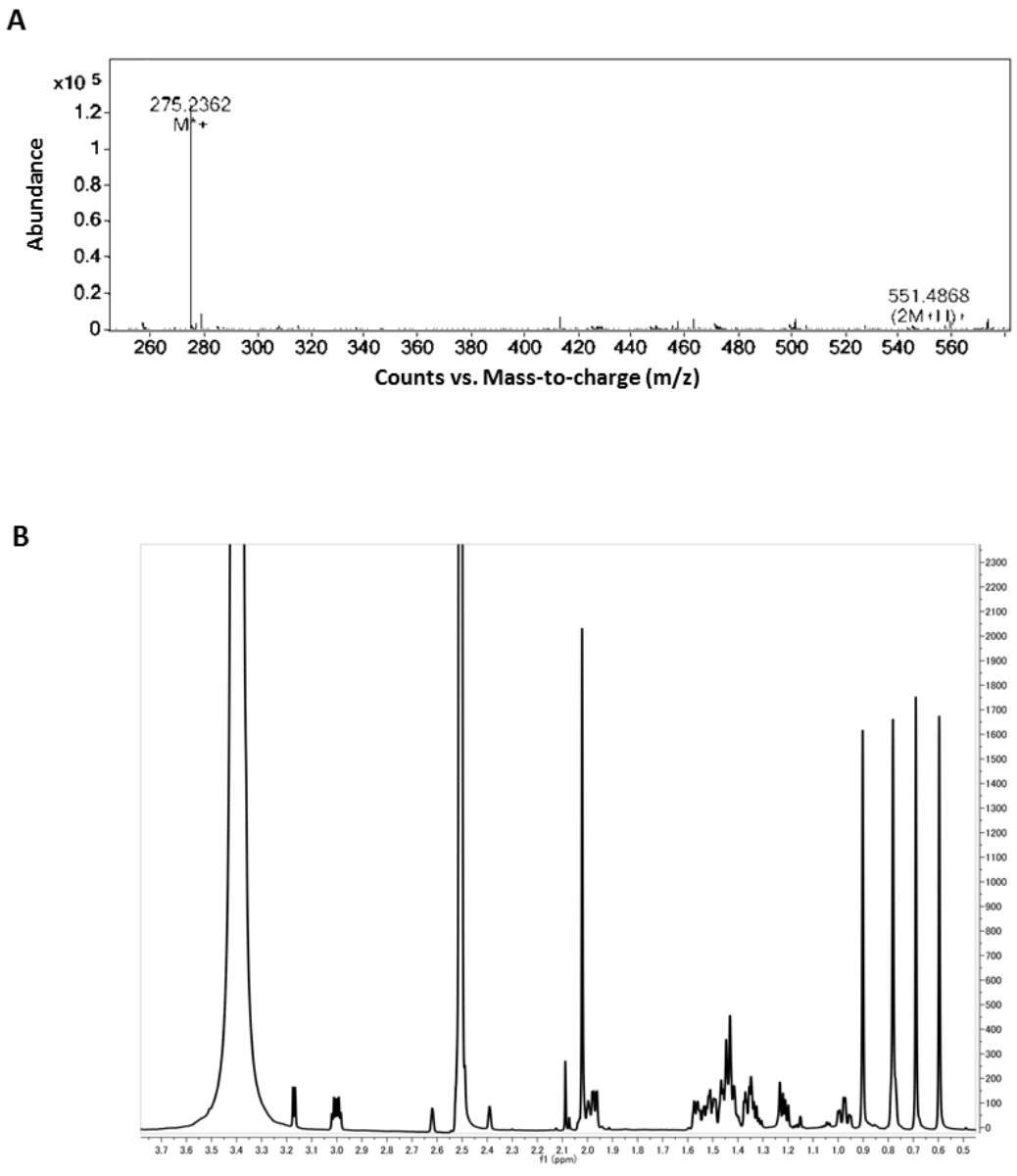

Supplemental Figure 2.10 HRESIMS analysis and ^{1}H-NMR spectrum of arabidonol.

(A) Detection of pseudomolecular ion peak at *m/z* 275.2362, $[M\text{-}OH]^{+}$. The *m/z* 551.4868 ion is for $(2M+H)^{+}$ or $C_{38}H_{63}O_2$ calculated for 551.4823.

(B) Full ^{1}H-NMR spectrum of arabidonol.

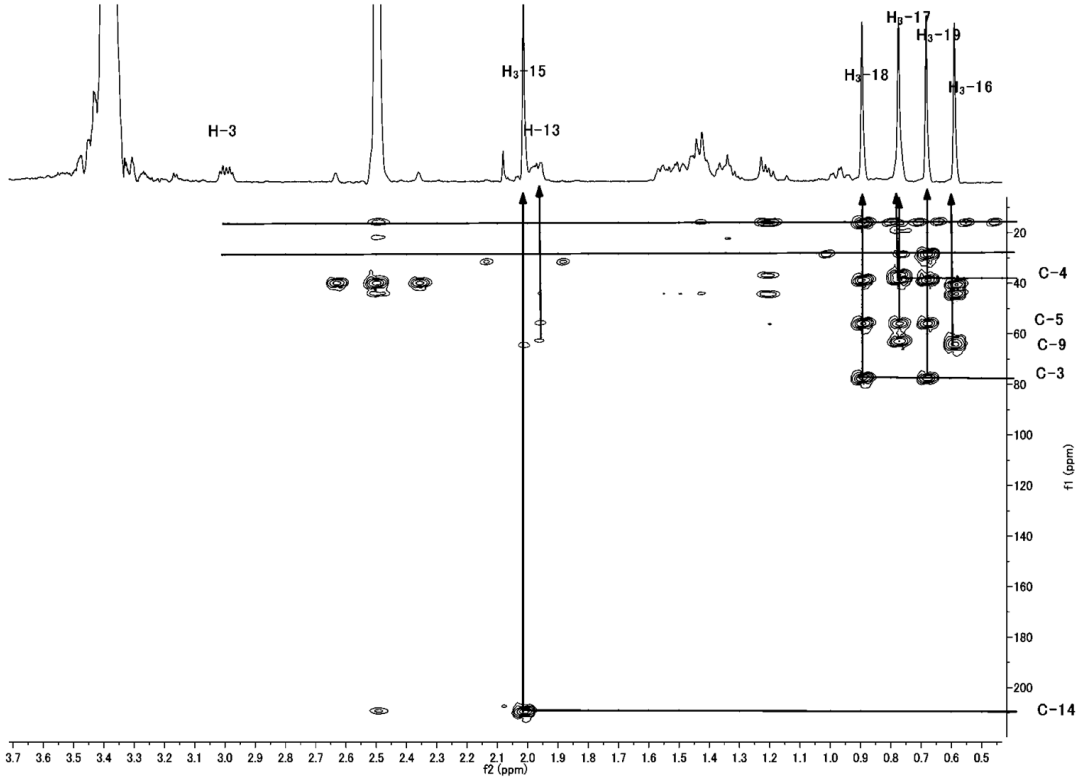

Supplemental Figure 2.11 Full HMBC NMR spectrum of arabidonol.

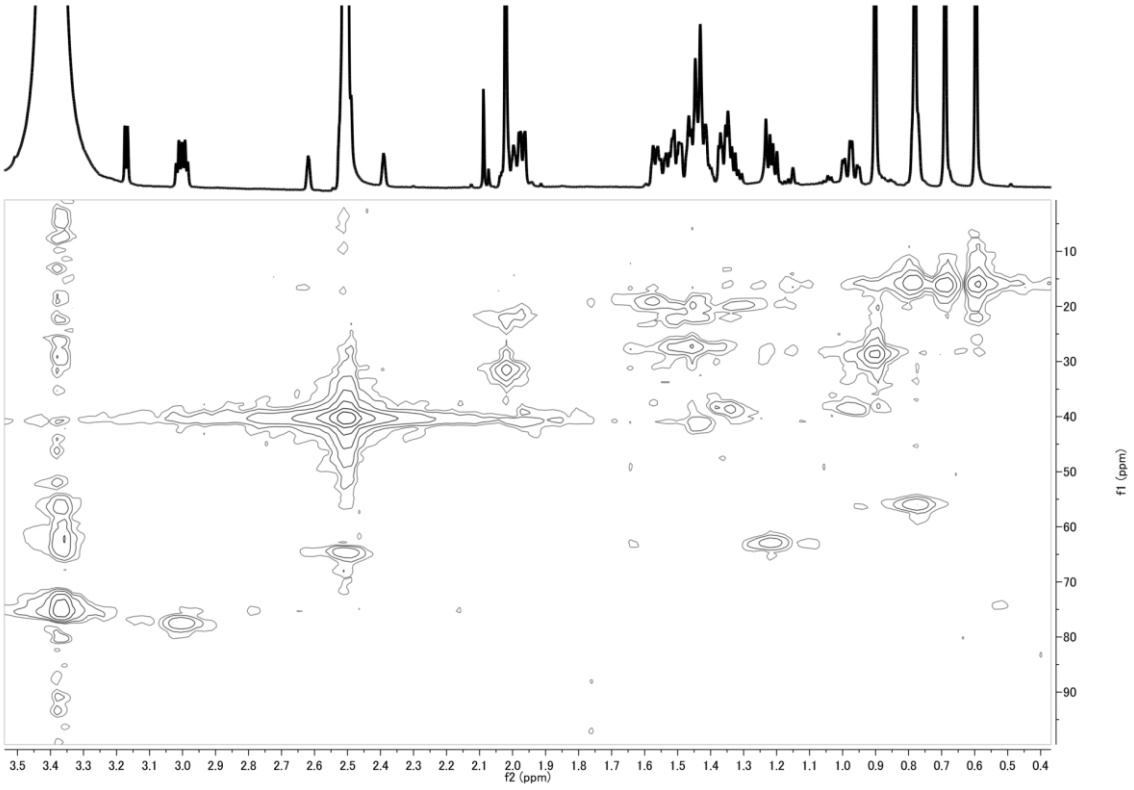

Supplemental Figure 2.12 HMQC NMR spectrum of arabidonol.

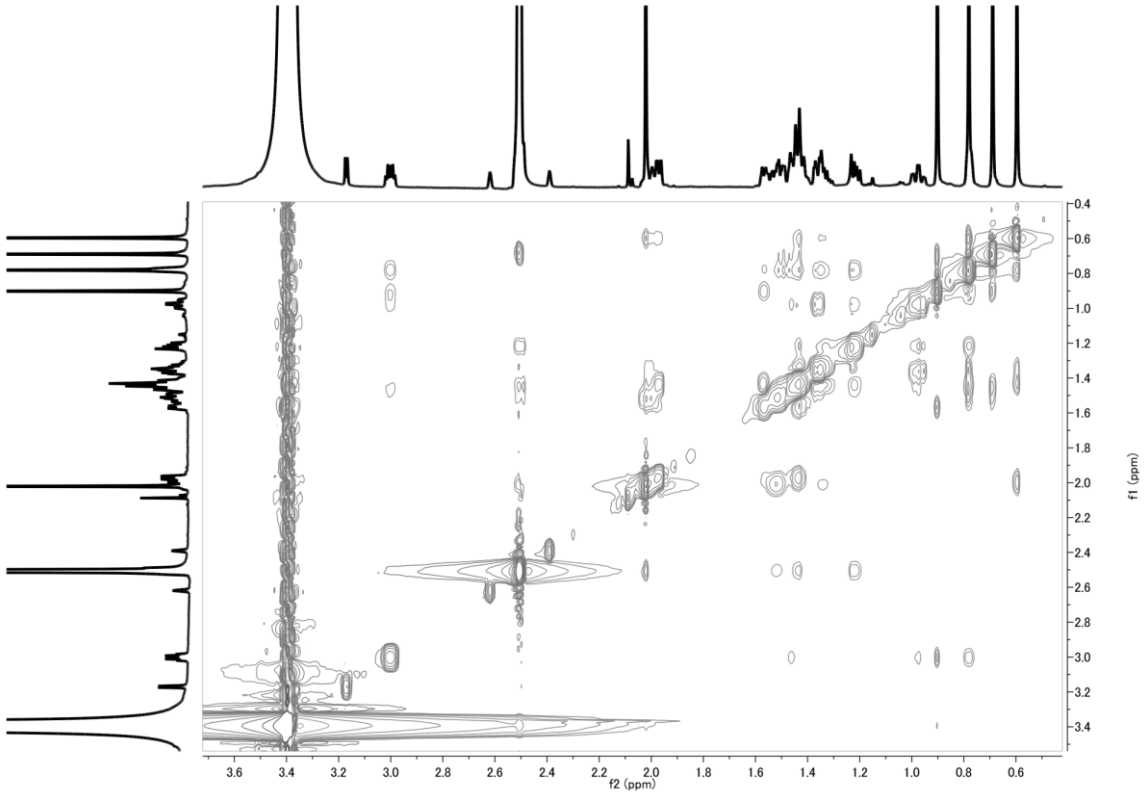

Supplemental Figure 2.13 NOESY NMR spectrum of arabidonol.

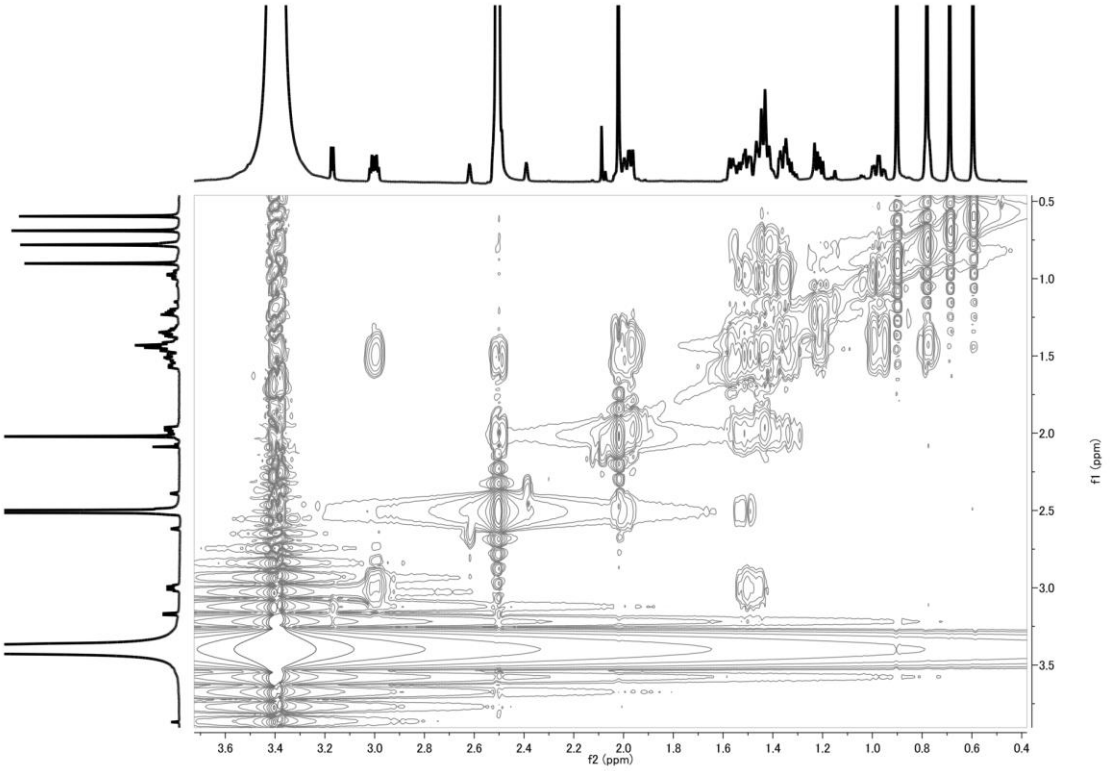

Supplemental Figure 2.14 COSY NMR spectrum of arabidonol.

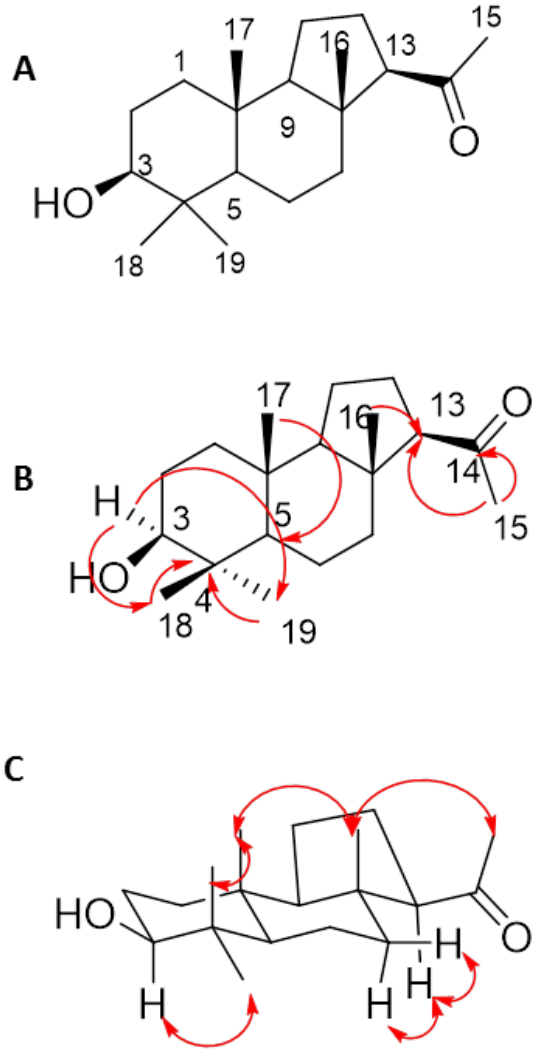

Supplemental Figure 2.15 Structure of arabidonol.

(A) Structure of arabidonol with atom numbering.

(B) Key HMBC correlations observed in arabidonol.

(C) Key NOE correlations observed in arabidonol

	Proton	Carbon
1	0.97 td, (13.3, 3.9) 1.34 m	38.7
2	1.45 m	27.3
3	3.00 dd (11, 5)	77.4
4		38.7
5	0.70 overlapped	55.9
6	1.56 m	19.7
7	1.49 overlapped	40.5
8		44.0
9	1.22 dd (12.8, 7.3)	63.4
10		38.6
11	1.99 m	21.9
12	1.43 overlapped	22.0
13	2.5 overlapped with the solvent signal	64.1
14		209.2
15	2.01 s	31.4
16	0.58 s	15.7
17	0.78 s	15.4
18	0.88 s	16.2
19	0.68 s	15.8

Supplemental Table 2.3 Proton and carbon chemical shifts for arabidiol and key correlations from NMR spectra.

Primer	Sequence	Experiment
P1	5'-CACCATGGATGCAATCGTCGTTGACTC-3'	CYP705A1 cDNA amplification
P2	5'-TTAAAGATGGGAAATTAAAGAGTTTTGGG-3'	CYP705A1 cDNA amplification
P3	5'-CACCATGTGGAGACTAAGAATTGGAGCTAAGG-3'	ABDS cDNA amplification
P4	5'-TCAAGGCTGAAGCCGCCGTAG-3'	ABDS cDNA amplification
P5	5'-GGGGACAACTTTGTATAGAAAAGTTGTTGAAAAATGC ACGGTCAATTCTACCTTC-3'	Cloning CYP705A1 promoter with attB4 (forward)
P6	5'-GGGGACTGCTTTTTTGTACAAACTTGTTGTTGCTGAAAA GCAAAGAAGAGGC-3'	Cloning CYP705A1 promoter with attB1 (reverse)
P7	5'-CTATGAATTC ATGGATGCAATCGTCGTTGACTC-3'	CYP705A1 forward with EcoRI for yeast expression
P8	5'-CTATGAGCTC TTAAAGATGGGAAATTAAAGAGTTTTGGG-3'	CYP705A1 reverse with SacI for yeast expression
P9	5'-CTATGAGCTCTTAACTTAAGGAAGCTAGAAACCTCTC-3'	mutCYP705A1 reverse with SacI for yeast expression
P10	5'-TGAGAGGTGGCAGAGATGTG-3'	CYP71A19, RT-PCR
P11	5'-ACCAAGTCCGATCTGGTGTC-3'	CYP71A19, RT-PCR
P12	5'-AGTAAGGACATTTGCCGCAC-3'	CYP71A20, RT-PCR
P13	5'-GACCGGTTGCTTCAGTTAGG-3'	CYP71A20, RT-PCR
P14	5'-CTCTCTCAGCCTCGGCTCTC-3'	CYP81D11, RT-PCR
P15	5'-TCAACAAATTCGACATCGCC-3'	CYP81D11, RT-PCR
P16	5'-ACGGTGATCACTGGCGTAAC-3'	CYP81D1, RT-PCR
P17	5'-ATGCCATGTGTGGGACTAGC-3'	CYP81D1, RT-PCR
P18	5'-CGAGGAAGAAGGAGAGCGTT-3'	CYP705A12, RT-PCR
P19	5'-TGAATCAACCTTTTTCCCCC-3'	CYP705A12, RT-PCR
P20	5'-CCAGGGGAGCTTCAATGTTC-3'	CYP708A3, RT-PCR
P21	5'-CCAACCAGCCGGAATTGTAT-3'	CYP708A3, RT-PCR
P22	5'-CGACGTGAACGTCTCCTCTC-3'	CYP705A1, RT-PCR
P23	5'-CCATTGCCCACTGTATTGCT-3'	CYP705A1, RT-PCR
P24	5'-CCGCAAGGGATCTCAAGAAG-3'	CYP71A12, RT-PCR
P25	5'-ATGAGAGGGAACTTTCGGCA-3'	CYP71A12, RT-PCR
P26	5'-TCGTGAACTCGTCACACTCG-3'	CYP81D8 , RT-PCR
P27	5'-TCTGAAACCAACCGCAAAAC-3'	CYP81D8 , RT-PCR
P28	5'-GCAGCGAGAGAAAAGAAGCA-3'	CYP76C4, RT-PCR
P29	5'-ATACGCTTGGGTCTCGTCCT-3'	CYP76C4, RT-PCR
P30	5'-GAGATGAGTAACGCCAAGCG-3'	CYP78A8, RT-PCR
P31	5'-ACCAAAACCGCAACAGTGTC-3'	CYP78A8, RT-PCR
P32	5'-ACGTACGGACTTGATGGACG-3'	CYP705A4, RT-PCR
P33	5'-CCGGGACAACTTCTTCTTCC-3'	CYP705A4, RT-PCR
P34	5'-CACTAAGCTGCTCCGACCAC-3'	CYP705A18, RT-PCR
P35	5'-TTGGACCGAGGTATCAGTGC-3'	CYP705A18, RT-PCR
P36	5'-GGACCTGATGGATGTGCTGT-3'	CYP705A13, RT-PCR
P37	5'-TCATGAACTCACGAACTGCG-3'	CYP705A13, RT-PCR
P38	5'-AGTTTATGGATGCCTTGTTGGC-3'	CYP705A1, qRT-PCR
P39	5'-ATTGCTATTGATGAGGCGTCAG -3'	CYP705A1, qRT-PCR
P40	5'-TCTACTTGCAGAGTGATAACGGA-3'	ABDS, qRT-PCR
P41	5'-CTCGATGACCGTGTCTTGAACAA-3'	ABDS, qRT-PCR
P42	5'-AGTCCTGCTTGGACGCTTCA-3'	UBC21, qRT-PCR
P43	5'-GAAGATTCCCTGAGTCGCAGTT-3'	UBC21, qRT-PCR

Supplemental Table 2.4 Sequence of primers used in different experiments.

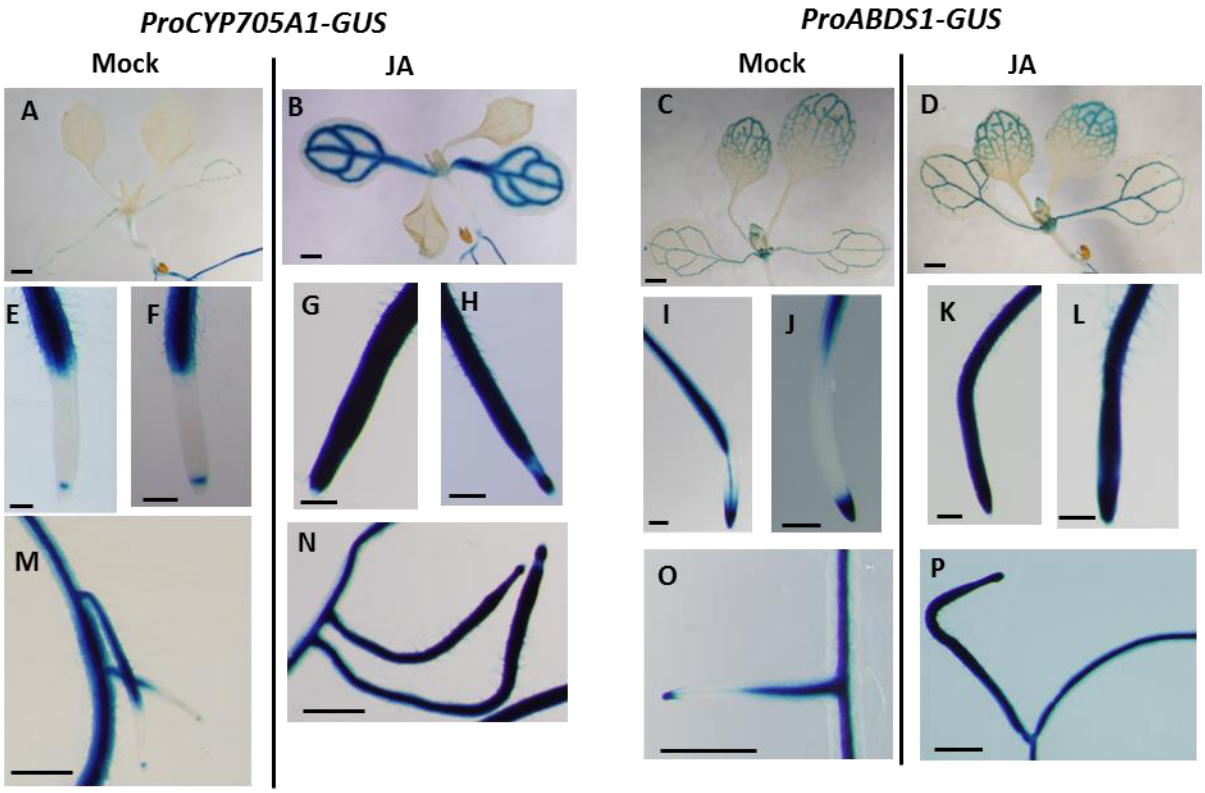

Supplemental Figure 2.16 Induced promoter-GUS activity of *CYP705A1* and *ABDS*.

GUS activity in twelve-day-old mock and JA-treated *ProCYP705A1:GUS* and *ProABDS:GUS* transgenic lines.

(A) to (D) Cotyledon and true leaves. Bar = 1 mm.

(E), (G), (I), (K) Main root tip. Bar = 200 µm.

(F), (H), (J), (L) Lateral root tip. Bar = 200 µm.

(M) to (P) Lateral –main root attachment site . Bar = 0.5 mm.

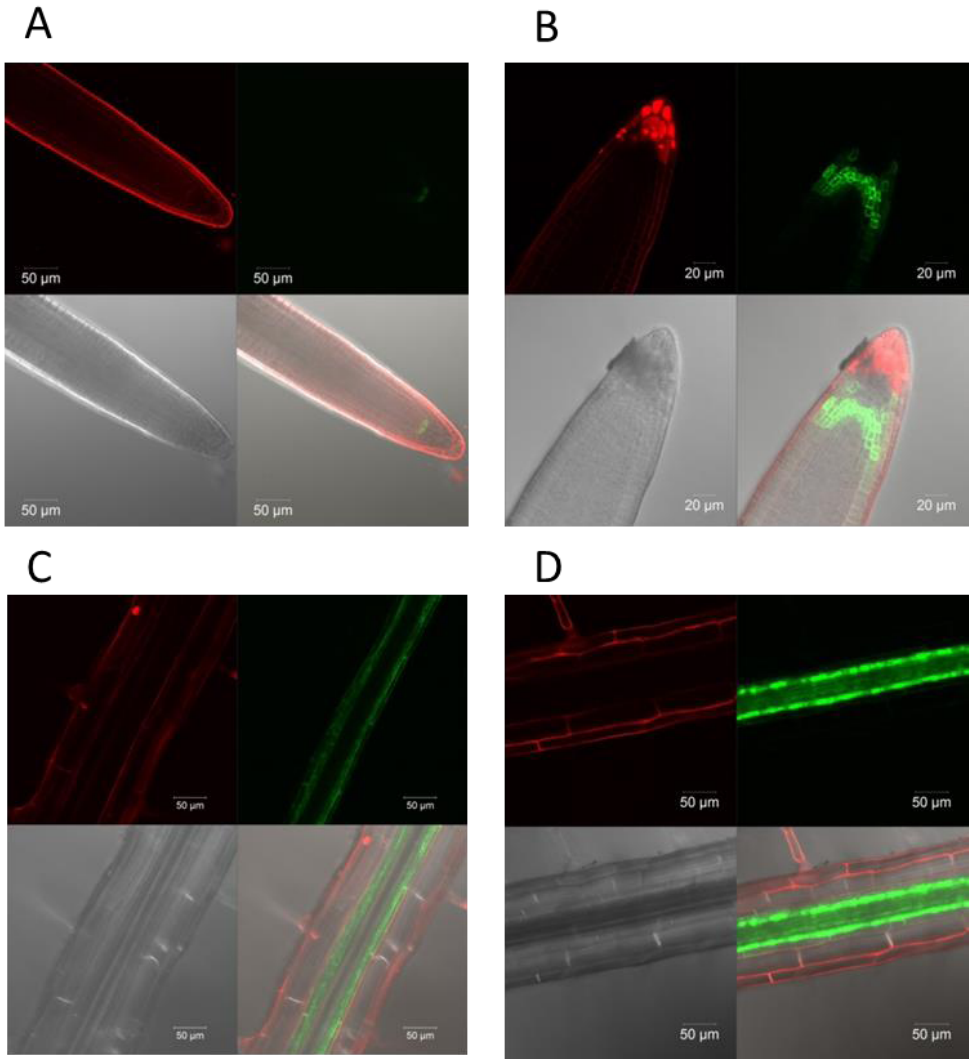

Supplemental Figure 2.17 Confocal microscopy analysis in response to JA treatment in *ProCYP705A1:CYP705A1-eYFP* lines.

Confocal microscopy analysis in twelve-day-old mock and JA treated *ProCYP705A1:CYP705A1-eYFP* plants. A localized induction of protein after JA treatment is observed.

(A) and (B) protein localization for CYP705A1 in root meristem zone. Bar = 50 µm.

(C) and (D) protein localization for CYP705A1 in root differentiation zone. Bar = 50 µm.

(A) and (C) are mock treatments. (B) and (D) are JA treatments.

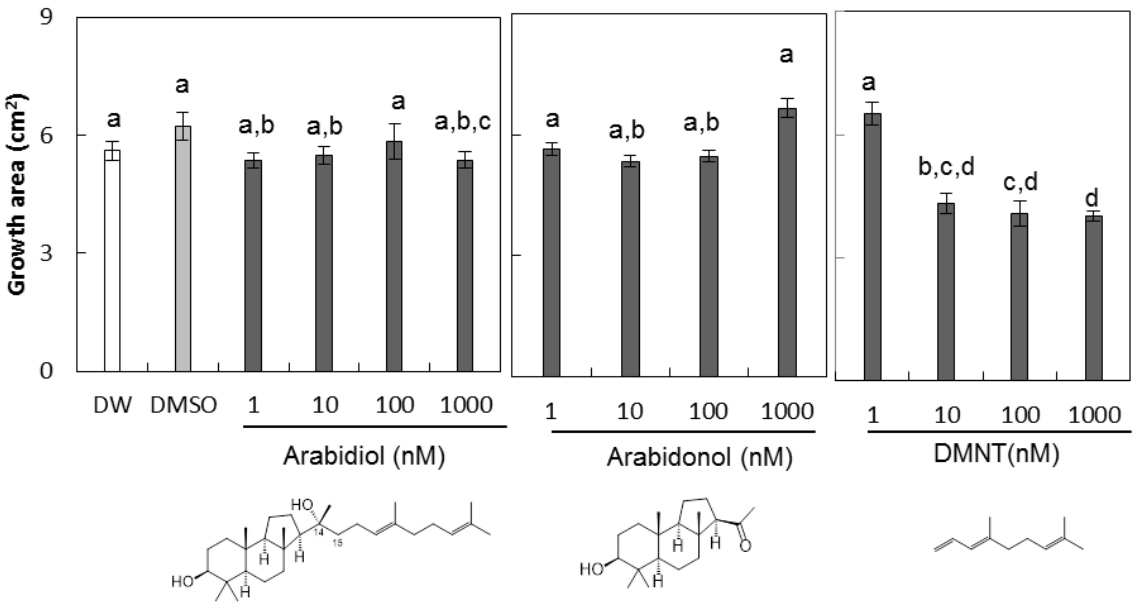

Supplemental Figure 2.18 Effect of arabidiol, arabidonol and DMNT on the growth of *P. irregulare* 110305.

Different amounts of chemicals were applied to 10 mL of fresh potato dextrose agar (PDA) plates. An agar plug with *Pythium* mycelium (2X2 mm) was positioned in the center of each plate and incubated at room temperature under dark condition. The *Pythium* growth zone was determined 2 days after inoculation. Data represents the mean value ± standard error mean of at least four replicates. $P<0.001$, one-way ANOVA, Tukey-Kramer HSD test.

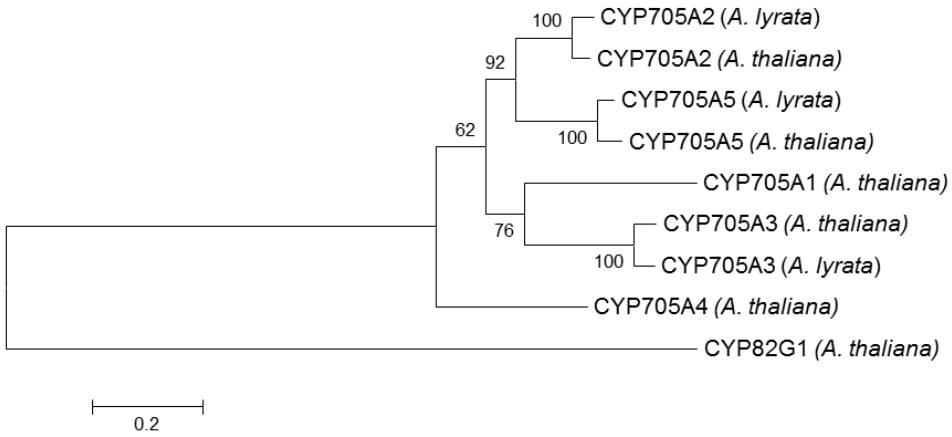

Supplemental Figure 2.19 Molecular Phylogenetic Analysis of *A. thaliana* and *A. lyrata* CYP705 members on the *ABDS* and *THAS* gene clusters

The TMTT synthase CYP82G1 from *A. thaliana* was used as an outgroup. Family tree evolutionary history was inferred by using the Maximum Likelihood method based on the JTT matrix-based model. The percentage of trees, in which the associated taxa cluster together, is shown next to the branches. Initial tree(s) for the heuristic search were obtained by applying the Neighbor-Joining method to a matrix of pairwise distances estimated using a JTT model. A discrete Gamma distribution was used to model evolutionary rate differences among sites (4 categories (+*G*, parameter = 1.8171). The tree is drawn to scale, with branch lengths measured in the number of substitutions per site. Evolutionary analyses were conducted in MEGA5 (Tamura et al., 2011) .

A1	I(115)	I(123)	T(213)	F(223)	F(224)	E(303)	F(304)	G(307)	A(308)	A(309)	D(310)	A(311)	P(371)	T(372)	V(375)	V(376)	M(491)	A(492)	%
A2	L	I	V	I	F	D	L	A	G	T	D	T	P	G	L	p	M	A	40
A3	L	L	V	I	F	E	F	G	G	T	D	T	P	S	L	I	M	V	45
A4	L	I	A	L	F	D	L	A	G	T	E	N	P	G	F	L	M	A	40
A5	L	I	V	H	F	D	L	A	G	T	E	A	P	G	V	V	M	A	50
			*	*					*	*				*					

Supplemental Figure 2.20 Sequence alignment of active site residues of CYP705A1 to CYP705A5.

Homology modeling of A2-A5 using the structure of CYP705A1 as the template gives evidence that several alterations in the active site may be associated with the lack of activity toward the oxidative degradation of arabidiol in A2-A5. The residues interacting with arabidiol (any atom in 5 Å including main chain) are listed and aligned to the equivalent residues in other member of this family (A2-A5).These major changes are highlighted with * in the table. The figure is prepared by WebLogo (Perkel, 2006)

SUPPLEMENTAL METHODS

Growth Inhibition Assay in Vitro

P. irregulare was cultured on half strength potato dextrose agar (PDA) (Difco213400) containing different concentrations of each chemical. *P. irregulare* plugs taken from water agar were placed in the center of the plate and incubated at room temperature under dark conditions for two days. The growth area was measured and calculated according to Adie et al (2008) with minor modifications. Hyphal growth from a single inoculate establishes a distinct growth zone, therefore two diameters (R_1, R_2), perpendicular to each other, were measured for each growth zone and the mean was obtained. The growth area was calculated:

$$Area = \pi \left(\frac{R_1 + R_2}{2} \right)^2$$

The growth inhibition assay was repeated at least twice with more than three replicates and the inhibitory effect of chemicals on *Pythium* growth was determined by comparison with the control growth area.

NMR Analysis of Arabidonol Structure

The ^{1}H NMR spectroscopic data of arabidonol (supplemental Figure 2.10B) displayed signals for four quaternary methyl groups (δ 0.58, 0.68, 0.78 and 0.88, each singlet), one singlet (δ 2.01, 3H) corresponding to one methyl group attached to a carbonyl, one oxymethine (δ 3.00, dd, J = 11, 5 Hz) (Supplemental Table 2). The Heteronuclear Single Quantum Coherence (HSQC) (Supplemental Figure 2.11) coupled with Heteronuclear Multiple Bond Correlation

(HMBC) experiment (Supplemental Figure 2.12) showed that arabidonol in fact had 19 carbons ascribable to four quaternary carbons including an acetyl carbonyl (δ 209.2, C-14), four methines, one of which attached to an oxygen (δ 77.4, C-3), six methylenes (δ 15.4, 15.7, 15.8, 16.2 and 31.4) and five methyls (δ 15.4, 15.7, 15.8, 16.2 and 31.4), (Supplemental Table 3). The four degrees of unsaturation deduced from HRESI mass spectroscopic data and the presence of carbonyl in the molecule demonstrated that arabidonol product must be a tricyclic compound. The allocation of the oxymethine to be at C-3, the acetyl group at C-13 and the presence of a five membered ring (ring C) were substantiated by the interpretation of HMQC and HMBC experiments. The long range cross-peaks from the proton at 3.00 ppm (H-3) to the methyl carbon at 16.2 ppm (C-18) and the methylene at C-2 (28.9), from the methyl protons at 0.88 (CH_3-18) to C-3 (77.4 ppm), C-19 (15.8 ppm), C-4 (37.8 ppm) and C-5 (55.9 ppm) allowed us to locate the hydroxyl group at C-3 and two methyl groups at C-4. The attachment of the acetyl group at C-13 was corroborated by long range correlations between the downfielded methyl group (δ 2.01) and both the carbonyl (δ 209.2) and the methine at δ 64.1. The important long range correlations which support the structure of arabidonol are summarized in Supplemental Figure 15B. The relative stereochemistry of arabidonol was deduced by 2D Nuclear Overhauser Effect SpectroscopY (NOESY) experiment (Supplemental Figure 2.13). The beta-orientation of the hydroxyl group at C-3 was deduced by the NOE correlations from the proton at 3.00 ppm (H-3) to CH_3-19; from CH_3-18 methyl to CH_3-17 and from CH_3-17 to CH_3-16. Moreover, the alpha-orientation of the proton at C-13 was substantiated by the NOE cross peak between H-13 and the two protons of C-7, and the methyl group at C-14 to CH_3-16 (Supplemental Figure 2.15C).

Computational Methods:

The protein sequence of CYP705A1 (excluding the first 37 residues involve in membrane binding) was blasted against the RCSB Protein Data Bank to search for the optimal template for homology modeling. Three cytochrome P450 conformations were selected based on maximum identity/similarity, high resolution and minimum gap in the structure. Three structures (PDB: 3RUK_C, 2HI4_A, 4I8V_A) were selected for multiple template comparative modeling using Modeller 9v11 (Marti-Renom et al. 2000). The simulation steps include single template modeling, multiple template modeling, and ab-initio loop refinement (Fiser et al. 2000). Each step includes 1000 independent simulation scored using DOPE (Shen and Sali 2006) and GA341 (Melo and Sali 2007) scoring functions. The selected final model was subjected to additional modeling to include the heme group into the protein structure. The loop carrying the cysteine residue bond to the heme group in PDB:3URK has 80% identity to the equivalent loop 439-449 in CYP705A1. The regional alignment of this loop in 3URK and CYP705A1 was used to incorporated the heme into the heme binding site of CYP705A1. The quality of the final model was verified using PROCHECK (Morris et al. 1992) and Anolea (Melo F 1997). Due to the high sequence identity (> 65%), the 3D structures of CYP705A2- CYP705A5 from *A. thaliana* were modeled using the structure of CYP705A1 as template.

Molecular dockings were performed using AutoDock-Vina (Trott and Olson 2010) with exhaustiveness of 10 and evaluation of 10 docked positions in each run. The protonation state of titratable residues in CYP705A1 structure were predicted by H++ (Gordon et al. 2005). The structure of the arabidiol molecule to be docked into the active site of modeled CYP705A1 was taken form the ZINC data base (ZINC 59211647) (Irwin et al. 2012). The ligands were fully flexible during docking and their Gasteiger partial charges (Gasteiger and Marsili 1980) of ligand and protein were determined by AutoDock Tools 1.5.4 (Morris et al. 1998; Morris et al.

2009). The partial charges distribution over for heme group was calculated as described previously (Lee et al. 2010) using Gaussian09A_02 (Frisch et al. 2009). The main binding cavity of modeled CYP705A1 was determined by using AutoLigand (Harris et al. 2008) and structural alignment to the templates of comparative modeling. The analysis of the binding cavity shows the side chain of M454 of CYP705A1 (conserved among CYP705A1- CYP705A5) is directly extended to the center of the binding site that fills a major part of the binding cavity. Since in the template this methionine is replaced by a glycine, to avoid biased docking to the orientation of this Met, another rotamer for Met form the PyMol rotamer library was picked for CYP705A1. The most favored docked structure for each compound was selected based on the lowest binding energy using three independent replicated docking experiments.

LITERATURE CITED:

Adie, B.A., Perez-Perez, J., Perez-Perez, M.M., Godoy, M., Sanchez-Serrano, J.J., Schmelz, E.A., and Solano, R. (2007). ABA is an essential signal for plant resistance to pathogens affecting JA biosynthesis and the activation of defenses in Arabidopsis. Plant Cell **19,** 1665-1681.

Agrios, G. (1997). Plant pathology. (San Diego: Academic Press).

Akhtar, M., and Wright, J.N. (1991). A unified mechanistic view of oxidative reactions catalysed by P-450 and related Fe-containing enzymes. Nat Prod Rep **8,** 527-551.

Alonso-Blanco, C., El-Assal, S.E., Coupland, G., and Koornneef, M. (1998). Analysis of natural allelic variation at flowering time loci in the Landsberg erecta and Cape Verde Islands ecotypes of Arabidopsis thaliana. Genetics **149,** 749-764.

Alonso, J.M., Stepanova, A.N., Leisse, T.J., Kim, C.J., Chen, H., Shinn, P., Stevenson, D.K., Zimmerman, J., Barajas, P., Cheuk, R., Gadrinab, C., Heller, C., Jeske, A., Koesema, E., Meyers, C.C., Parker, H., Prednis, L., Ansari, Y., Choy, N., Deen, H., Geralt, M., Hazari, N., Hom, E., Karnes, M., Mulholland, C., Ndubaku, R., Schmidt, I., Guzman, P., Aguilar-Henonin, L., Schmid, M., Weigel, D., Carter, D.E., Marchand, T., Risseeuw, E., Brogden, D., Zeko, A., Crosby, W.L., Berry, C.C., and Ecker, J.R. (2003). Genome-wide insertional mutagenesis of *Arabidopsis thaliana*. Science **301,** 653-657.

Arimura, G., Ozawa, R., Shimoda, T., Nishioka, T., Boland, W., and Takabayashi, J. (2000). Herbivory-induced volatiles elicit defence genes in lima bean leaves. Nature **406,** 512-515.

Armstrong, G., and Armstrong, J. (1981). Formae speciales and races of *Fusarium oxysporum* causing wilt diseases. (Pennsylvania State University Press).

Bakkali, F., Averbeck, S., Averbeck, D., and Idaomar, M. (2008). Biological effects of essential oils - A review. Food Chem Toxicol **46,** 446-475.

Bechtold, N., Ellis, J., and Pelletier, G. (1993). In-Planta Agrobacterium-Mediated Gene-Transfer by Infiltration of Adult Arabidopsis-Thaliana Plants. Comptes Rendus Acad. Sci. Ser. III-Sci. Vie-Life Sci. **316,** 1194-1199.

Birnbaum, K., Shasha, D.E., Wang, J.Y., Jung, J.W., Lambert, G.M., Galbraith, D.W., and Benfey, P.N. (2003). A gene expression map of the Arabidopsis root. Science **302,** 1956-1960.

Bohlmann, J., Meyer-Gauen, G., and Croteau, R. (1998). Plant terpenoid synthases: Molecular biology and phylogenetic analysis. Proceedings of the National Academy of Sciences **95,** 4126-4133.

Boland, W., Gabler, A., Gilbert, M., and Feng, Z.F. (1998). Biosynthesis of C-11 and C-16 homoterpenes in higher plants; Stereochemistry of the C-C-bond cleavage reaction. Tetrahedron **54,** 14725-14736.

Brady, S.M., Orlando, D.A., Lee, J.Y., Wang, J.Y., Koch, J., Dinneny, J.R., Mace, D., Ohler, U., and Benfey, P.N. (2007). A high-resolution root spatiotemporal map reveals dominant expression patterns. Science **318,** 801-806.

Brandenburg, E. (1950). Uber die bildung von toxinen in der gattung *Pythium* und ihre wirkung auf die pflanzen. Nachrichtenbl. Deut. Pflanzenschutzdienst. **2,** 69-70.

Chen, F., Tholl, D., Bohlmann, J., and Pichersky, E. (2011). The family of terpene synthases in plants: a mid-size family of genes for specialized metabolism that is highly diversified throughout the kingdom. The Plant Journal **66,** 212-229.

De Boer, J.G., Posthumus, M.A., and Dicke, M. (2004). Identification of volatiles that are used in discrimination between plants infested with prey or nonprey herbivores by a predatory mite. Journal of Chemical Ecology **30,** 2215-2230.

Deacon, J.W. (1979). Cellulose decomposition by *Pythium* and its relevance to substrate-groups of fungi. Transactions of the British Mycological Society **72,** 469-477.

DeVore, N.M., and Scott, E.E. (2012). Structures of cytochrome P450 17A1 with prostate cancer drugs abiraterone and TOK-001. Nature **482,** 116-U149.

Dicke, M., Sabelis, M.W., Takabayashi, J., Bruin, J., and Posthumus, M.A. (1990). Plant strategies of manipulating predatorprey interactions through allelochemicals: Prospects for application in pest control. Journal of Chemical Ecology **16,** 3091-3118.

Donath, J., and Boland, W. (1995). Biosynthesis of acyclic homoterpenes: Enzyme selectivity and absolute configuration of the nerolidol precursor. Phytochemistry **39,** 785-790.

Dudareva, N., Negre, F., Nagegowda, D.A., and Orlova, I. (2006). Plant volatiles: Recent advances and future perspectives. Critical Reviews in Plant Sciences **25,** 417-440.

Ehlting, J., Sauveplane, V., Olry, A., Ginglinger, J.F., Provart, N.J., and Werck-Reichhart, D. (2008). An extensive (co-)expression analysis tool for the cytochrome P450 superfamily in Arabidopsis thaliana. BMC Plant Biol **8,** 47.

Field, B., and Osbourn, A.E. (2008). Metabolic diversification—Independent assembly of operon-like gene clusters in different plants. Science **320,** 543-547.

Field, B., Fiston-Lavier, A.S., Kemen, A., Geisler, K., Quesneville, H., and Osbourn, A.E. (2011). Formation of plant metabolic gene clusters within dynamic chromosomal regions. Proc Natl Acad Sci U S A **108,** 16116-16121.

Fridman, E., and Pichersky, E. (2005). Metabolomics, genomics, proteomics, and the identification of enzymes and their substrates and products. Current Opinion in Plant Biology **8,** 242-248.

Frost, C.J., Appel, H.M., Carlson, J.E., De Moraes, C.M., Mescher, M.C., and Schultz, J.C. (2007). Within-plant signalling via volatiles overcomes vascular constraints on systemic signalling and primes responses against herbivores. Ecology Letters **10,** 490-498.

Fulton, D.C., Kroon, P.A., and Threlfall, D.R. (1994). Enzymological aspects of the redirection of terpenoid biosynthesis in elicitor-treated cultures of *Tabernaemontana divaricata*. Phytochemistry **35,** 1183-1186.

Gibeaut, D.M., Hulett, J., Cramer, G.R., and Seemann, J.R. (1997). Maximal biomass of Arabidopsis thaliana using a simple, low-maintenance hydroponic method and favorable environmental conditions. Plant Physiology **115,** 317-319.

Hansen, B.G., Kerwin, R.E., Ober, J.A., Lambrix, V.M., Mitchell-Olds, T., Gershenzon, J., Halkier, B.A., and Kliebenstein, D.J. (2008). A novel 2-oxoacid-dependent dioxygenase involved in the formation of the goiterogenic 2-hydroxybut-3-enyl glucosinolate and generalist insect resistance in Arabidopsis. Plant Physiol **148,** 2096-2108.

Herde, M., Gartner, K., Kollner, T.G., Fode, B., Boland, W., Gershenzon, J., Gatz, C., and Tholl, D. (2008). Identification and regulation of TPS04/GES, an Arabidopsis geranyllinalool synthase catalyzing the first step in the formation of the insect-induced volatile C16-homoterpene TMTT. Plant Cell **20,** 1152-1168.

Huang, M., Abel, C., Sohrabi, R., Petri, J., Haupt, I., Cosimano, J., Gershenzon, J., and Tholl, D. (2010). Variation of herbivore-induced volatile terpenes among Arabidopsis ecotypes depends on allelic differences and subcellular targeting of two terpene synthases, TPS02 and TPS03. Plant Physiol **153,** 1293-1310.

Huffaker, A., Pearce, G., and Ryan, C.A. (2006). An endogenous peptide signal in Arabidopsis activates components of the innate immune response. Proceedings of the National Academy of Sciences **103,** 10098–10103.

Kaiser, R. (1991). In: Perfumes: Art, Science and Technology. (London: Elsevier Applied Science).

Kalemba, D., Kusewicz, D., and Świąder, K. (2002). Antimicrobial properties of the essential oil of *Artemisia asiatica* Nakai. Phytotherapy Research **16,** 288-291.

Kappers, I.F., Aharoni, A., van Herpen, T.W., Luckerhoff, L.L., Dicke, M., and Bouwmeester, H.J. (2005). Genetic engineering of terpenoid metabolism attracts bodyguards to Arabidopsis. Science **309,** 2070-2072.

Karimi, M., Inze, D., and Depicker, A. (2002). GATEWAY vectors for Agrobacterium-mediated plant transformation. Trends Plant Sci **7,** 193-195.

Koch, E., and Slusarenko, A. (1990). Arabidopsis is susceptible to infection by a downy mildew fungus. The Plant Cell **2,** 437-445.

Larbat, R., Kellner, S., Specker, S., Hehn, A., Gontier, E., Hans, J., Bourgaud, F., and Matern, U. (2007). Molecular cloning and functional characterization of psoralen synthase, the first committed monooxygenase of furanocoumarin biosynthesis. Journal of Biological Chemistry **282,** 542-554.

Lee, S., Badieyan, S., Bevan, D.R., Herde, M., Gatz, C., and Tholl, D. (2010). Herbivore-induced and floral homoterpene volatiles are biosynthesized by a single P450 enzyme (CYP82G1) in Arabidopsis. Proc Natl Acad Sci U S A **107,** 21205-21210.

Manici, L.M., Lazzeri, L., Baruzzi, G., Leoni, O., Galletti, S., and Palmieri, S. (2000). Suppressive activity of some glucosinolate enzyme degradation products on *Pythium irregulare* and *Rhizoctonia solani* in sterile soil. Pest Management Science **56,** 921-926.

Mann, C.M., Cox, S.D., and Markham, J.L. (2000). The outer membrane of *Pseudomonas aeruginosa* NCTC 6749 contributes to its tolerance to the essential oil of *Melaleuca alternifolia* (tea tree oil). Letters in Applied Microbiology **30,** 294-297.

Mary, W., Crombie, L., and Crombie, L. (1986). Distribution of avenacins A-1, A-2, B-1 and B-2 in oat roots: Their fungicidal activity towards `take-all' fungus. Phytochemistry **25,** 2069-2073.

McGarvey, D.J., and Croteau, R. (1995). Terpenoid metabolism. The Plant Cell **7,** 1015-1026.

Mumm, R., and Dicke, M. (2010). Variation in natural plant products and the attraction of bodyguards involved in indirect plant defense. Canadian Journal of Zoology-Revue Canadienne De Zoologie **88,** 628-667.

Mylona, P., Owatworakit, A., Papadopoulou, K., Jenner, H., Qin, B., Findlay, K., Hill, L., Qi, X., Bakht, S., Melton, R., and Osbourn, A. (2008). Sad3 and Sad4 are required for saponin biosynthesis and root development in oat. Plant Cell **20,** 201-212.

Oliver, J., Castro, A., Gaggero, C., Cascón, T., Schmelz, E., Castresana, C., and Ponce de León, I. (2009). *Pythium* infection activates conserved plant defense responses in mosses. Planta **230,** 569-579.

Perkel, J.M. (2006). WebLogo: Data visualization for everyone. Scientist **20,** 67-67.

Pichersky, E., Noel, J.P., and Dudareva, N. (2006). Biosynthesis of plant volatiles: nature's diversity and ingenuity. Science **311,** 808-811.

Ruben, D.M., and Stanghellini, M.E. (1978). Ultrastructure of oospore germination in *Pythium aphanidermatum*. American Journal of Botany **65,** 491-501.

Schlink, K. (2010). Down-regulation of defense genes and resource allocation into infected roots as factors for compatibility between *Fagus sylvatica* and *Phytophthora citricola*. Functional & Integrative Genomics **10,** 253-264.

Shimura, K., Okada, A., Okada, K., Jikumaru, Y., Ko, K.W., Toyomasu, T., Sassa, T., Hasegawa, M., Kodama, O., Shibuya, N., Koga, J., Nojiri, H., and Yamane, H. (2007). Identification of a biosynthetic gene cluster in rice for momilactones. Journal of Biological Chemistry **282,** 34013-34018.

Staswick, P.E., Yuen, G.Y., and Lehman, C.C. (1998). Jasmonate signaling mutants of Arabidopsis are susceptible to the soil fungus Pythium irregulare. Plant J **15,** 747-754.

Takahashi, S., Yeo, Y., Greenhagen, B.T., McMullin, T., Song, L., Maurina-Brunker, J., Rosson, R., Noel, J.P., and Chappell, J. (2007). Metabolic engineering of sesquiterpene metabolism in yeast. Biotechnol Bioeng **97,** 170-181.

Tamura, K., Peterson, D., Peterson, N., Stecher, G., Nei, M., and Kumar, S. (2011). MEGA5: molecular evolutionary genetics analysis using maximum likelihood, evolutionary distance, and maximum parsimony methods. Mol Biol Evol **28,** 2731-2739.

Tholl, D., Sohrabi, R., Huh, J.H., and Lee, S. (2011). The biochemistry of homoterpenes--common constituents of floral and herbivore-induced plant volatile bouquets. Phytochemistry **72,** 1635-1646.

Urban, P., Mignotte, C., Kazmaier, M., Delorme, F., and Pompon, D. (1997). Cloning, yeast expression, and characterization of the coupling of two distantly related Arabidopsis thaliana NADPH-cytochrome P450 reductases with P450 CYP73A5. J Biol Chem **272,** 19176-19186.

Vaughan, M.M., Wang, Q., Webster, F.X., Kiemle, D., Hong, Y.J., Tantillo, D.J., Coates, R.M., Wray, A.T., Askew, W., O'Donnell, C., Tokuhisa, J.G., and Tholl, D. (2013). Formation of the unusual semivolatile diterpene rhizathalene by the Arabidopsis class I terpene synthase TPS08 in the root stele is involved in defense against belowground herbivory. Plant Cell **25,** 1108-1125.

Vijayan, P., Shockey, J., Lévesque, C.A., Cook, R.J., and Browse, J. (1998). A role for jasmonate in pathogen defense of Arabidopsis. Proceedings of the National Academy of Sciences **95,** 7209-7214.

Vitha, S., Benes, K., Michalova, M., and Ondrej, M. (1993). Quantitative Beta-Glucuronidase Assay in Transgenic Plants. Biol Plantarum **35,** 151-155.

Xiang, T., Shibuya, M., Katsube, Y., Tsutsumi, T., Otsuka, M., Zhang, H., Masuda, K., and Ebizuka, Y. (2006). A new triterpene synthase from Arabidopsis thaliana produces a tricyclic triterpene with two hydroxyl groups. Org Lett **8,** 2835-2838.

Xie, D.X., Feys, B.F., James, S., Nieto-Rostro, M., and Turner, J.G. (1998). COI1: An Arabidopsis gene required for jasmonate-regulated defense and fertility. Science **280,** 1091-1094.

Ye, J., Coulouris, G., Zaretskaya, I., Cutcutache, I., Rozen, S., and Madden, T.L. (2012). Primer-BLAST: a tool to design target-specific primers for polymerase chain reaction. BMC Bioinformatics **13,** 134.

Yuan, W.M., and Crawford, D.L. (1995). Characterization of *Streptomyces lydicus* WYEC108 as a potential biocontrol agent against fungal root and seed rots. Applied and Environmental Microbiology **61,** 3119-3128.

Zimmermann, P., Hirsch-Hoffmann, M., Hennig, L., and Gruissem, W. (2004). GENEVESTIGATOR. Arabidopsis microarray database and analysis toolbox. Plant Physiology **136,** 2621-2632.

3. Identification of Downstream Modification Products in the Arabidiol Catabolic Pathway in *Arabidopsis* Roots

Other Contributors:

Liva Harinantenaina, postdoctoral associate in the Chemistry Department at Virginia Tech, did the NMR analysis.

ABSTRACT

Terpenoids represent the largest class of specialized or secondary metabolites and serve various functions in plant organism interactions. There are large numbers of functionally active terpenoid metabolites, which are derived by degradation of larger terpene skeletons such as C_{40} tetraterpenes. We have recently demonstrated that the root-specific triterpene alcohol, arabidiol, undergoes oxidative degradation to the volatile irregular C_{11} homoterpene or norterpenoid DMNT and the C_{19} tricyclic ketone arabidonol in a reaction catalyzed by the cytochrome P450 monooxygenase CYP705A1 (Sohrabi et al., unpublished). This breakdown reaction is induced upon infection of *Arabidopsis* roots with the oomycete *Pythium irregulare* and treatment with the defense hormone jasmonic acid and represents an alternative pathway to produce the common stress-induced volatile DMNT via catabolism of a regular terpenoid precursor. In contrast to DMNT, no defensive activity could be associated with arabidonol. Moreover, arabidonol could not be detected *in planta*, which raises the question of its conversion to potentially biologically active downstream products. Here we present genetic and biochemical evidence that arabidonol is modified in a jasmonate-independent manner to at least three products, of which two, a putative stereoisomer and its putative acetylated form, are released from root tissue. Analysis of gene expression data sets paired with functional expression in yeast provided no indication that genes located on the arabidiol synthase (*ABDS*) gene cluster are involved in the observed modification steps. *Arabidopsis* accession-specific and interspecific differences of the profiles of the modification products provide grounds for the identification of gene loci involved in this new pathway by applying QTL or genome synteny analysis.

INTRODUCTION

Plants produce a large number of structurally diverse terpenoid chemicals which play various roles in cell physiology as well as the interaction with the surrounding environment. Among terpenoids, the C30 triterpenoids with more than 20,000 skeletons have functions in plant growth and development by serving as precursors of membrane and steroid hormones and as possible growth-regulating signals (Nes and Heftmann, 1981; Benveniste, 2004; Boutte and Grebe, 2009). Additionally, triterpenes are involved in plant defense responses and responses to other environmental factors such as nutrient and water availability (Phillips et al., 2006; Augustin et al., 2011). Triterpenoids undergo several types of modifications via sequential reactions catalyzed by cytochrome P450 monooxygenases (P450), acyl transferases, and glycosyl-transferases, which give rise to diverse saponin metabolites (Osbourn et al., 2011). Saponin glycosides such as avenacins secreted from oat roots are biologically active compounds with potent antimicrobial properties (Mary et al., 1986). Moreover, modified triterpenoids have been used as medicine due to their pharmacological properties such as anti-proliferative and anti-cancer activities (Osbourn et al., 2011).

All terpenoids are derived from five carbon isopentenyl diphosphate (IPP) units. Sequential condensation of these C5 building blocks gives rise to the formation of regular terpenes such as monoterpenes (C10), sesquiterpenes (C15) diterpenes (C20), triterpenes (C30) and tetraterpenes (C40) (Bohlmann et al., 1998; Fridman and Pichersky, 2005; Chen et al., 2011). Norisoprenoids with an irregular (non-5x) number of carbon atoms are biosynthesized by the breakdown of regular terpene precursors. For example, the degradation of carotenoids by carotenoid cleavage enzymes and subsequent modification steps results in the production of norisoprenoids (also referred to as apocarotenoids) with C8-C18 atoms. These compounds have

gained increased attention because of their role as volatile aroma compounds in fruits such as tomato and melon (Winterhalter and Rouseff, 2001). In addition, non-volatile carotenoid derivatives can undergo multiple diverse enzymatic reactions and are converted to products that play important roles as hormones (e.g. strigolactones), signaling molecules, and chromophores (Walter et al., 2010). There are only limited numbers of volatile norterpenoid derived from the degradation of triterpenoids. For example, the violet fragrance from dried rhizomes of certain *Iris* (sword lily) species is due to compounds called irones (Jaenicke and Marner, 1990).

Recently, we discovered a new pathway to produce volatile compounds from triterpene precursors. *Arabidopsis* produces the triterpenoid alcohol arabidiol specifically in root tissues by the activity of the enzyme arabidiol synthase (*ABDS*) (Sohrabi et al., unpublished). Degradation of the arabidiol triterpene metabolite by the P450 CYP705A1 leads to the formation of the volatile irregular C_{11} homo-or norterpenoid DMNT and a C19 norterpenoid ketone called arabidonol (Figure 3.1).The *CYP705A1* and *ABDS* are highly co-regulated and are part of a gene cluster with a second triterpenoid synthase called baroul synthase and several P450s. We have reported that volatile DMNT emission is induced in response to root inoculation with an oomycete pathogen *Pythium irregulare* and treatment with defense hormone jasmonic acid (JA). Although we did not find biological activity for arabidonol our results suggested that DMNT volatile plays a role in inhibiting oospore germination (Sohrabi et al., unpublished). Since we were unable to detect arabidonol in vivo, we assumed that the compound could be further converted into derivatives with possible defensive activities. Here we report the detection of arabidonol downstream modification products in root exudates of *Arabidopsis thaliana* and predict a sequence of enzymatic reactions for these modification steps based on exogenous application of isolated intermediates to the root tissue. Additionally, NMR based structural

elucidation of the modification products is presented. Although we predicted that P450s on the gene cluster of the *ABDS*/*CYP705A1* might be involved in further modification for arabidonol *in planta*, no biochemical activity was detected for selected candidates upon yeast expression. We present natural variation in arabidonol modification steps in two *Arabidopsis* accessions L*er* and Cvi and discuss an evolutionary history for arabidiol degradation and cleavage in *Arabidopsis*.

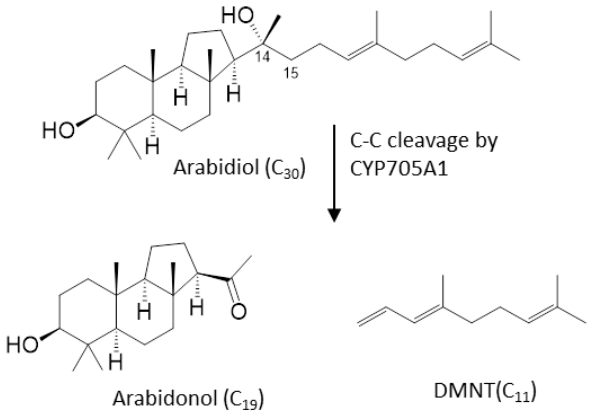

Figure 3.1 The arabidiol degradation pathway.

The pathway for arabidiol degradation in *Arabidopsis* roots is shown. Arabidiol cleavage at the C_{14}-C_{15} bond by CYP705A1 leads to the formation of the volatile DMNT (C_{11}) and the norterpenoid arabidonol (C_{19}).

RESULTS

Arabidiol-Derived Compounds are Detected in Arabidopsis Root Tissue and Exudates

Previous experiments indicated that in jasmonate-treated *Arabidopsis* roots the triterpenoid alcohol, arabidiol, undergoes a rapid breakdown into DMNT and arabidonol, since arabidiol was only detected in *cyp705a1-1* plants, which are impaired in the degradation of this precursor. The degradation of arabidiol is easily monitored by the trapping and analysis of DMNT. However, arabidonol was undetectable in organic extracts of roots indicating a rapid

turnover or conversion, similar to that of arabidiol, into downstream derivatives. We, therefore, searched for possible conversion products of arabidonol in organic extracts of JA-treated axenically grown root tissues of wild type plants in comparison to those of the arabidonol biosynthetic mutant *cyp705a1* (Figure 3.2 A). When we examined root extracts of Col-0 wild type plants, a single compound potentially derived from arabidiol degradation was detected named Deg-R (for R for root) with a mass spectrum similar to that of arabidonol but with a different retention time at T_R = 27.8 min. This compound was not found in the *cyp705a1* mutant. (Figure 3.2 B).

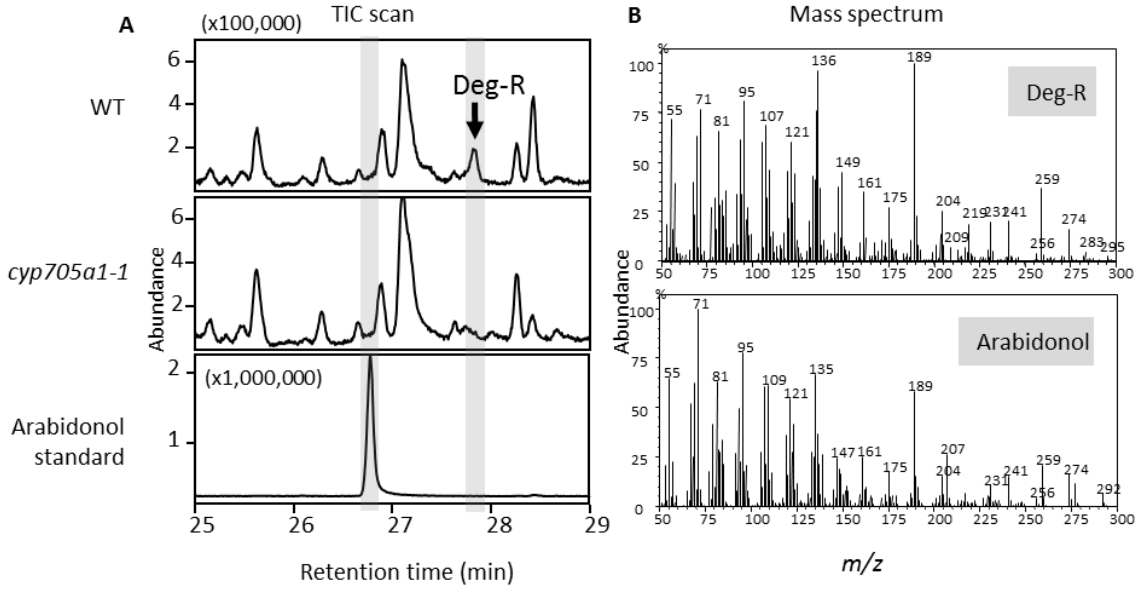

Figure 3.2 Detection of arabidiol-derived compounds in *Arabidopsis* root tissue.

(A) GC chromatograms of ethyl acetate extracts of root tissues of wild type and *cyp705a1* plants treated with 100 µM JA for 24 h. A peak representing a putative arabidiol degradation product (named Deg-R) was detected in wild type roots but was absent in the *cyp705a1* mutant. Arabidonol was not detected in roots. The lower panel shows an arabidonol standard. (B) Mass spectra of arabidonol and Deg-R. A molecular ion of m/z of 295 was found for Deg-R in contrast to the molecular ion of 292 for arabidonol.

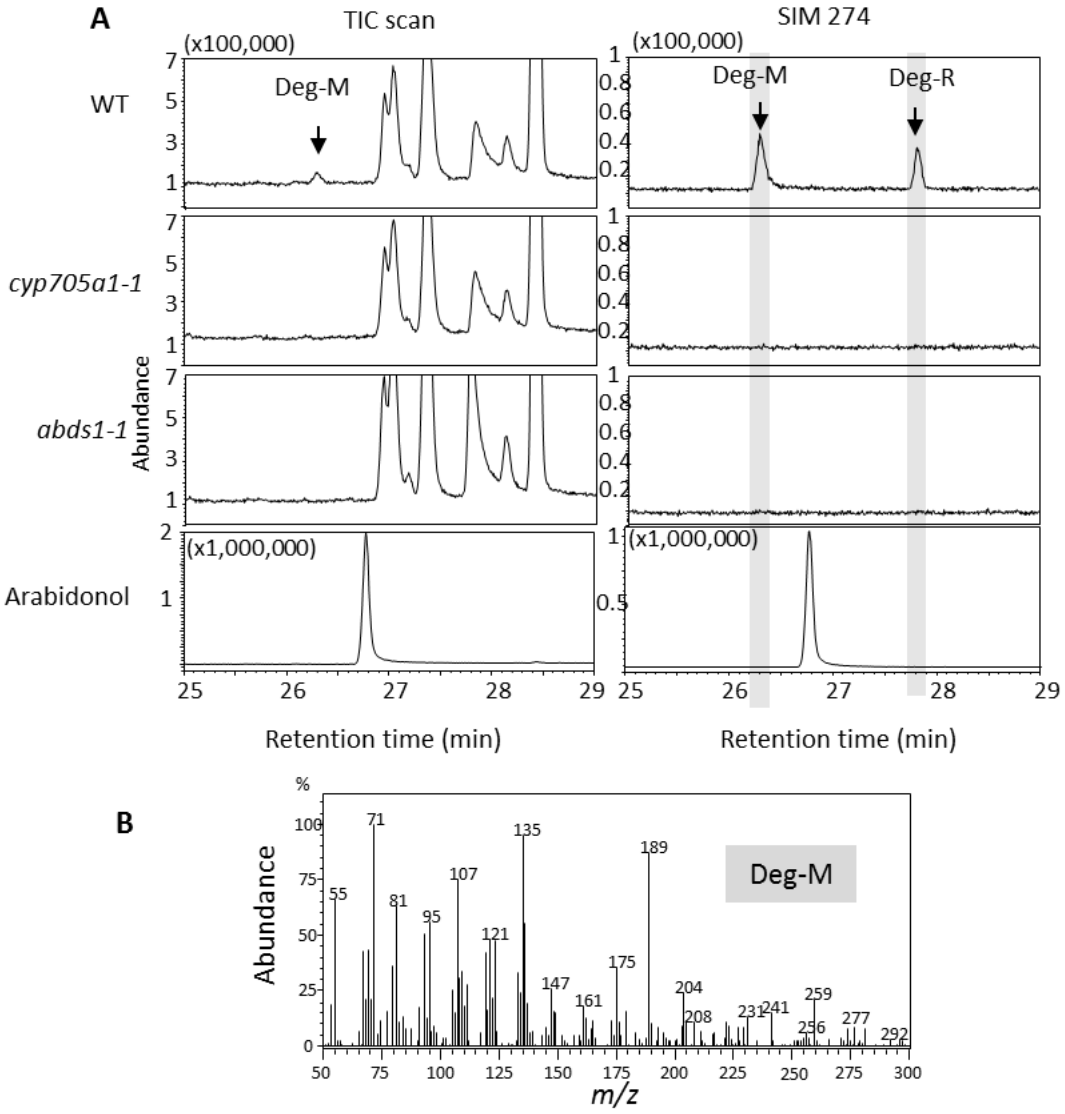

Figure 3.3 Detection of arabidiol-derived compounds in Arabidopsis root exudates.

(A) GC chromatograms of ethyl acetate extracts of liquid medium of axenically grown roots of wild type plants and *cyp705a1* and *abds* mutants. Upon 24 h of JA treatment a second compound in addition to Deg-R was detected called Deg-M with a retention time different to that of arabidonol. Left panel: Total ion chromatograms (TIC). Right panel: Single ion chromatograms (SIM) monitoring the 274 ion distinctive of arabidonol. The bottom chromatogram shows a pure arabidonol standard. **(B)** Mass spectrum of Deg-M.

Since the exudation of specialized metabolites from plant roots has been reported previously (Bais et al., 2005; Badri et al., 2009), we also considered the possibility that arabidonol or any conversion product could be released into the rhizosphere. When exudates were extracted from axenically grown cultures of JA-treated wild type plants, we detected Deg-R and a second compound named Deg-M (M for medium) with a retention time of T_R = 26.3 min and a mass spectrum similar to that of arabidonol. Deg-M was absent in exudates of the *cyp705a1-1* and *abds-1* mutants (Figure 3.3). Based on these results, we concluded that arabidonol is converted into at least two other products, which are in part secreted by the root tissue.

Arabidonol is Converted into Deg-M, Deg-R, and a Third Compound, Deg-I, in Planta

To further examine the conversion of arabidonol into the observed putative derivatives, we performed feeding experiments with arabidonol using axenically grown *abds-1* plants (Figure 3.4A). Prior to these experiments, arabidonol was purified from yeast lines co-expressing *ABDS* and *CYP705A1* (see Methods). The compound was then applied at 3 µM concentration to three weeks old cultures of the *abds-1* mutant without JA treatment followed by organic extraction from root tissue at different time points. To evaluate whether arabidonol could be directly modified by root exudates, plant root exudates were obtained 24 h after growth medium replacement from axenically grown *Arabidopsis* roots and inoculated with arabidonol in a new container for 30 h. No modification of arabidiol was observed under these experimental conditions indicating that the conversion of arabidonol occurs in the root tissue most likely by specific enzymatic activities (Figure 3.4.A). Feeding with arabidonol for 1.5 h, 3 h and 30 h resulted in the production and secretion of Deg-M and Deg-R. The compounds were found at

different ratios depending on the duration of the precursor application. At early stages of feeding, Deg-M and only trace amounts of Deg-R were detected from the organic extracts of the culture medium (Figure 3.4A). At late time points, the amount of the Deg-R was increased leading to the

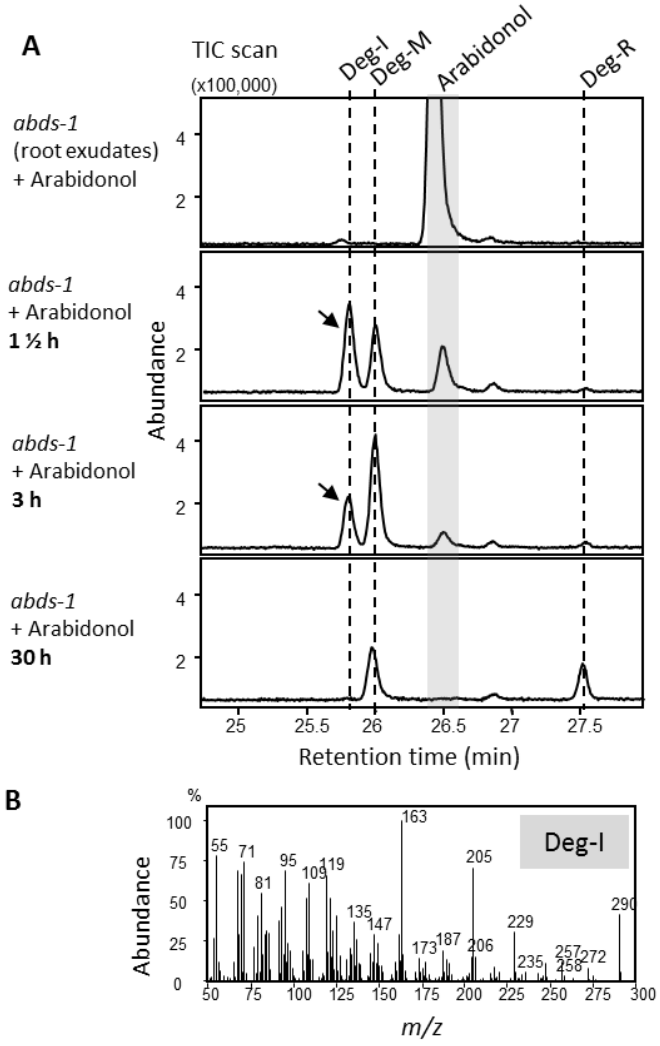

Figure 3.4 Arabidonol is converted into several modification products *in planta.*

(A) GC-MS chromatogram of organic extracts upon arabidonol feeding is shown. No conversion of arabidonol was observed upon exposure only to root exudates obtained axenically grown *abds-1* plants (in the absence of root tissue–upper panel). When applied in the presence of root tissue, arabidonol was initially converted into Deg-M and Deg-I between 1-3 h of arabidonol application and also produced small amounts of Deg-R. Upon treatment for 30 h, the amounts of Deg-M and Deg-I decreased while the levels of Deg-R increased. (B) The mass spectrum of Deg-I with a molecular ion of 290 is depicted. The arrow points to appearance of the Deg-I peak.

same ratio of both derivatives as was observed in JA-treated wild type plants (Figure 3.3). Surprisingly, a third compound was detected after 1.5 h at retention time T_R =26.1 min with a mass spectrum again similar to that of arabidonol (Figure 3.4B). This compound was also found at 3 h of arabidonol application though at lower amounts and was present at trace amounts 24 h after feeding suggesting that it is as a possible intermediate in the arabidonol modification pathway, therefor named Deg-I.

Purification and Structure Elucidation of Arabidonol Modification Products

Our initial attempt to purify the detected modification products directly from JA-treated *Arabidopsis* roots was not successful because of insufficient amounts of compounds and the complexity of the background matrix. However, since we found arabidonol to be efficiently converted into downstream products upon its application to axenic plant cultures, we used this bioconversion approach to produce the derivatives at levels sufficient for NMR analysis. For the production of Deg-I, *abds-1* plants were treated with 4-6 mg of purified arabidonol for 3 h prior to an extraction of the compound from the culture medium with ethyl acetate. In separate experiments ethyl acetate extractions of roots and culture medium were done 24 h after arabidonol feeding to extract Deg-R and Deg-M, respectively. The extracts were subjected to flash chromatography and thin layer chromatography (TLC) purification as described under Methods.

Deg-M and Deg-R samples with more than 90% purity were analyzed by NMR spectroscopy (^{1}H-NMR, ^{13}C-NMR, HMBC, and QMBC), which suggested the molecular structures shown in Figure 3.6. The difference between Deg-M and arabidonol was limited to the C3-OH position with a conversion from β in arabidonol into α in Deg-M indicating

epimerization reaction. In Deg-R, in addition to the C3-OH epimerization from β into α, the C3-OH has been modified by the addition of an acetyl group, evident from appearance of the second carbonyl correlation in HMBC analysis. NMR analysis of Deg-I is still in progress, but our preliminary analysis suggests a dehydrogenation reaction at the C_3-OH position of arabidonol which follows by its immediate conversion into Deg-M. According to the structural analysis, a putative pathway for the modification of arabidonol was developed as shown in Figure 3.5.

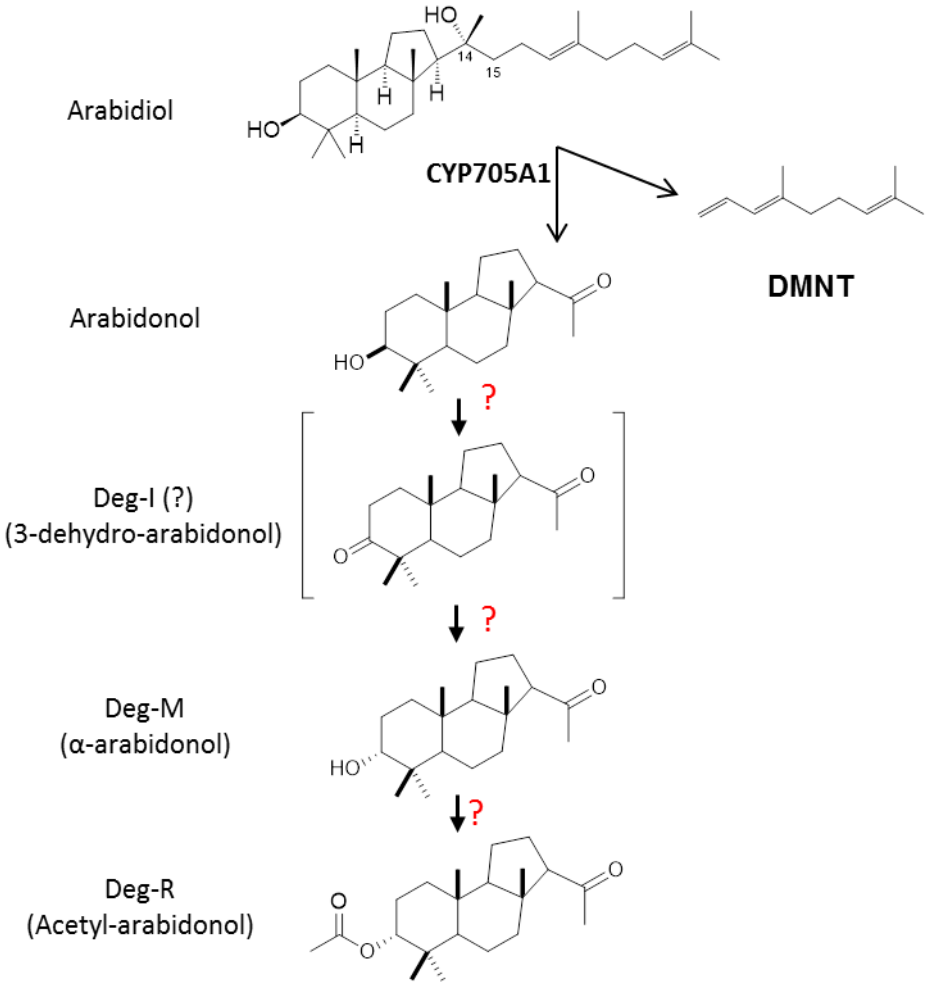

Figure 3.5 Putative pathway for the formation of arabidonol derivatives.

Structural analysis of compounds was performed using ^{1}H-NMR and ^{13}C-NMR analysis. The structures of arabidonol derivatives are shown. We predict Deg-I as 3-dehydro-arabidonol. Deg-M is suggested to be a product of epimerization of arabidonol at the C_3 position. Deg-R is modified by addition of an acetyl group to for acetyl-arabidonol.

Application of Individual Derivatives to Confirm the Sequence of Arabidonol Modification Steps

We performed feeding experiments with the purified individual compounds to further examine the suggested sequence of the modification reactions. Compounds were applied for 30 h to axenically grown *abds-1* plants and products were extracted from the culture medium and analyzed by GC-MS (Figure 3.6). Upon feeding with arabidonol, we detected Deg-I, the α-arabidonol isomer, Deg-M, and small amounts of acetyl-arabidonol (Deg-R) similar to results presented in Figure 3.4. Application of Deg-I resulted in substantial production of Deg-M suggesting an immediate conversion of this intermediate (Figure 3.6A). Feeding with Deg-M only yielded Deg-R suggesting Deg-M to be a substrate of a subsequent acetyl transferase reaction. Upon feeding with Deg-R no derivatives were detected (Figure 3.6B) indicating that the acetylated form of arabidonol might be converted into a more polar product, which is not extractable by ethyl acetate. Collectively, these results confirm the suggested sequential modification pathway of epimerization via a Deg-I intermediate followed by an acylation of the C_3 hydroxyl group to yield acetyl-arabidonol (Figure 3.5).

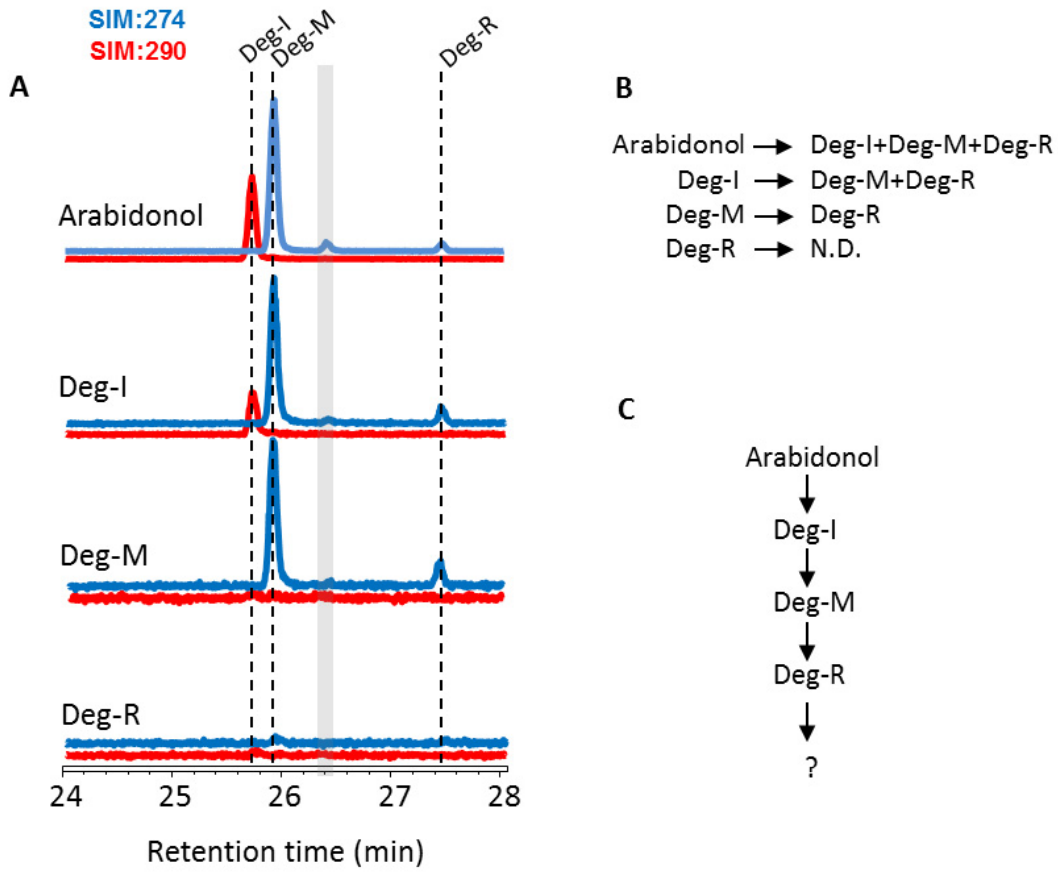

Figure 3.6 Arabidonol is converted to acetyl-arabidonol via two intermediates.

(A) Feeding studies were performed with arabidonol, Deg-I, Deg-M and Deg-R in axenically grown root cultures of *abds-1* plants for 3 h. Single ion monitoring (SIM) mode analysis result is shown for characteristic ion from MS spectrum profiles (*m/z* 290 for Deg-I and *m/z* 274 for arabidonol, Deg-M and Deg-R). (B) The compounds detected after feeding with each modification product are listed. N.D., not detected. (C) Suggested order of compound modifications in the arabidonol conversion pathway.

Functional Expression of the Putative Acyltransferase At4g15390 in Yeast

As an approach to identify genes involved in the modification of arabidonol, we looked for genes on the *ABDS* gene cluster that may encode enzymes catalyzing the suggested conversion steps (isomerases, dehydrogenases, or acyl transferases). Although genetic linkage of the genes on the *ABDS* cluster region may suggest a role in the same biosynthetic pathway, our

analysis of publically available microarray experiments indicated that most of the clustered genes are not highly co-regulated with *ABDS*/*CYP705A1* and are expressed only at low levels in roots (Supplemental Figures 3.1 and 3.2). One of the clustered genes (At4g15390) has been annotated as a putative acyltransferase gene (Figure 2.8). Although this gene is not co-regulated with *ABDS* and *CYP705A1*, it is expressed at high levels in roots suggesting a possible acyltransferase activity in converting Deg-M into acetyl-arabidonol. Expression of this gene in yeast in the presence of externally applied Deg-M did not lead to the detection of acetyl-arabidonol (data not shown). Therefore, we concluded that other possible acyltransferase enzymes, which are not physically linked to the *ABDS* cluster, might be involved in this reaction.

Genetic and Evolutionary Approaches for the Identification of Genes Involved in the Arabidiol Catabolic Pathway

We previously used QTL analysis as a successful approach in combination with gene expression analysis to identify the *CYP705A1* gene, which is responsible for the degradation of arabidiol (Sohrabi et al., unpublished). The QTL approach was based on the analysis of recombinant inbred lines (RILs) of the two *Arabidopsis* accessions Cvi and L*er*. Since Cvi is impaired in the formation of DMNT, we reasoned that this accession might also be unable to modify arabidonol. However, upon feeding of axenically grown Cvi plants with arabidonol, we found a conversion of the compound into all downstream products that have been detected in the Col-0 accession (Figure 3.7). By contrast, in the L*er* accession, arabidonol was converted only to Deg-M but not further converted into Deg-R (Figure 3.7). This result suggests accession-dependent natural variation in the acylation of arabidonol. A further analysis of the arabidonol

modification in recombinant inbred lines from a cross between L*er* x Cvi will be required to associate this natural variation with corresponding biosynthetic genomic loci.

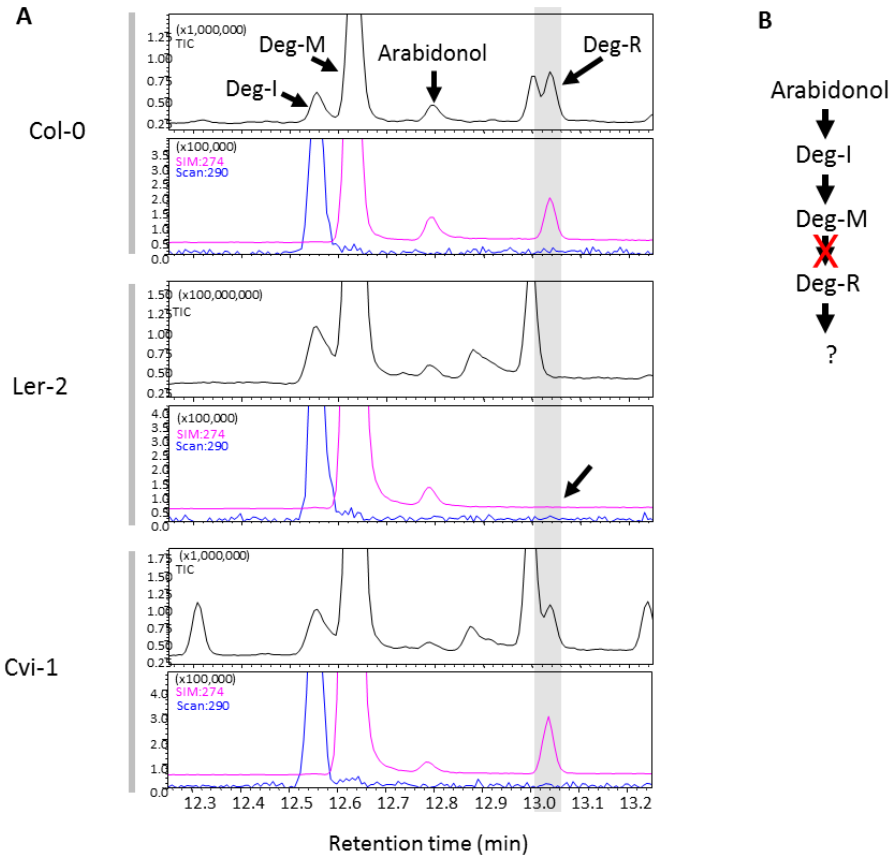

Figure 3.7 Natural Variation in the Modification of Arabidiol-Derived Compounds Between Different Accessions of *Arabidopsis*.

(A) The total ion chromatograms (TIC) and SIM analysis profiles for *m/z 290* and 274 are shown. Arabidonol was applied at 30 µM concentration for 3 h to axenic cultures of Col-0, Cvi, and L*er* plants. Roots of Col-0 and Cvi converted arabidonol into the downstream products (Deg-I, Deg-M, and Deg-R), but in L*er* only Deg-I and Deg-M were detected. The TIC and SIM scan profiles are shown. (B) The predicted pathway for arabidonol modification is shown. The red X indicates the step impaired in the L*er* accession.

Our previous genome synteny analysis of the *ABDS* gene cluster in *Arabidopsis* suggested that the arabidiol biosynthesis and degradation pathway emerged recently after divergence of *A. thaliana* and *A. lyrata* from their common ancestor. Therefore, we postulated

that the ability to modify arabidonol should have evolved after this divergence and no modification of arabidonol should be observed in *A. lyrata*. To test this hypothesis, axenically grown *A. lyrata* plants were fed with 30 µM arabidonol for 3 h. Interestingly, we found that *A. lyrata* roots converted arabidonol primarily into the intermediate compound Deg-I and produced only trace amounts Deg-M and no acetyl-arabidonol was detected (Figure 3.8). However, the ability of *A. lyrata* to convert Deg-M into acetyl-arabidonol was not evaluated in a separate feeding experiment in this study.

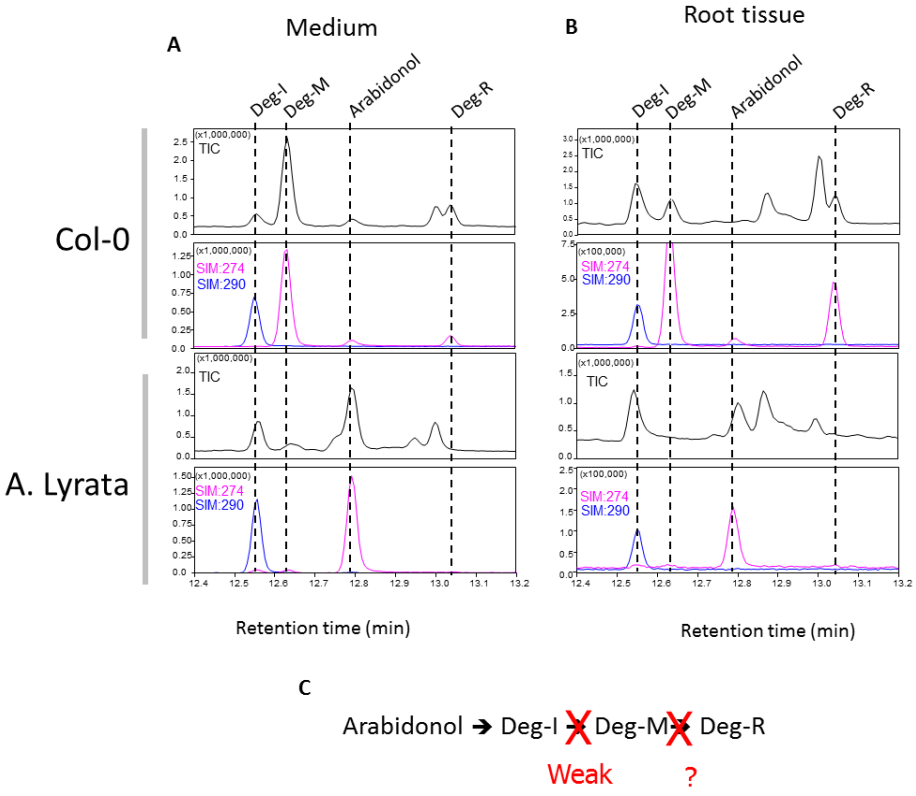

Figure 3.8 Arabidonol is modified differently in *A. thaliana* and *A. lyrata*.

(A) and (B)The TIC and SIM analysis profiles for *m/z 290* and 274 are shown. *A. thaliana Col-0* and *A. lyrata* plants were grown axenically and treated with arabidonol for 3 h. Organic extractions were done from culture medium (A) and root tissue (B). Only conversion to Deg-I and at a very low level to Deg-M was observed in as the culture medium and roots after arabidonol feeding while no Deg-R was detected in *A. lyrata*. (C) The predicted pathway for arabidonol modification is shown. The red X indicates steps in the pathway with possible difference between *A. thaliana* and *A. lyrata.*

DISCUSSION

The Arabidiol Catabolic Pathway Contains Several Modification Steps

We have previously reported that the triterpene alcohol, arabidiol, is degraded into the volatile C_{11}-homo/norterpene, DMNT, and the C_{19} ketone, arabidonol, in a reaction that is induced upon treatment with JA and the soil-borne pathogen *P. irregulare*. Since arabidonol could only be detected as a product of CYP705A1 when this enzyme was expressed in yeast, but was absent in planta, we assumed that the cleavage product was further modified or catabolized. Upon JA treatment we have detected two compounds with high mass spectrum similarity to arabidonol, which were absent from *abds-1* plants, suggesting that they were possible arabidonol derivatives. Because of the unavailability of a labeled arabidonol substrate and the lack of knowledge about the enzymatic nature of the modification reactions, we used a biotransformation approach by applying purified precursors. This approach was successful in obtaining modification products at sufficiently high amounts for subsequent NMR analysis. Biotransformation has been used widely in pharmaceutical industry to produce value-added phyto-pharmaceuticals in hairy root cultures of various plant species by biochemical reactions such as glycosylation, oxidation, reduction, isomerization, cyclization, acetylation and hydrolysis (Banerjee et al., 2012).

Our feeding experiments with arabidonol suggested modification of arabidonol into at least three products. We have suggested Deg-I as putative intermediate in epimerization of arabidonol into Deg-M. Previous studies on the brassinosteroid hormone biosynthesis pathway have shown the presence of a ketone intermediate in C_3-epimerization of teasterone (β-C_3-OH) to typhasterol (α-C_3-OH). In this pathway, teasterone is modified to a 3-dehydroteasterone

intermediate via dehydrogenation and later converted to typhasterol by a reductase activity (Suzuki et al., 1994; Park et al., 1999). Therefore, we predict that Deg-I might similarly serve as a ketone intermediate in arabidonol epimerization to Deg-M. Interestingly, it has been shown that the rice CYP90D2 converts teasterone into 3-dehydroteasterone (Hong et al., 2003) and we predict that a similar P450 mediated reaction might result in arabidonol conversion to Deg-I.

The β orientation at the C_3-OH group is the most abundant orientation in sterols and triterpenoids and in their corresponding glycosides is linked to sugar moieties via a β-glycosidic bond (Haralampidis et al., 2002; Benveniste, 2004). However, triterpenoid glycosides have been reported with an α orientation at their C_3-OH such as saponin QS-21, derived from the bark of the *Quillaja saponaria* Molina tree (Jacobsen et al., 1996). Additionally, modifications such as β to α epimerization for cholesterol in animal systems which have been reported to increase the phosphatidylcholine chain order in membranes and decrease membrane permeability (Rog and Pasenkiewicz-Gierula, 2003). However the ability of Deg-M to partition in membranes and its potential effects on membrane fluidity and permeability is not clear.

Our results suggest that Deg-M (putative α-arabidonol) is further modified to Deg-R via acetylation. In triterpene glycoside biosynthesis there are several examples of acylation at C_3-OH of the triterpene moiety prior to glycosidic bond formation (Augustin et al., 2011). At this time, it is not clear whether acetyl-arabidonol is further modified *in planta*. Since feeding with acetyl-arabidonol did not result in any detectable products, further modification reactions such as additional glycosylations and hydroxylations cannot be excluded. There are also examples of diterpene glycosides with biological activities such as stevioside, a stevia glycoside derived from the steviol diterpene (Hanson and De Oliveira, 1993) with inhibitory effect on monosaccharide metabolism in the rat liver (Ishii et al., 1987) Also, 17-hydroxygeranyllinalool diterpene

glycosides in *Nicotiana attenuata* are produced as JA-dependent anti-feeding diterpene glycosides (Heiling et al., 2010).

We have shown that α-arabidonol and its acetylated form occur in root exudates. It should be noted that these compounds have not been described in previous studies of *Arabidopsis* root exudation (Badri et al., 2009; Badri et al., 2012). Root exudation of phytochemicals from plants has been shown to play a role in plant interactions with microbial communities as well as other plant species (Bais et al., 2006; Badri and Vivanco, 2009). Therefore, we predict that the JA-induced production of the detected compounds might contribute to the interaction of *Arabidopsis* with microbial communities in the rhizosphere (Carvalhais et al., 2013).

Our previous experiments on evaluating the *in vitro* bioactivity of the arabidiol-derived degradation products suggested a role only for DMNT but not arabidonol in the inhibition of *Pythium* oospore germination and mycelium growth. It is possible that the detected arabidonol derivatives play a role in the defense against *Pythium* since the secretion of α-arabidonol and acetyl-arabidonol suggest a potential role as phytoalexins in the rhizosphere. To obtain a better understanding of the biological function of the arabidonol derivatives in the *Arabidopsis*-*Pythium* interaction or any other Arabidopsis root-pathosystem, a more comprehensive study of the effects of these metabolites in vivo and in vitro is required.

Our results have shown that the biotransformation of arabidonol is JA-independent. This is an interesting aspect of regulation of arabidiol biosynthesis and degradation in *Arabidopsis*. The transcripts of *ABDS* and *CYP705A1* are induced upon JA treatment in roots leading to the subsequent increased production of DMNT and arabidonol *in planta*. The immediate conversion of arabidonol into its downstream products may happen via enzymatic activities catalyzed by

constitutively expressed genes in roots. The reason for uncoupling JA-dependency of arabidonol production from its constitutive downstream modification is not clear yet but a possible cell auto toxicity effect for arabidonol derivatives could be considered.

We have found two degradation products of arabidiol in exudates from *Arabidopsis* roots in response to treatment with the defense hormone jasmonic acid. Recent findings suggest an involvement of ATP-binding cassette (ABC) transporters in the secretion of phytochemicals (including terpenes) from roots in *Arabidopsis* and other plant species (Loyola-Vargas et al., 2007; Sugiyama et al., 2007; Badri and Vivanco, 2008). ABC transporters, which are the largest family of transporters, use ATP to pump a diverse array of substrates across plasma membranes (Goossens et al., 2003; Bednarek et al., 2010). We hypothesize a role of ABC transporters in the secretion of arabidiol-derived metabolites in *Arabidopsis* roots, which are induced in the presence of the terpene metabolite as was previously reported for a diterpene-specific transporter in *Nicotiana* leaves (Jasinski et al., 2001). Additionally, several ABC transporters have been reported in the secretion of specialized phytochemicals from *Arabidopsis* roots (Badri et al., 2008; Badri et al., 2009). However, we currently cannot exclude other transporters such as those of the major facilitator superfamily or ion channels and, therefore, further studies are required to identify the respective transporter gene candidates.

Identification of Arabidonol Modifying Enzymes

Previous studies on the biosynthesis of diterpenes and triterpenes have revealed that genes encoding multiple steps of the corresponding pathways are clustered and often co-regulated in an operon-type fashion (Field and Osbourn, 2008; Swaminathan et al., 2009). Our previous genome synteny analysis has suggested recent evolution of the arabidiol production and

cleavage pathway as a gene cluster in *Arabidopsis* (Sohrabi et al.). In *A. lyrata,* a baroul synthase like protein with 84% amino acid sequence identity to *ABDS* along with two members of the *Brassicaceae* specific CYP705 family (CYP705A2 and CYP705A3) are present. Additionally, there are several different genes families on the ABDS region, which are highly syntenic between three genomes including *Brassicaceae* specific P450 CYP702, acyltransferases, glycosyltransferases and ABC transporters (Supplemental figure 3.1). We assumed that some genes on this cluster such as CYP705 and CYP702 members with so far unidentified function may play a role in the downstream modification of arabidonol. We did not necessarily expect these genes to be induced by JA since the modification reactions proofed to be JA-independent. However, we expected candidate genes to be expressed in the same tissue or cells as *ABDS* and *CYP705A1*. Against our expectation, most other genes on the cluster are not co-regulated at the tissue level with the *ABDS*/*CYP705A1* gene module and a putative acyltransferase with high expression in roots does not appear to modify α-arabidonol when expressed in yeast. We predict that other loci are responsible for the observed modification steps. A QTL analytical approach using Cvi x Ler recombinant inbred lines could be used to pinpoint putative genes involved in the acetylation of α-arabidonol.

Comparison of *A. thaliana* with its close relative, *A. lyrata*, showed that the enzymatic step to produce the intermediate compound Deg-I is conserved in both species, while this does not seem to be the case for the downstream reactions. This finding may suggest that the enzymatic activity for the modification of arabidonol into Deg-I was present in the common ancestor of *A. lyrata* and *A. thaliana* before their divergence and the subsequent evolution of the arabidiol biosynthetic and cleavage steps in *A. thaliana*. Such evolutionary scheme has been reported for the biosynthesis of arabidopyrones in *Arabidopsis*, in which a highly conserved

extradiol ring-cleavage dioxygenase was capable of converting a novel enzymatic reaction product (a catechol-substituted substrate) derived from gene duplication and neofunctionalization events (Weng et al., 2012). It is likely that the conversion of Deg-I into Deg-M is similarly associated with an existing enzymatic activity with low substrate specificity, which is capable of accepting arabidonol as an additional substrate. On the other hand, the enzymatic step for modification of Deg-I into α-arabidonol was partially active in *A. lyrata* and may have gone through subsequent evolutionary specialization to establish a new activity. Whether the final acyltransferase step is entirely absent in *A. lyrata* needs to be further investigated by the specific application of pure α-arabidonol compound. Together, our studies on *Arabidopsis* accessions and close relatives demonstrate genotype-dependent plasticity in the assembly of the arabidiol catabolic pathway and present an example of a secondary metabolic pathway that is dependent on gene-cluster specific and unspecific gene activities.

METHODS

Plant Materials and Growth Conditions

Arabidopsis mutants (*abds-1* and *cyp705a1-1)* used in this study were described in Chapter 2. The Cvi and *Ler* accessions were part of the RIL population described previously (Alonso-Blanco et al., 1998). *Arabidopsis lyrata* was acquired from the ABRC stock center (Alonso et al., 2003). Axenic plants were maintained as described by Hetu et al. (2005). Two days before treatment and harvesting of the root tissue, the MS medium was changed to reduce the sucrose level to 1%. JA treatment was done by applying 100 μM JA (Sigma Aldrich, St. Louis, MO) directly to the liquid medium of the root culture. All plants were grown in short day

(10-h light/14-h dark photoperiod) under 150 μmol m^{-2} s^{-1} photosynthetically active radiation (PAR) at 22°C.

Production and Purification of Arabidonol from Yeast Expression Lines

To produce arabidonol in larger quantities, we used transgenic WAT11 (Urban et al., 1997) yeast lines expressing *ABDS* and *CYP705A1*. Yeast cells were grown as described previously (Sohrabi et al.) with minor modification. Briefly, for large scale purification of arabidonol, 9 L of yeast culture was prepared in YPI medium and induced with 2% of galactose. DMNT levels were monitored every day to ensure continuous degradation of arabidiol and production of arabidonol. After 5 days of galactose induction, yeast cells were separated from the growth medium by centrifugation at 7000 rpm. The water from the growth medium was removed by sublimation in a lyophilizer (Labconco) over a period of 5 days and the dried out material was used for extraction of arabidonol. The residual lyophilized material from the medium was resuspended in 1 L of double distilled water followed by three times extraction with 1 L of ethyl acetate. The ethyl acetate extracts were combined and organic solvent was removed to dryness under low pressure using a rotary evaporator (Cole-Parmer). Then, the extract was subjected to flash chromatography over silica gel (Merck grade 9385, pore size 60 Å, 230-400 mesh (Sigma)). For transferring the extract to the column, first, a slurry of extract was prepared by adding 50 mL of ethyl acetate and 3 g of silica gel to the round bottom flask followed by rotary evaporation to obtain dried silica particles attached to the extracts. Then the silica gel with the extract was loaded onto a preconditioned silica gel flash chromatography column and several fractions were collected as described previously (Sohrabi et al.). Aliquots of fractions containing arabidonol were individually loaded on preparative thin layer chromatography (TLC) plates (20

x 20 cm silica gel pore size 60 Å (250 µm) with 2.5 x 20 cm concentration zone) and developed with a 5:2 mixture of hexanes:ethyl acetate as described before (Sohrabi et al.). Silica gel was scraped from the plates at an R_f value similar to that of arabidonol and the purity of the extracted compound was evaluated by GC-MS analysis.

Analysis of Arabidonol Derivatives in Plants

Extraction of arabidonol derivatives from plants was performed with plant material from axenically grown cultures. Arabidonol dissolved in DMSO was applied at 3 or 30 µM concentration and cultures were incubated over a range of different times. Arabidonol derivatives were extracted with 10 mL ethyl acetate from 1 g of ground root material. One volume of water was added to the mixture for phase separation and the top organic layer was collected followed by two additional extractions with 10 mL of ethyl acetate each time. Ethyl acetate extracts were combined, dried down using a rotary evaporator, and passed through a small silica gel column (2 cm) that was prepared in glass pasture pipettes for removal of highly polar ethyl acetate extracted compounds. Samples were dried using compressed N2 (Airgas) and resuspended in ethyl acetate and analyzed by GC-MS. Extraction of arabidonol derivatives from root exudates was done by extracting the MS growth medium of *abds-1* plants at different time points. Briefly, water from 15 mL of growth medium was evaporated to dryness using a lyophilizer and the sample was resuspended in 2 mL of double distilled water followed by three times extraction with 10 mL of ethyl acetate. Organic extracts were combined, dried under low pressure, resuspended in small amounts of ethyl acetate, and cleaned up by passing through a small silica gel column. Samples were concentrated under a N_2 stream subsequently analyzed by GC-MS.

Purification of Modification Products

In order to obtain large amounts of arabidonol derivatives, feeding experiments were done several times with aliquots of arabidonol ranging from 2-6 mg using axenically grown *abds-1* plants. To obtain Deg-I, feeding experiments were done in three axenic culture flasks for 3 h followed by three extractions per flask with equal volumes of ethyl acetate and medium. Ethyl acetate extracts were combined and dried under low pressure and loaded onto a silica gel flash chromatography column (standard joint and PTFE Stopcock, 10" with 10 mm internal diameter glass column, Kemtech America) preconditioned with 4:1 hexanes:ethyl acetate. Then, 10 mL fractions were collected and a small aliquot was analyzed by GC-MS. A method was developed for TLC purification of Deg-I by evaluating different developing solvent conditions and identifying the TLC behavior of Deg-I. This was done by comparing R_f value of compounds between fractions containing high levels of Deg-I with the ethyl acetate extract before flash chromatography separation. In summary, fractions containing Deg-I were subjected to TLC purification by developing with 4:1 hexanes:ethyl acetate and Deg-I was localized by running a small aliquot of the ethyl acetate extract before flash chromatography separation followed by *p*-anisaldehyde-sulfuric acid staining (Hahn-Deinstrop, 2007).

For purification of α-arabidonol (Deg-M), arabidonol feeding was done for 24 h. The same procedure for flash chromatography and TLC analysis was used. α-Arabidonol was found in later fractions upon elution with 4:1 hexanes:ethyl acetate compared to Deg-I and showed a different TLC behavior more similar to arabidonol. α-Arabidonol was verified with GC-MS at each step during separation and purification steps.

For purification of acetyl-arabidonol (Deg-R), arabidonol feeding was done for 24 h. Instead of the culture medium the root tissue was used for extraction since higher amounts of

acetyl-arabidonol were found in root extracts. Ground root material from three axenic cultures treated with 6 mg of arabidonol was mixed with 50 mL of double distilled and extracted three times with 50 mL of hexanes. The hexanes extract was condensed and loaded onto the flash chromatography column as described above. Upon eluting compounds from the column with 4:1 hexanes:ethyl acetate, the fraction containing acetyl-arabidonol were verified with GC-MS and used for TLC purification. Finally, acetyl-arabidonol was also verified by GC for purity.

NMR Analysis of Modification Products

Purified samples were dissolved in $CDCl_3$ and submitted to NMR analysis at Chemistry department at Virginia Tech. ^{1}H and ^{13}C NMR spectra were recorded on a JEOL Eclipse 500 and Bruker Avance 600 spectrometers in CDCl3 or CD3OD with TMS as internal standard.

Supplemental Materials

Supplemental Figure 3.1 Genes on the *ABDS*/*BARS* cluster are not highly co-regulated under normal developmental condition.

Results were obtained from GENVESTIGATOR (Zimmermann et al., 2004). The expression values for genes are presented as gene expression potential percentage. A darker red color suggests higher expression.

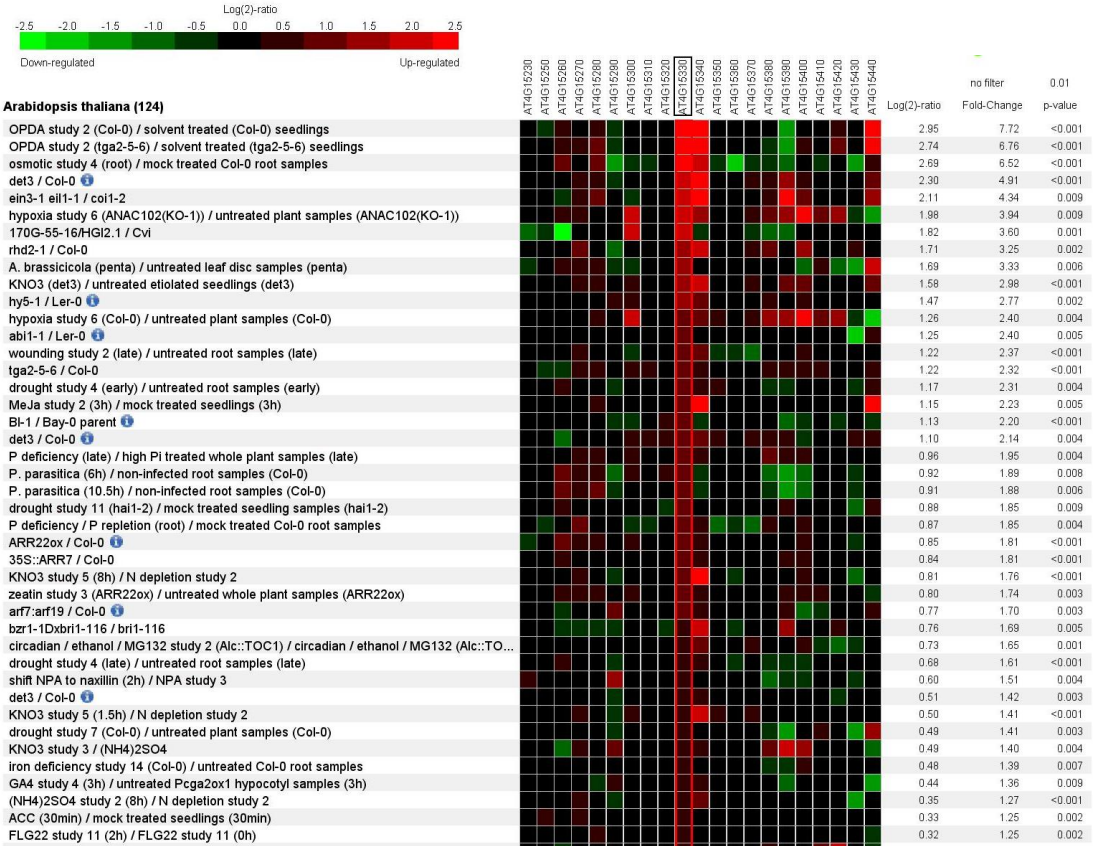

Supplemental Figure 3.2 Genes of the *ABDS*/*BARS* cluster are not co-regulated under stress conditions.

Results were obtained from GENVESTIGATOR (Zimmermann et al., 2004). The expression values for genes are presented as fold change in log (2) ratios. A red color presents up-regulation and green down-regulation.

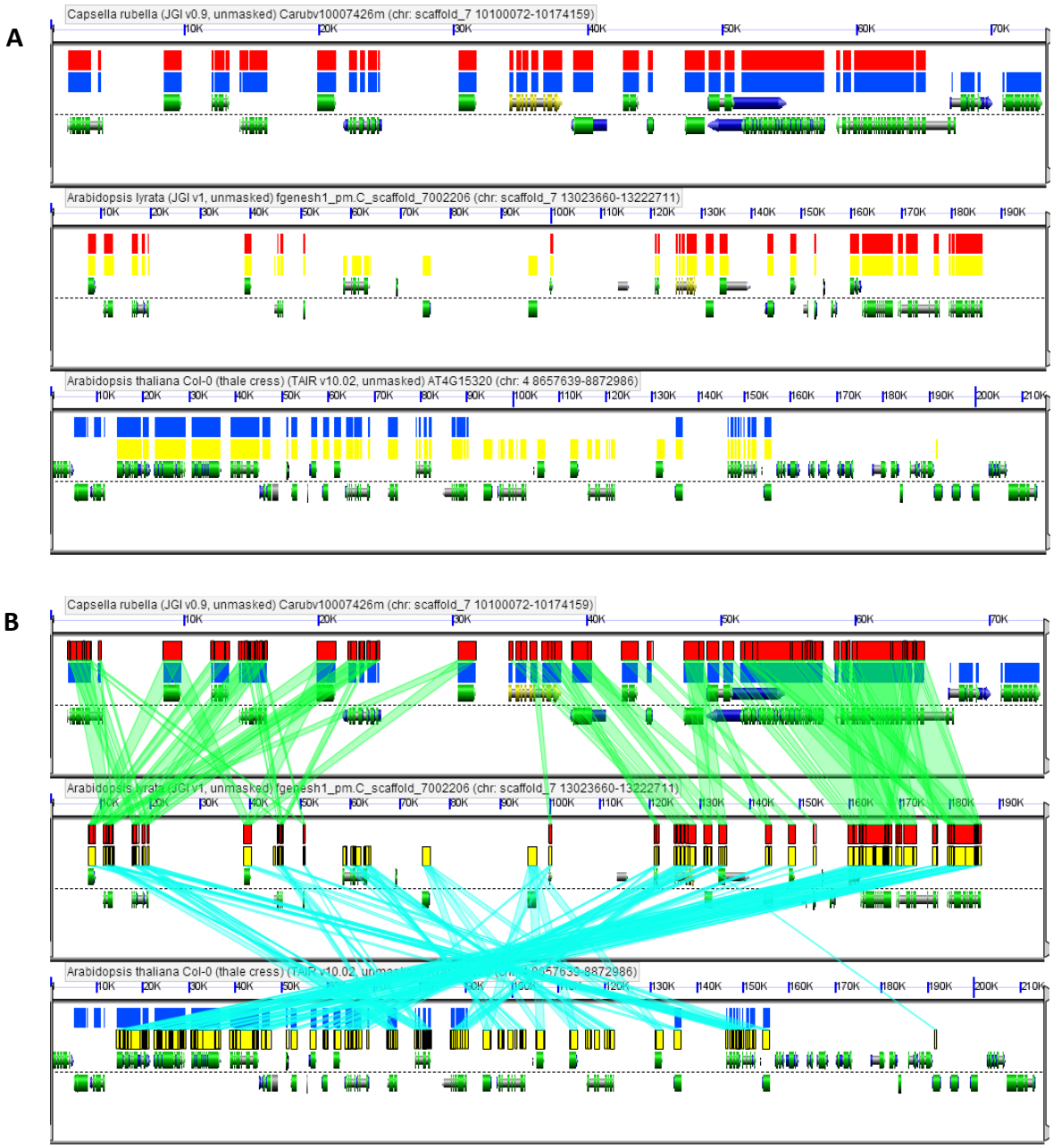

Supplemental Figure 3.3 Genome evolution analysis of the ABDS/BARS region.

The CYP705A1 activity has evolved most likely along with ABDS activity in *A. thaliana*. Only a single triterpene synthase ortholog in *A. lyrata* was found for the *ABDS*/*BARS* region presumable encoding a BARS activity. Other genes on the genome are highly syntenic between *C. rubella*, *A. lyrata* and *A. thaliana*, but the orientation and copy number has gone through several changes. Comparative genome analysis was done online using the GeVO tool (http://synteny.cnr.berkeley.edu/CoGe/) (Lyons and Freeling, 2008). (A) and (B) Syntenic regions between *C. rubella* and *A. lyrata*, *C. rubella* and *A. thaliana*, *A. lyrata* and *A. thaliana* are color coded in red, blue and yellow, respectively. (B) Syntenic regions between *C. rubella* and *A. lyrata*, and *A. thaliana* and *A. lyrata* are connected by green and cyan lines, respectively.

Literature Cited

Alonso-Blanco, C., El-Assal, S.E., Coupland, G., and Koornneef, M. (1998). Analysis of natural allelic variation at flowering time loci in the Landsberg erecta and Cape Verde Islands ecotypes of Arabidopsis thaliana. Genetics **149,** 749-764.

Alonso, J.M., Stepanova, A.N., Leisse, T.J., Kim, C.J., Chen, H., Shinn, P., Stevenson, D.K., Zimmerman, J., Barajas, P., Cheuk, R., Gadrinab, C., Heller, C., Jeske, A., Koesema, E., Meyers, C.C., Parker, H., Prednis, L., Ansari, Y., Choy, N., Deen, H., Geralt, M., Hazari, N., Hom, E., Karnes, M., Mulholland, C., Ndubaku, R., Schmidt, I., Guzman, P., Aguilar-Henonin, L., Schmid, M., Weigel, D., Carter, D.E., Marchand, T., Risseeuw, E., Brogden, D., Zeko, A., Crosby, W.L., Berry, C.C., and Ecker, J.R. (2003). Genome-wide insertional mutagenesis of *Arabidopsis thaliana*. Science **301,** 653-657.

Augustin, J.M., Kuzina, V., Andersen, S.B., and Bak, S. (2011). Molecular activities, biosynthesis and evolution of triterpenoid saponins. Phytochemistry **72,** 435-457.

Badri, D.V., and Vivanco, J.M. (2009). Regulation and function of root exudates. Plant Cell and Environment **32,** 666-681.

Badri, D.V., Chaparro, J.M., Manter, D.K., Martinoia, E., and Vivanco, J.M. (2012). Influence of ATP-Binding Cassette Transporters in Root Exudation of Phytoalexins, Signals, and in Disease Resistance. Frontiers in plant science **3,** 149.

Badri, D.V., Quintana, N., El Kassis, E.G., Kim, H.K., Choi, Y.H., Sugiyama, A., Verpoorte, R., Martinoia, E., Manter, D.K., and Vivanco, J.M. (2009). An ABC transporter mutation alters root exudation of phytochemicals that provoke an overhaul of natural soil microbiota. Plant Physiol **151,** 2006-2017.

Badri, D.V., Loyola-Vargas, V.M., Broeckling, C.D., De-la-Pena, C., Jasinski, M., Santelia, D., Martinoia, E., Sumner, L.W., Banta, L.M., Stermitz, F., and Vivanco, J.M. (2008). Altered profile of secondary metabolites in the root exudates of Arabidopsis ATP-binding cassette transporter mutants. Plant Physiology **146,** 762-771.

Bais, H.P., Prithiviraj, B., Jha, A.K., Ausubel, F.M., and Vivanco, J.M. (2005). Mediation of pathogen resistance by exudation of antimicrobials from roots. Nature **434,** 217-221.

Bais, H.P., Weir, T.L., Perry, L.G., Gilroy, S., and Vivanco, J.M. (2006). The role of root exudates in rhizosphere interations with plants and other organisms. Annual Review of Plant Biology **57,** 233-266.

Banerjee, S., Singh, S., and Rahman, L.U. (2012). Biotransformation studies using hairy root cultures - A review. Biotechnol Adv **30,** 461-468.

Bednarek, P., Kwon, C., and Schulze-Lefert, P. (2010). Not a peripheral issue: secretion in plant-microbe interactions. Current Opinion in Plant Biology **13,** 378-387.

Benveniste, P. (2004). Biosynthesis and accumulation of sterols. Annu Rev Plant Biol **55,** 429-457.

Bohlmann, J., Meyer-Gauen, G., and Croteau, R. (1998). Plant terpenoid synthases: Molecular biology and phylogenetic analysis. Proceedings of the National Academy of Sciences **95,** 4126-4133.

Boutte, Y., and Grebe, M. (2009). Cellular processes relying on sterol function in plants. Curr Opin Plant Biol **12,** 705-713.

Carvalhais, L.C., Dennis, P.G., Badri, D.V., Tyson, G.W., Vivanco, J.M., and Schenk, P.M. (2013). Activation of the jasmonic acid plant defence pathway alters the composition of rhizosphere bacterial communities. PLoS One **8,** e56457.

Chen, F., Tholl, D., Bohlmann, J., and Pichersky, E. (2011). The family of terpene synthases in plants: a mid-size family of genes for specialized metabolism that is highly diversified throughout the kingdom. The Plant Journal **66,** 212-229.

Field, B., and Osbourn, A. (2008). Metabolic diversification - Independent assembly of operon-like gene clusters in plants. Science **320,** 543 - 547.

Fridman, E., and Pichersky, E. (2005). Metabolomics, genomics, proteomics, and the identification of enzymes and their substrates and products. Curr. Opin. Plant Biol. **8,** 242-248.

Goossens, A., Hakkinen, S.T., Laakso, I., Oksman-Caldentey, K.M., and Inze, D. (2003). Secretion of secondary metabolites by ATP-binding cassette transporters in plant cell suspension cultures. Plant Physiology **131,** 1161-1164.

Hahn-Deinstrop, E. (2007). In Applied Thin-Layer Chromatography (Wiley-VCH Verlag GmbH & Co. KGaA.

Hanson, J.R., and De Oliveira, B.H. (1993). Stevioside and related sweet diterpenoid glycosides. Natural Product Reports **10,** 301-309.

Haralampidis, K., Trojanowska, M., and Osbourn, A.E. (2002). Biosynthesis of triterpenoid saponins in plants. Advances in biochemical engineering/biotechnology **75,** 31-49.

Heiling, S., Schuman, M.C., Schoettner, M., Mukerjee, P., Berger, B., Schneider, B., Jassbi, A.R., and Baldwin, I.T. (2010). Jasmonate and ppHsystemin regulate key Malonylation steps in the biosynthesis of 17-Hydroxygeranyllinalool Diterpene Glycosides, an abundant and effective direct defense against herbivores in Nicotiana attenuata. Plant Cell **22,** 273-292.

Hong, Z., Ueguchi-Tanaka, M., Umemura, K., Uozu, S., Fujioka, S., Takatsuto, S., Yoshida, S., Ashikari, M., Kitano, H., and Matsuoka, M. (2003). A rice brassinosteroid-deficient mutant, ebisu dwarf (d2), is caused by a loss of function of a new member of cytochrome P450. Plant Cell **15,** 2900-2910.

Ishii, E.L., Schwab, A.J., and Bracht, A. (1987). Inhibition of monosaccharide transport in the intact rat liver by stevioside. Biochemical pharmacology **36,** 1417-1433.

Jacobsen, N.E., Fairbrother, W.J., Kensil, C.R., Lim, A., Wheeler, D.A., and Powell, M.F. (1996). Structure of the saponin adjuvant QS-21 and its base-catalyzed isomerization product by 1H and natural abundance 13C NMR spectroscopy. Carbohydrate research **280,** 1-14.

Jaenicke, L., and Marner, F.J. (1990). The Irones and Their Origin. Pure Appl Chem **62,** 1365-1368.

Loyola-Vargas, V.M., Broeckling, C.D., Badri, D., and Vivanco, J.M. (2007). Effect of transporters on the secretion of phytochemicals by the roots of Arabidopsis thaliana. Planta **225,** 301-310.

Lyons, E., and Freeling, M. (2008). How to usefully compare homologous plant genes and chromosomes as DNA sequences. Plant Journal **53,** 661-673.

Mary, W., Crombie, L., and Crombie, L. (1986). Distribution of avenacins A-1, A-2, B-1 and B-2 in oat roots: Their fungicidal activity towards `take-all' fungus. Phytochemistry **25,** 2069-2073.

Nes, W.D., and Heftmann, E. (1981). A Comparison of Triterpenoids with Steroids as Membrane-Components. Journal of Natural Products **44,** 377-400.

Osbourn, A., Goss, R.J., and Field, R.A. (2011). The saponins: polar isoprenoids with important and diverse biological activities. Nat Prod Rep **28,** 1261-1268.

Park, S.H., Han, K.S., Kim, T.W., Shim, J.K., Takatsuto, S., Yokota, T., and Kim, S.K. (1999). In vivo and in vitro conversion of teasterone to typhasterol in cultured cells of Marchantia polymorpha. Plant and Cell Physiology **40,** 955-960.

Phillips, D.R., Rasbery, J.M., Bartel, B., and Matsuda, S.P. (2006). Biosynthetic diversity in plant triterpene cyclization. Curr Opin Plant Biol **9,** 305-314.

Rog, T., and Pasenkiewicz-Gierula, M. (2003). Effects of epicholesterol on the phosphatidylcholine bilayer: a molecular simulation study. Biophys J **84,** 1818-1826.

Sohrabi, R., Huh, J.H., Badieyan, S., Harinantenaina, L., Kliebenstein, D.J., Kingston, D.G., Sobrado, P., and Tholl, D. An alternative biosynthetic route to the pathogen-induced volatile homoterpene DMNT via triterpene degradation in Arabidopsis roots (Manuscript in preparation).

Sugiyama, A., Shitan, N., and Yazaki, K. (2007). Involvement of a soybean ATP-binding cassette - Type transporter in the secretion of genistein, a signal flavonoid in legume-Rhizobium Symbiosis(1). Plant Physiology **144,** 2000-2008.

Suzuki, H., Fujioka, S., Takatsuto, S., Yokota, T., Murofushi, N., and Sakurai, A. (1994). Biosynthesis of Brassinolide from Teasterone Via Typhasterol and Castasterone in Cultured-Cells of Catharanthus-Roseus. J Plant Growth Regul **13,** 21-26.

Swaminathan, S., Morrone, D., Wang, Q., Fulton, D.B., and Peters, R.J. (2009). CYP76M7 is an ent-cassadiene C11alpha-hydroxylase defining a second multifunctional diterpenoid biosynthetic gene cluster in rice. Plant Cell **21,** 3315-3325.

Urban, P., Mignotte, C., Kazmaier, M., Delorme, F., and Pompon, D. (1997). Cloning, yeast expression, and characterization of the coupling of two distantly related Arabidopsis thaliana NADPH-cytochrome P450 reductases with P450 CYP73A5. J Biol Chem **272,** 19176-19186.

Walter, M.H., Floss, D.S., and Strack, D. (2010). Apocarotenoids: hormones, mycorrhizal metabolites and aroma volatiles. Planta **232,** 1-17.

Weng, J.K., Li, Y., Mo, H., and Chapple, C. (2012). Assembly of an evolutionarily new pathway for alpha-pyrone biosynthesis in Arabidopsis. Science **337,** 960-964.

Winterhalter, P., and Rouseff, R. (2001). Carotenoid-Derived Aroma Compounds: An Introduction. In Carotenoid-Derived Aroma Compounds (American Chemical Society), pp. 1-17.

Zimmermann, P., Hirsch-Hoffmann, M., Hennig, L., and Gruissem, W. (2004). GENEVESTIGATOR. Arabidopsis microarray database and analysis toolbox. Plant Physiol. **136,** 2621-2632.

4. Final Discussion and Future Perspectives

Plants are constantly exposed to various changes and threats in their surrounding environment. To cope with these changes, plants rely on different mechanisms including the biosynthesis of chemicals with enormous structural diversity. Although these naturally occurring chemicals used to be considered as waste products of a "luxurious metabolism", they are now accepted as important players in ecological interactions with various biological roles, which has evolved through natural selection (Hartmann, 2007). Phytochemical have been studied extensively in various parts of plants, but knowledge of their biological role in the rhizosphere is still limited. During my research I have focused on understanding the biochemical pathway for the production of the volatile terpene DMNT emitted from *Arabidopsis* roots in response to the root pathogen *Pythium irregulare* and treatment with the defense hormone JA. The discovery of an alternative *Brassicaceae*-specific pathway for volatile homoterpene formation via the degradation of the triterpene precursor arabidiol, as presented in chapter II, raises new questions regarding the placidity and evolution of specialized metabolic pathways in plants. In chapter III we have tried to obtain a better understanding of these biochemical and evolutionary processes by further studying the catabolism of arabidiol-derived metabolites in *Arabidopsis* roots. In this chapter, I highlight the significance of my discoveries in a broader context and present possible future research directions.

Regulation and Functions of Phytochemicals in the Rhizosphere

Similar to aerial plant structures, roots are constantly exposed to numerous beneficial and pathogenic organisms in the rhizosphere and interact with these organisms largely via the release of chemical compounds derived from both primary and specialized metabolic pathways. Primary metabolites such as fatty acids and amino acids serve as attractants to beneficial microbial

communities in the rhizosphere (Jaeger et al., 1999) via recruiting plant growth promoting rhizobacteria to confer enhanced plant growth and immunity (Rudrappa et al., 2008). Additionally, specialized metabolites are found to orchestrate plant-organismal interactions belowground. For example, flavonoids are well-known for their function in establishing plant interactions with mycorrhizal fungi by promoting spore germination and attachment (Scervino et al., 2005). Phytochemicals in roots can also be induced as defense compounds against bacterial and fungal pathogens known as phytoallexins. For example, triterpenoid glycosides such as avenacins secreted from oat roots are involved in the defense against various soil-borne pathogens (Papadopoulou et al., 1999). Furthermore, phytochemicals are also involved in allelopathy interactions belowground. One of the best known examples are aromatic compounds such as juglone produced by the black walnut *Juglans spp*, which have strong allelopathic properties (Hejl and Koster, 2004). Interestingly, rice (*Oryza sativa*) produces diterpene lactones called momilactones, which function as both antimicrobial and allelopathic factors (Wang et al., 2011).

Emission of volatile specialized metabolites such as terpenes from aerial tissues has been reported to show several biological functions and it is expected to see similar activities for volatiles released belowground. Although the mobility of root emitted volatiles in the soil is limited and is dependent on overall physicochemical properties, it has been shown that volatile terpenes such as the C_{15} (*E*)-β-caryophyllene can easily diffuse into air pockets surrounding root tissue and attract insect-parasitizing nematodes (Rasmann et al., 2005). Additionally, volatiles from roots can show allelopathic activities (Romagni et al., 2000) and possibly effect microbial communities in close vicinity of roots in the rhizosphere (Hammer et al., 2003). We have observed emission of the homoterpene DMNT in response to *Arabidopsis* root inoculation with

the oomycete pathogen *Pythium irregulare* and demonstrated that upon cleavage of arabidiol, in addition to DMNT a C19 ketone called arabidonol is produced, which is subsequently converted to several derivatives. *Pythium irregulare* is an oomycete pathogen categorized as a hemibiotroph since it forms haustoria-like structures in the early stage of infection but also produces both phytotoxins and lytic enzymes that degrade plant tissue (Deacon, 1979), which are typical features of necrotrophs (Oliver and Ipcho, 2004). Studies of *Pythium* pathogenicity with *Arabidopsis* suggests that plant defense responses involve the plant hormones, JA and ethylene (Staswick et al., 1998; Vijayan et al., 1998; Geraats et al., 2002). *Pythium* is not only affecting terpene metabolism, as shown in this study, but can also induce the production of indole glucosinolates, lignin, and phenylpropanoids within 48 h of infection (Bednarek et al., 2005; Adie et al., 2007). It is not clear whether the detected arabidiol-derived metabolites act individually or synergistically with other defensive metabolites in this particular pathosystem. Synergistic effects have been reported as an example for terpene mixtures resulting in increased toxic effects on larvae of the generalist lepidopteran *Spodoptera litura* when compared to individual compounds (Hummelbrunner and Isman, 2001). Since many oomycetes including *Pythium* change lifestyles from biotrophs to necrotrophs, studying the functions of induced and constitutive defense chemicals in a time-dependent manner would provide insight into dynamic interactions of the various defense-related phytochemicals. Further studies are required to measure the bioactivity of non-volatile arabidiol catabolism products against pathogens individually or in combination with volatile DMNT.

Cell-Type or Tissue Specificity of Chemical Defense in Roots

Plants are exposed to different selective pressures from organismal communities aboveground and belowground and, therefore, have evolved different chemical defense profiles in these tissues. To dissect the functions of chemical defense metabolites in roots, it is important to understand their tissue or cell type-specific organization. The radial structure of roots with a distinct concentric organization of different cell types makes roots an ideal system for studying cell type specificity. Previous studies reported that the monoterpene 1,8-cineole is synthesized in the epidermis and cortex of *Arabidopsis* roots (Chen et al., 2004) while the production of the sesquiterpene (*Z*)-γ-bisabolene occurs primarily in the sub-epidermal layers and the root cortex (Ro et al., 2006). Additionally, cell type specific biosynthesis of triterpenes has been reported in the epidermis of *Arabidopsis* and oat roots (Jenner et al., 2005). Similarly in this study we have shown that formation of basal DMNT levels is primarily restricted to the pericycle and quiescent center in root meristematic zone. Such cell-type specificity requires a highly coordinated expression of genes involved in the same biosynthetic pathway as recently shown for the thalianol biosynthesis and modification in *Arabidopsis* (Field and Osbourn, 2008) and is also evident in our promoter activity assays for both *ABDS* and *CYP705A1* genes primarily in the root differentiation zone. However, unlike *ABDS*, the *CYP705A1* is expressed only in the quiescent center but not in other cell layers in meristematic zone suggesting that presumably presence of arabidiol in quiescent center could have inhibitory effects on functions of cells in this center. This is supported by a recent study in which accumulation of triterpene intermediates led to disruption of membrane trafficking and inhibition of root growth in oat roots (Mylona et al., 2008). Whether arabidiol accumulation in quiescent center could result in interference with stem cell maintenance and regeneration in *Arabidopsis* roots is not clear. This question could be

addressed by expressing *ABDS* gene under control of a strong quiescent center specific promoter in the *cyp705a1-1* background and evaluating root growth phenotype in these plants.

A cell-specific distribution of defense metabolites in roots may be critical for warding off soil-borne, root-attacking organisms such as nematodes, microbial pathogens and insect larvae with different invasion and feeding strategies (Maron, 1998; Wardle, 2006; Rasmann and Agrawal, 2008). Allocation of defense phytochemicals to the epidermis or root tips appears to be important in inhibiting penetration of pathogens at early stages of infection and whereas their accumulation in the vascular tissue seems to be important for example in defending against phloem feeding insects such as root aphids. Here we showed that the degradation of arabidiol produces basal levels of DMNT and arabidonol derivatives primarily in the root pericycle. Upon activation of the JA signaling pathway, the degradation of arabidiol was enhanced in almost all cell types in the root meristem and elongation zones; however, this was not the case in the root differentiation zone, where the expression of the CYP705A1 protein remained restricted to the pericycle. Combined with our bioassays in this study, we postulate that DMNT might be involved in defending newly emerged root cells in the meristematic and elongation zones against pathogen penetration, and in the vascular tissue upon possible successful pathogen propagation in the root tissue. Further studies are required to evaluate cell type specific expression of genes involved in the modification of arabidonol under normal growth condition and pathogen attack and establish a correlation between organization of the arabidiol catabolism products and their potential bioactivity. Additionally since arabidonol derivatives are found in root exudates we postulate that these phytochemicals might play a role in plant interaction with root attacking organism in the rhizosphere acting as a potential defense compound in rhizosphere. Whether

detection of these metabolites in root exudates is mediated via specific or non-specific transport processes should be further evaluated in details.

Evolution of DMNT Formation in *Arabidopsis*

Our study has shown that DMNT in Arabidopsis is produced specifically by the P450 enzyme CYP705A1 in roots and not by the leaf-specific homoterpene synthase CYP82G1. Whereas CYP705A1 is only found in *Brassicaceae*, the taxonomic distribution of the CYP82 members for most cases overlaps with the occurrence of homoterpenes in various plant families (Nelson et al., 2008). Although no CYP82 member has been identified in monocots they are yet capable of producing homoterpenes (Tholl et al., 2011) (Figure 1.1). We predict that in monocots a P450 presumably from a different family might be involved in homoterpene formation though the nature of the substrate it is not clear.

The arabidiol synthase (*ABDS*) gene is localized on chromosome 4 as part of a gene cluster with a second triterpene synthase (*BARS*), several *Brassicaceae*-specific P450s in CYP702 and CYP705 families including CYP705A1, and three glucosyltransferases. Recently, several functional operon-like gene clusters have been described in maize, oat, *Arabidopsis*, and rice plants (Osbourn and Field, 2009). The formation of metabolic gene clusters in specialized metabolism is suggested to enhance gene regulation and reduce possible cytotoxic effects of intermediates (Osbourn, 2010). Plant gene clusters are most likely assembled by recruitment of genes from somewhere else in the genome via gene duplication, neofunctionalization, and genome reorganization (Field and Osbourn, 2008; Swaminathan et al., 2009). Based on our genome synteny analysis it is evident that one oxidosqualene cyclase gene along with CYP705 members have been recruited to a genomic region with several CYP702, acyltransferase and

glycosyltransferase in the common ancestor of *A. thaliana* and *A. lyrata.* Subsequent gene duplication and neofunctionalization of the oxidosqualene cyclase and CYP705 members has resulted in metabolic diversification and evolution of an alternative pathway for volatile DMNT in *Arabidopsis* roots. Whether other genes residing on the gene cluster can modify arabidiol catabolism metabolites awaits further thorough biochemical and molecular investigations. It is somewhat remarkable that there seems to be a strict tissue-specific metabolic difference in *Arabidopsis* in the formation of homoterpenes, since TMTT and DMNT are produced by two different pathways above and belowground without overlap in the enzymatic machineries. The reason for the evolution of this distinct metabolic separation remains elusive but it might indicate tissue-dependent "micro-environments" that facilitate metabolic pathway evolution under particular selective pressures. It should be noted that CYP82G1 and the geranyllinalool synthase TPS04 are co-expressed in leaves to produce TMTT under stress conditions. However, these genes are not part of a cluster in contrast to *ABDS* and *CYP705A1*, which raises questions about the plasticity or stringency of gene cluster evolution.

Production of DMNT by the degradation of arabidiol presents, to our knowledge, the first biochemical and molecular characterization of volatile terpene formation from a C_{30} precursor. Few other examples are known to date for the production of volatile breakdown products from large precursors. As an example formation of the irones the violet fragrance from dried rhizomes of certain sword lily species is via degradation of iridal triterpenes (Jaenicke and Marner, 1990). Another example for the breakdown of large precursors into volatile terpene products is the formation of apocarotenoids from carotenoid precursors (Winterhalter and Rouseff, 2001). For example, *β*-ionone, *β*-damascenone and dihydroactinidiolide are volatile carotenoid derivatives found in the scent of flowers such as *Rosa hybrid* (rose), or *Freesia hybrida*, or in fruit and

vegetable aroma such as *Averrhoa carambola* (starfruit) or *Lycopersicon esculentum* (tomato) (Winterhalter and Rouseff, 2001). Additionally, as novel plant hormones, strigolactones are derived from carotenoid degradation. The compounds can inhibit shoot branching by interfering with auxin transport (Beveridge et al., 2000). Strigolactones are also involved in plant signaling to promote branching of mycorrhizal fungi (Akiyama et al., 2005) and induce seed germination of parasitic plants (Bouwmeester et al., 2003; Akiyama and Hayashi, 2006) in the rhizosphere. Our discovery of arabidiol as a precursor of volatile DMNT and non-volatile arabidonol, which undergoes further modifications *in planta* highly resembles carotenoid catabolic pathways which similarly produced volatiles and non-volatiles from a large precursor. . The concept of making functional small molecules by the catabolism of larger precursor compounds, which do or may have other roles, represents an efficient way to produce functional units at different stages of a metabolic cycle and suggests that the role of catabolic reactions in regulating plant development or plant-environment interactions might have been underestimated. In our case, further experiments should be developed to study the role of arabidonol derivatives in plant-organismal interaction in the rhizosphere and evaluate their effect on plant developmental processes.

Literature Cited

Adie, B.A., Perez-Perez, J., Perez-Perez, M.M., Godoy, M., Sanchez-Serrano, J.J., Schmelz, E.A., and Solano, R. (2007). ABA is an essential signal for plant resistance to pathogens affecting JA biosynthesis and the activation of defenses in Arabidopsis. Plant Cell **19,** 1665-1681.

Akiyama, K., and Hayashi, H. (2006). Strigolactones: Chemical signals for fungal symbionts and parasitic weeds in plant roots. Annals of Botany **97,** 925-931.

Akiyama, K., Matsuzaki, K.I., and Hayashi, H. (2005). Plant sesquiterpenes induce hyphal branching in arbuscular mycorrhizal fungi. Nature **435,** 824-827.

Bednarek, P., Schneider, B., Svatos, A., Oldham, N., and K, H. (2005). Structural complexity, differential response to infection, and tissue specificity of indolic and phenylpropanoid secondary metabolism in *Arabidopsis* roots. Plant Physiology **138,** 1058–1070.

Beveridge, C.A., Symons, G.M., and Turnbull, C.G.N. (2000). Auxin inhibition of decapitation-induced branching is dependent on graft-transmissible signals regulated by genes *Rms1* and *Rms2*. Plant Physiology **123,** 689-698.

Bouwmeester, H.J., Matusova, R., Zhongkui, S., and Beale, M.H. (2003). Secondary metabolite signalling in host-parasitic plant interactions. Current Opinion in Plant Biology **6,** 358-364.

Chen, F., Ro, D.K., Petri, J., Gershenzon, J., Bohlmann, J., Pichersky, E., and Tholl, D. (2004). Characterization of a root-specific Arabidopsis terpene synthase responsible for the formation of the volatile monoterpene 1,8-cineole. Plant Physiology **135,** 1956-1966.

Deacon, J.W. (1979). Cellulose decomposition by *Pythium* and its relevance to substrate-groups of fungi. Transactions of the British Mycological Society **72,** 469-477.

Field, B., and Osbourn, A. (2008). Metabolic diversification - Independent assembly of operon-like gene clusters in plants. Science **320,** 543 - 547.

Geraats, B.P.J., Bakker, P.A.H.M., and van Loon, L.C. (2002). Ethylene insensitivity impairs resistance to soilborne pathogens in tobacco and *Arabidopsis thaliana*. Molecular Plant-Microbe Interactions **15,** 1078-1085.

Hammer, K.A., Carson, C.F., and Riley, T.V. (2003). Antifungal activity of the components of Melaleuca alternifolia (tea tree) oil. Journal of Applied Microbiology **95,** 853-860.

Hartmann, T. (2007). From waste products to ecochemicals: fifty years research of plant secondary metabolism. Phytochemistry **68,** 2831-2846.

Hejl, A.M., and Koster, K.L. (2004). Juglone disrupts root plasma membrane H+-ATPase activity and impairs water uptake, root respiration, and growth in soybean (*Glycine max*) and corn (*Zea mays*). Journal of Chemical Ecology **30,** 453-471.

Hummelbrunner, L.A., and Isman, M.B. (2001). Acute, sublethal, antifeedant, and synergistic effects of monoterpenoid essential oil compounds on the tobacco cutworm, *Spodoptera litura* (Lep., Noctuidae). Journal of Agricultural and Food Chemistry **49,** 715-720.

Jaeger, C.H., III, Lindow, S.E., Miller, W., Clark, E., and Firestone, M.K. (1999). Mapping of sugar and amino acid availability in soil around roots with bacterial sensors of sucrose and tryptophan. Applied and Environmental Microbiology **65,** 2685-2690.

Jaenicke, L., and Marner, F.J. (1990). The irones and their origin. Pure Appl Chem **62,** 1365-1368.

Jenner, H., Townsend, B., and Osbourn, A. (2005). Unravelling triterpene glycoside synthesis in plants: phytochemistry and functional genomics join forces. Planta **220,** 503-506.

Maron, J.L. (1998). Insect herbivory above- and belowground: Individual and joint effects on plant fitness. Ecology **79,** 1281-1293.

Mylona, P., Owatworakit, A., Papadopoulou, K., Jenner, H., Qin, B., Findlay, K., Hill, L., Qi, X., Bakht, S., Melton, R., and Osbourn, A. (2008). Sad3 and Sad4 are required for saponin biosynthesis and root development in oat. Plant Cell **20,** 201-212.

Nelson, D., Ming, R., Alam, M., and Schuler, M. (2008). Comparison of cytochrome p450 genes from six plant genomes. Tropical Plant Biol. **1,** 216-235.

Oliver, R.P., and Ipcho, S.V.S. (2004). Arabidopsis pathology breathes new life into the necrotrophs-vs.-biotrophs classification of fungal pathogens. Molecular Plant Pathology **5,** 347-352.

Osbourn, A. (2010). Gene clusters for secondary metabolic pathways: an emerging theme in plant biology. Plant Physiol **154,** 531-535.

Osbourn, A.E., and Field, B. (2009). Operons. Cellular and molecular life sciences : CMLS **66,** 3755-3775.

Papadopoulou, K., Melton, R.E., Leggett, M., Daniels, M.J., and Osbourn, A.E. (1999). Compromised disease resistance in saponin-deficient plants. Proceedings of the National Academy of Sciences **96,** 12923-12928.

Rasmann, S., and Agrawal, A.A. (2008). In defense of roots: A research agenda for studying plant resistance to belowground herbivory. Plant Physiology **146,** 875-880.

Rasmann, S., Kollner, T.G., Degenhardt, J., Hiltpold, I., Toepfer, S., Kuhlmann, U., Gershenzon, J., and Turlings, T.C.J. (2005). Recruitment of entomopathogenic nematodes by insect-damaged maize roots. Nature **434,** 732-737.

Ro, D.K., Ehlting, J., Keeling, C.I., Lin, R., Mattheus, N., and Bohlmann, J. (2006). Microarray expression profiling and functional characterization of AtTPS genes: Duplicated Arabidopsis thaliana sesquiterpene synthase genes At4g13280 and At4g13300 encode root-specific and wound-inducible (Z)-gamma-bisabolene synthases. Archives of Biochemistry and Biophysics **448,** 104-116.

Romagni, J.G., Allen, S.N., and Dayan, F.E. (2000). Allelopathic effects of volatile cineoles on two weedy plant species. Journal of Chemical Ecology **26,** 303-313.

Rudrappa, T., Czymmek, K.J., Paré, P.W., and Bais, H.P. (2008). Root-secreted malic acid recruits beneficial soil bacteria. Plant Physiology **148,** 1547-1556.

Scervino, J.M., Ponce, M.A., Erra-Bassells, R., Vierheilig, H., Ocampo, J.A., and Godeas, A. (2005). Flavonoids exhibit fungal species and genus specific effects on the presymbiotic growth of *Gigaspora and Glomus*. Mycological Research **109,** 789-794.

Staswick, P., Yuen, G., and CC., L. (1998). Jasmonate signaling mutants of Arabidopsis are susceptible to the soil fungus *Pythium irregulare*. The Plant Journal **15,** 747-754.

Swaminathan, S., Morrone, D., Wang, Q., Fulton, D.B., and Peters, R.J. (2009). CYP76M7 is an ent-cassadiene C11alpha-hydroxylase defining a second multifunctional diterpenoid biosynthetic gene cluster in rice. Plant Cell **21,** 3315-3325.

Tholl, D., Sohrabi, R., Huh, J.H., and Lee, S. (2011). The biochemistry of homoterpenes--common constituents of floral and herbivore-induced plant volatile bouquets. Phytochemistry **72,** 1635-1646.

Vijayan, P., Shockey, J., Lévesque, C.A., Cook, R.J., and Browse, J. (1998). A role for jasmonate in pathogen defense of Arabidopsis. Proceedings of the National Academy of Sciences **95,** 7209-7214.

Wang, Q., Hillwig, M.L., and Peters, R.J. (2011). CYP99A3: functional identification of a diterpene oxidase from the momilactone biosynthetic gene cluster in rice. Plant J **65,** 87-95.

Wardle, D.A. (2006). The influence of biotic interactions on soil biodiversity. Ecology Letters **9,** 870-886.

Winterhalter, P., and Rouseff, R. (2001). Carotenoid-derived aroma compounds: An introduction. In Carotenoid-Derived Aroma Compounds (American Chemical Society), pp. 1-17.